Feasibility Analysis of ORC Systems: Thermo-Economic and Technical Considerations for Flexible Design

A thesis submitted in partial fulfilment of the requirements for the degree of Doctor of Philosophy in Mechanical Engineering

University of Canterbury

2016

Denny Budisulistyo

TABLE OF CONTENTS

LIST OF FIGURES

LIST OF TABLES

ACKNOWLEDGEMENTS

A special thanks to my senior supervisor Professor Susan Krumdieck for useful discussions, advises, all supports and clear ideas that inspired much of this thesis. I would also like to thank my co-supervisor and wider supervisor team, Associate Professor Mark Jermy, Associate Professor Mathieu Sellier, Dr. Sid Becker, Dr. Hyung-Chul Jung, Dr. Nick Baines, and Hezy Ram who were all helpful during this thesis work.

I would like to acknowledge my thesis examiners: Professor Roberto Gabbrielli and Dr. Nugroho Agung Pambudi who have given a lot of advises and suggestions for improving this thesis.

I would like to acknowledge the fellow students participating in the Above Ground Geothermal and Allied Technologies (AGGAT) programme who contributed in various ways to the ideas and experimentation in this thesis work: Michael Southon, Choon Seng Wong, Leighton Taylor, Sandeep Siwach, James Hewett, Sungjin Choi and Richard Wijninckx.

Finally, I would like to thank my family Swanny and Carol, my parents Han and Christiana and my sisters Henny, Yanny, and Fanny who all are patient and keep me motivated throughout my studies.

ABSTRACT

Geothermal energy conversion engineering is currently carried out nearly exclusively in-house by the technology providers, primarily Ormat and more recently Turboden and Exergy. Geothermal power has a long history of sustainable and economic baseload generation, but each new development requires a much more complex feasibility engineering process than other fossil fuel or renewable energy prospects. The development potential for geothermal energy is vastly greater than for wind or solar, but a critical gap exists in methodologies for the assessment of the technical and economic feasibility of a particular resource development at the exploratory stages of the project. This thesis contributes a sequential approach for carrying out the feasibility study for flexible design (FSFFD) for organic Rankine cycle (ORC) energy conversion technology. The FSFFD approach addresses all of the key ORC design choices to achieve the best performance within the constraints of the available component technologies and cost. The FSFFD approach involves three processes: 1) thermodynamic and economic feasibility studies for key components, 2) flexible design methodology for best resource utilization, and 3) a novel lifetime strategy for anticipating the geothermal resource degradation in the design of plant capacity.

The feasibility studies are conducted to investigate the influence of the heat exchanger design and cycle configurations on the ORC cost and performance. Component selection and cycle configuration options are modelled to obtain the most profitable design considering thermodynamics, economics and technical aspects. The results show that the plate exchanger is the most economical exchanger for ORC systems, even though shell and tube are the current standard. The two-stage thermodynamic cycle configuration provides higher net electrical power output, and

higher thermal and exergy efficiencies than the one-stage designs. However, the increased investment cost and the added technical complexity of two-stage designs can make these designs less feasible than one-stage designs.

The FSFFD approach uses a two-stage design methodology. The first exploration methodology assesses design alternatives for a new binary geothermal power plant. This methodology is suitable for investigating the potential geothermal resource over which the binary geothermal power plant will be installed. The second development methodology obtains the cost-optimum design that is the best match to a heat resource. A breakdown of all typical costs of the geothermal plant projects is calculated in the exploration methodology, although it still deals with uncertainty costs in the preliminary stage, especially the drilling costs. The development methodology was tested with the experimental data from a lab-scale ORC system. The study of the lab-scale ORC system optimised the current ORC design with three ranges of heat input (condition 1, condition 2 and condition 3) – which was not clear to the original designers. The size of the current evaporator and condenser is significantly larger than the required heat transfer areas, but the size of the current gas-oil exchanger is significantly smaller especially under the low heat input conditions.

Finally, a novel lifetime strategy is developed to optimise the binary geothermal power plant taking into consideration the resource degradation. The best design point is selected over the whole plant life considering the typical decrease of thermal input found by research of past developments. The results demonstrate that the initial geothermal resource temperature, pressure, and flowrate are not the best design point to develop the most profitable plant design, although current practice uses these values. This thesis also proposes how to improve the lifetime plant performance in

two ways through operational parameters adjustments and adaptive designs. The results show that adjustment of mass flow rates of n-pentane and cooling air can maintain the performance over the whole plant life. After the half-life of the operation, the working fluid pumps need to be replaced to maintain the plant performance. The two adaptive designs discussed in this thesis are installing a recuperator and reducing the heat transfer area of preheater and vaporizer.

Chapter 1 - Introduction

1.1. Introduction

Coal is the main source of baseload power generation for the world. Requirement for coal has grown rapidly over the last decade [1]. World coal consumption increases from 2012 to 2040 at an average rate of 0.6% per year, from 152 quadrillion Btu to 180 quadrillion Btu in 2040. The power generation consumed 59% of world coal consumption in 2012 and remains close to that share of coal consumption through 2040 [2]. However, the coal-fired power generation must be shut down over the next several decades to mitigate the most destructive climate change damage. The only baseload renewables of scale are hydro and geothermal energies. Recently, the installed capacity of geothermal power generation in the world has increased significantly [3]. An increase about 1.7 GWe in the five year term 2010-2015 has been achieved (about 16%), which is greater than the average value of about 200 MW/year in the period 2000-2005. The total installed capacity of geothermal power plant worldwide in 2015 is 12.6 GWe. Figure 1.1 shows a world map of the installed capacity of geothermal power plants in 2015. Figure 1.2 shows the progress of plant installed capacity from 1995 to 2015 and the forecast of the installed capacity in 2020 [3]. The forecast increase for period 2015-2020 is 8.8 GWe and the total capacity at 21.4 GWe is predicted to be installed worldwide in 2020.

There are many reasons to be optimistic about future geothermal development. The cost of geothermal development is cost competitive with fossil fuels in most locations. Geothermal power plants can also provide power without consuming fresh water. Geothermal resources are divided into two types according to what the wells

produce. Steam-dominated resources produce steam with very little water and water-dominated resources produce the opposite [4].

Among geothermal energy resources, the low-to-moderate temperature liquid-dominated resources with temperatures < 160^0C are the majority of geothermal resources worldwide [5]. Binary power plants that based on Organic Rankine Cycle (ORC) technology are the best energy conversion system to exploit these low temperature resources from both a technical and environmental aspects [6]. The ORC technology has several benefits [7]:

- It can be used to convert low temperature of renewable heat resources into electricity. The heat resources commonly include geothermal, biomass and solar resources.
- It can increase energy utilisation from industrial processes by recovering the waste heat of industrial processes and convert it into electricity. As a result, this increases an overall conversion energy efficiency of the primary system. The approach is known as combined heat and power generation (CHP) through a bottoming cycle.
- The CHP systems can reduce building energy consumptions because the ORC technology can produce electricity from high temperature level of fossil fuels and the rejected heat of the systems with low temperature is still able to meet the needs of the buildings

The ORC technology can become a “bridge to the future” to minimize the risk of energy scarcity and environmental issues.

Nowadays the binary power plants are the most widely used type of geothermal power plant. They constitute 44% of the total geothermal power plant units in 2010, but contribute only 10% of the total geothermal power [8]. The average power rating

per unit is small, only 2.3 MW/unit, but medium and large binary power plants can produce power output at least 5 MW. Several binary units have been recently added to existing flash-steam plants to recover more electricity generation [9]. Table 1.1 shows the number of binary plants installed worldwide at the end of 2006 [10].

New Zealand has a total of 1,005 MWe of installed geothermal capacity which is typically contributing about 16% of the national electricity generation in 2015. The country currently produces about 75% of its electricity from renewable sources and is strategically targeting 90% renewable generation by 2025 [11]. New Zealand has the opportunity to learn from the geothermal developments; the country has to become a leader in geothermal development.

The geothermal developments include four different areas: thermal engineering, geochemistry, geophysics and reservoir engineering. The developments in our research group are focused on thermal engineering, which includes optimization, troubleshooting, maintenance, operation and design adaptation. This thesis addresses knowledge gaps of the binary geothermal power plant developments especially for the energy conversion technology.

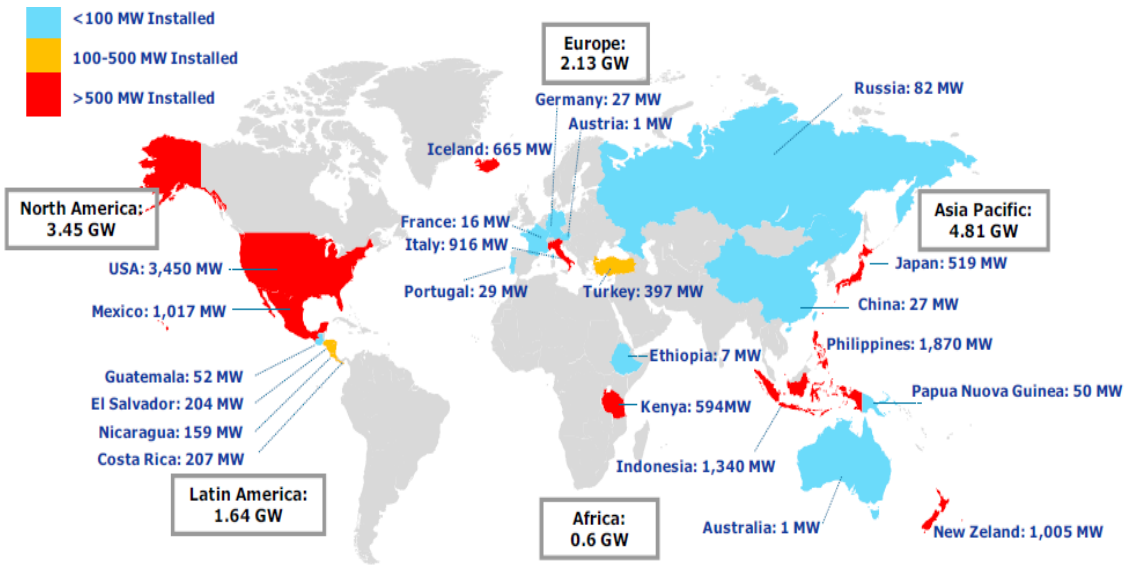

Figure 1.1: Installed capacity of geothermal power plant worldwide in 2015

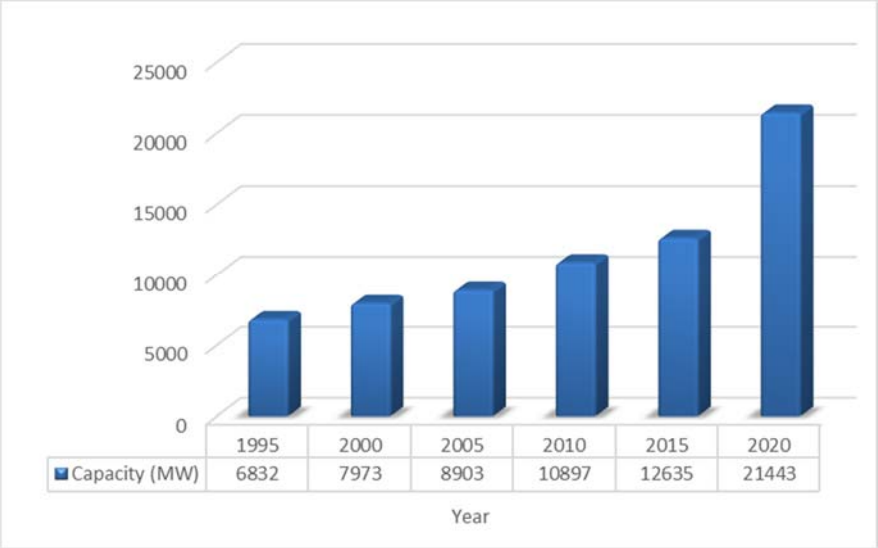

Figure 1.2: Total worldwide installed capacity from 1995 to 2015 and forecast for 2020.

Table 1.1: Number of installed binary plants worldwide.

Country	Binary	Flash + Binary
USA	139	10
New Zealand	10	14
Philippines	13	5
Iceland	8	-
Guatemala	1	7
Portugal	5	-
Austria	3	-
Germany	3	-
Kenya	1	2
Mexico	2	-
Japan	2	-
Costa Rica	2	-
Australia	2	-
Ethiopia	2	-
Austria	2	-
Turkey	2	-
China	1	-
Nicaragua	1	-
Thailand	1	-
El Salvador	1	-
France	1	-
Total	202	38

1.2. The design problems

Designing the ORC plant is a challenging task because the system has a low thermal efficiency especially for the system utilizing low temperature resources. Quoilin et al. Quoilin, Van Den Broek [7] reported that the thermal efficiency of the current high temperature ORC plant does not exceed 24% and the low temperature ORC plant would have a lower efficiency.

Designing ORC plant addresses hard problems because this is usually open-ended and ill-structured. These problems are the common problems in designing engineering systems [12, 13]:

- Design problems are *open-ended* because they usually have many acceptable solutions. A unique solution is generally not obtained, and one may have to choose from a range of acceptable solutions.
- Design problems are *ill-structured* because their solutions cannot normally be found by applying mathematic formulas or algorithms in a structure way.

Trade-off is generally necessary as a part of design processes to take both technical and economic aspects into account and produce a design flexibility, because certain characteristics of the system may have to relax in order to achieve some other goals for example greater cost effectiveness or higher system performance. The algorithms for comparing any two alternate designs on the aggregation of cost and performance objectives are required in *trade-off*. This thesis implements a cost-performance trade-offs. The trade-offs define how performance objectives should be traded with cost objectives [14].

1.3. Motivation

Designing thermal systems like the ORC systems usually involves complexities arising from non-linear mechanisms, partial differential equations, coupled phenomena and other complications. Therefore, the design variables selected in the initial designs cannot always satisfy the given requirements and constraints. Each step of the design process requires in-depth engineering knowledge and experience, known as knowledge-based engineering (KBE). However, open literature on the subject is limited due to business purpose. Main ORC manufacturers such as Ormat, Turboden, and Exergy have essentially built up their own KBE. New Zealand has currently 260 low enthalpy geothermal energy sites with temperatures < 150^0C and 170 other sites such as disused coal mines, abandoned oil and gas wells, and water wells outside of typical geothermal areas and in onshore sedimentary basins [15]. However, the country has limited research funding support fundamental mechanical engineering science that would be needed for development of KBE.

1.4. The Contribution

The aim of this thesis is to develop an approach for a feasibility study for flexible design (FSFFD) for the ORC development which includes thermodynamic, component, resource, and cost considerations. The five main design variables are:

1) Type of working fluids e.g. n-pentane or refrigerants
2) Type of main components, e.g. flat plate or shell and tube heat exchanger
3) Type of cycle configurations e.g. standard Rankine or with re-heat
4) Design parameters e.g. pinch points, degree of superheat or subcooling
5) Size of main components e.g. heat duty and power output.

Up to the time of writing this thesis, there are no studies in the literature that propose the comprehensive guidelines to investigate the thermodynamic and

economic feasibility through design and optimization of the ORC which take into account all of the five main design variables as well as the resource degradation. The FSFFD approach is also unique in the literature as it considers the selection of standard main components which are available in the market as a starting point for designing and optimising the ORC system. The approach is used to design the ORC plant utilizing low temperature heat resources. This new method is named the FSFFD approach and is compared to the design approaches reported in the current literature in Table 1.2.

Table 1.2: Differences between current and proposed approaches

Differences	Current approaches described in literature review	Proposed FSFFD approach described in this thesis
1. Design variables	< 5 variables	5 variables
2. Starting design point	No reference	Selection of available main components
3. Selection and design	Both are not described clearly	Both are considered as interchangeable terms during development process

The implementation of FSFFD approach involves three processes:

1) Feasibility study to investigate the influence of heat exchanger and cycle selections on the design optimization.
2) Design methodology is used for two purposes:
   (a) To assess design alternatives for a new binary geothermal power plant based on thermodynamic and economic analyses
   (b) To design and optimize the ORC systems based on a design to resource (DTR) method.
3) Lifetime design strategy to mitigate the performance reduction due to geothermal resource degradation over whole plant life.

This thesis proposes a way to achieve a relevant and feasible design of an ORC because the process is started by selecting the standard main components that are

available in the market. The process takes into account different design options, trade-off and initial limitations of the system.

1.5. FSFFD approach

1.5.1. Definition

The feasibility study for flexible design (FSFFD) approach provides sequential studies to work through the feasibility and optimization process for the ORC plants utilizing a low temperature resource. As a result, the development of the ORC designs based on FSFFD approach should be achieved faster and provides more flexibility and helps to reduce risk and uncertainties in the feasibility stage.

1.5.2. FSFFD approach description

The design process of the ORC system based on FSFFD approach is illustrated in Figure 1.4. The modelling of the ORC plant is an extremely important step in developing a numerical model in the FSFFD approach. The FSFFD approach consists of four steps:

1) Initial step

The starting point for FSFFD approach is to gather all requirements of preliminary data and range of options:

a. *Development: conceptual design* that consists of the basic approach and the general features of the systems. The initial design must be well defined in terms of the following [16]:

- Overall geometry and configuration of the system
- Different components that comprise the system
- Interaction between the various components
- Given fixed quantities in the system

The detailed explanations of the ORC system for the initial design are given in Chapter 2 including the basic cycle, the process flow diagram, selection guidance of the ORC main components and technology of the systems.

b. *Resource: heat resource and heat sink* conditions are used to design a thermodynamic cycle of the ORC plant. An acceptable design is obtained from various design variables considered by comparing the simulation results with problem statement. All the requirements and constraints must be satisfied by an acceptable design. There are two different strategies for designing of a thermal system based on a numerical model which are adjusting design variables and developing different designs [16]. This thesis uses the adjusting design variables as the design strategy because the fixed set of operating conditions (heat source and heat sink of the ORC system) is applied to simplify the design evaluation.

c. *Design variables* that influence the thermodynamic cycle performance of ORC are type of working fluids, type of main components, type of cycle configurations or designs, design parameters and size of main components. The initial selection of the design variables is based on information available from other similar designs, on current engineering practice and on experience. The selection of design variables in the ORC design is a critical step in the design procedure, and considerable effort must be exerted to obtain a design which is acceptable or as close as possible to an acceptable design.

2) Simulation step

A simplified model of the ORC system may be developed for this initial design of the system by utilizing approximations and idealizations of the processes. Therefore its behaviour and characteristics may be analysed. Both analytical and experimental procedures are employed to model a system. The analytical and/or

numerical results must be validated, preferably by comparison with available experimental data to ensure the accuracy of the models representing the actual system (real-world). Simulation is the evaluation process of the model to determine the behaviour of the system under a variety of conditions so that the design can be evaluated for satisfactory performance. The design variables influence a variety of conditions. This process is known as *numerical simulation*.

3) Evaluation step

The next step in the design process is the evaluation of the various designs. Two types of evaluation are considered here: thermodynamic and economic approaches. The objective of the thermodynamic evaluation is to minimize the thermodynamic in-efficiencies: exergy destruction and exergy loss. The objective of the economic evaluation is to minimize the levelized costs of the plant investment. These approaches have been used by several ORC researchers in their works [17-19]. In addition, the ORC system utilising geothermal resources operates under off-design conditions for most of their operation [20]. Therefore, it is important to analyse the behaviour and performance of the systems under off-design conditions. The acceptable designs are evaluated using the criteria of success used by most engineering companies such as return on investment (ROI), net present value (NPV) and energy return on investment (EROI). These criteria have represented standard investment evaluation criteria with and without considering the time value of money [21, 22]. In case that the component costs are not calculated, the ratio of total net power to total heat transfer areas ($W_{net}/A_{tot,\ HE}$) is proposed an optimization criterion. The criterion is similar to the objective function that was proposed by Madhawa et al. [23] to optimise a cost-effective design of the ORC plants. The iterative process is repeated by varying the design variables to evaluate

the design alternatives based on the requirements and constraints given in the problem statement. If an acceptable design is not obtained, the design variables and/or initial design are varied and the processes of modelling, simulation and design evaluation are repeated until an acceptable design is obtained.

4) Result step

The best designs are selected based on the criteria of success used in the evaluation step. The acceptable criteria are the highest value of ROI, NPV, and EROI among alternatives

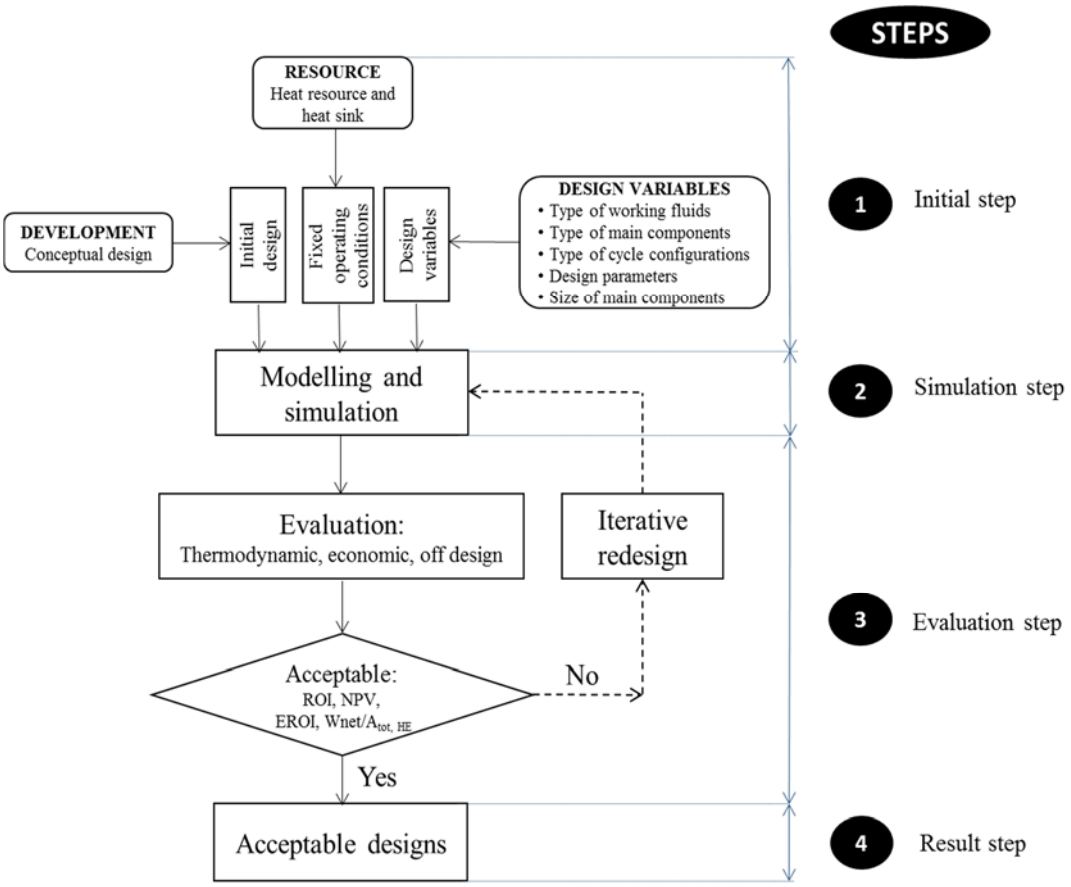

Figure 1.3: Design process of ORC system by using FSFFD approach (adapted from Jaluria [16]).

A base of expertise for designing and optimization of ORC plants in this thesis is proposed by employing the simulation models and the experimentation of the ORC

test rig in our thermodynamic laboratory. The numerical models of ORC system is accomplished via simulation of the system thermodynamics in the software package Engineering Equation Solver (EES) [24], Aspen plus and Aspen exchanger design and rating (EDR) [25]. The detail ORC test rig used in the research work is explained in Chapter 6. The application of ORC in this research work focus on the application of ORC development for binary geothermal plants and waste heat recovery (WHR) systems.

1.6. Research Questions

In the course of researching the current state of the art in ORC design outside of the main technology suppliers, a set of key questions kept arising in discussions with experienced geothermal developers and utility operators.

1. The heat exchanger costs contribute the majority of the total plant investment cost [23]. How can the heat exchanger design reduce the ROI of the binary geothermal power plant?
2. A potential geothermal well located in Taupo Volcanic Zone (TVZ), New Zealand is available. Is this feasible to be utilized for a new binary geothermal power plant? Several thermodynamic cycle configurations with 1-stage turbine and 2-stage turbine are provided to increase the plant performance. Which cycle configuration is the most favourable design for the geothermal resource?
3. A design methodology for conducting the pre-feasibility study which assesses a potential low temperature geothermal resource is required because New Zealand has a lot of resources across the country [15]. How can an assessment be conducted systematically and considering five main design variables in a design methodology?

4. How can the ORC systems be designed and optimised to obtain the best design based on a design to resource (DTR) method? Some constraints in the investigation are the available main components, the available working fluid and the available heat resource. What is the best heat exchanger design (in terms of size) required by the ORC test rig in our laboratory to achieve better performance? To answer this question, the experiments have been conducted to validate the calculations of heat transfer coefficients in the real test rig operations.
5. How can the binary geothermal power plant be designed to achieve the most profitable design considering a geothermal resource degradation over the whole plant life?

The aforementioned challenges were successfully investigated in this thesis and the FSFFD approach was developed, so that the initial feasibility investigation for a geothermal development prospect could provide a solid foundation for investment decisions.

1.7. Outline of the Thesis

The aim of this thesis is to develop the FSFFD approach for the ORC design development. The organisation of the work in this thesis is presented in Figure 1.4. The work began with feasibility studies of the main design variables, followed by developing design methodologies and design strategy considering lifetime of power plant operations. Every chapter is outlined as follows:

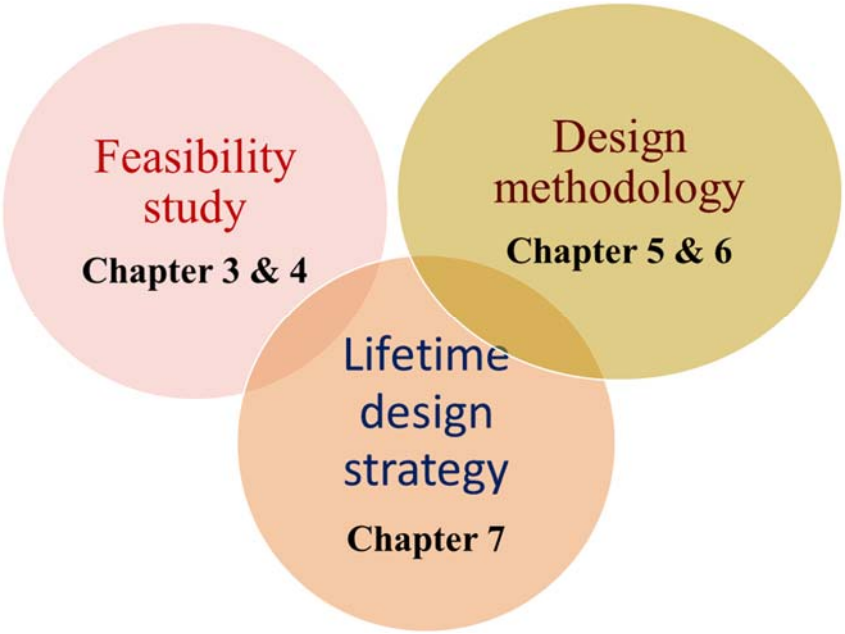

Figure 1.4: Organization of the work in this thesis

Chapter 2 summarises the literature review of organic Rankine cycle (ORC) technology in energy conversion units for low temperature heat resources. The literature review includes a basic ORC technology, a review of the ORC main component selections, modelling and simulating the ORC design and off-design consideration in the ORC models. The gaps in the research were also identified in this chapter.

Feasibility Study

Chapter 3 describes the effect of heat exchanger design on the plant ROI. The analysis aims to analyse and evaluate the heat exchanger design; therefore the new plant design can have a better ROI. The analysis is applied to the Chena geothermal power plant. The ROI of the existing Chena geothermal power plant is used as a base case for the comparison analysis.

Chapter 4 describes comparative thermodynamic and economic analysis of different thermodynamic cycle configurations in the pre-feasibility study of a binary

geothermal power plant. The analysis used a constant pressure ratio and an absolute pressure level to improve the accuracy of the turbine models.

Design Methodology

Chapter 5 describes a design methodology for assessing a potential geothermal resource over which the new binary geothermal power plant will be installed. The methodology is applied to the existing geothermal well located in Taupo Volcanic Zone (TVZ), New Zealand.

Chapter 6 describes a comprehensive design methodology for a cost-effective design of the ORC system using design to resource (DTR) method. The methodology considers selection of components required for a system as a step in the design process of the ORC system.

Design Strategy

Chapter 7 describes the design investigation of a binary geothermal power plant, which takes into account resource degradation over the whole plant life. The best design point is selected based on thermodynamic and economic point of view to obtain the most profitable plant design.

Chapter 8 describes the thesis summary and the implications of the lesson from each section and the author's point of view of this research work.

Chapter 2 – Literature Review

The aim of this thesis is to develop an approach for a feasibility study for flexible design (FSFFD) for the ORC development, which includes thermodynamic, component, resource, and cost considerations. This chapter presents conceptual designs of the organic Rankine cycle (ORC) technology, selection of the ORC main components, and art of ORC modelling and simulating the ORC designs from previous works. The literature review introduces five main variables that greatly influence the ORC performance during the design process. It also discusses off-design investigations of the ORC system from previous researchers. Thus, the literature review identifies gaps in the research: lack of investigation for heat exchanger and cycle configurations, lack of comprehensive guideline for the ORC design considering five main design variables and lack of a design strategy for designing the binary power plant considering the resource degradation.

2.1. Organic Rankine Cycle technology

The ORC has the same working principle and components as a typical Rankine cycle. The Rankine cycle has been traditionally used to produce electricity from steam. This is a proven form of technology and it uses water as the working fluid to produce electricity. Therefore, the Rankine cycle cannot be used to utilize resources with a temperature lower than the boiling point of water (100^0C). The principle of the conventional Rankine cycle is shown in Figure 2.1. The main components of the cycle are turbine, condenser, pump and evaporator. The cycle consists of four main ideal processes [26]:

1-2: Reversible adiabatic expansion in the turbine

2-3: Constant-pressure heat transfer in the condenser

3-4: Reversible adiabatic pumping process in the pump

4-1: Constant-pressure heat transfer in the evaporator

Water is classified as wet fluid and impacts to moisture content less than 10% in the turbine exhaust in Rankine cycle. The moisture forms water droplets and causes erosion of the turbine blades. A certain amount of superheat is required to avoid the condensation of steam in the turbine [27]. However, two main challenges are associated with the superheating of steam. First, superheat requires higher operating temperature of the steam. The low temperature heat resources may not be able to superheat the steam. Second, the heat transfer coefficients are lower in the vapour phase that impacts to increase the required heat transfer areas. This incurs a high capital cost and may not result feasible for the power plant. Therefore, Rankine cycle using a steam is not feasible for low temperature applications.

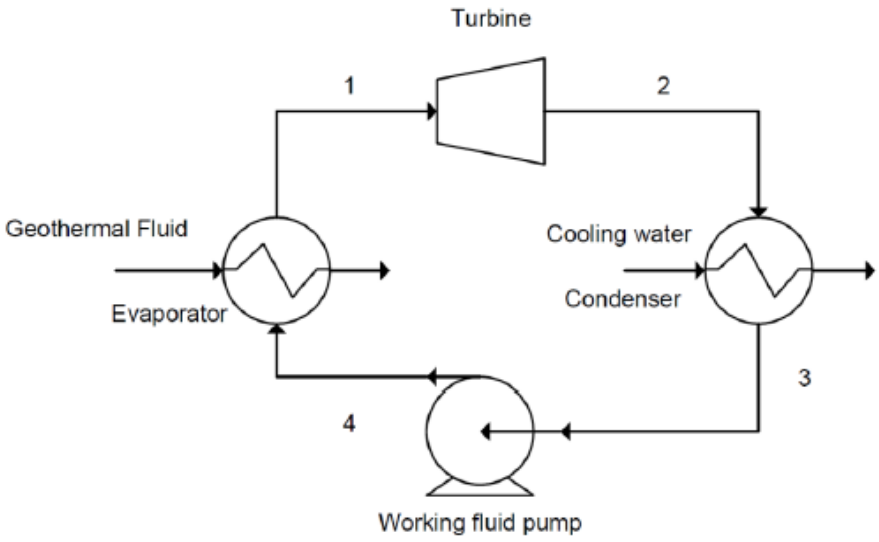

(a)

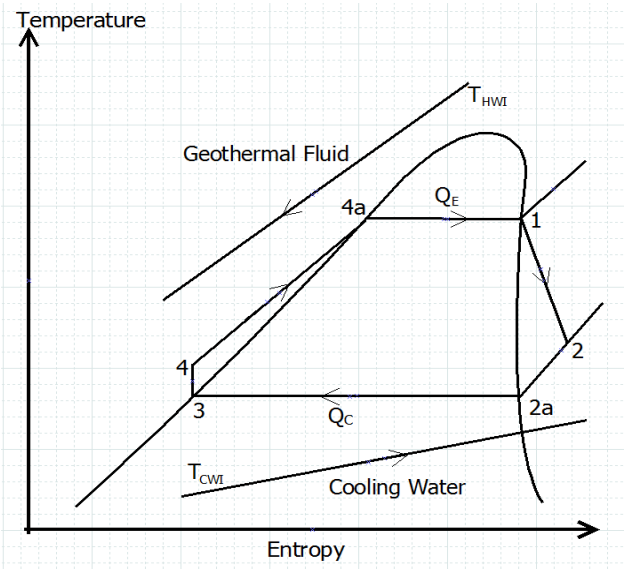

(b)

Figure 2.1: Schematic diagram (a) and temperature - entropy diagram of basic Rankine cycle (b)

The ORC is similar to the conventional Rankine cycle, but uses organic fluids such as 1,1,1,3,3-pentafluoropropane (R24fa), 1,1,1,2-tetrafluoroethane (R134a), n-pentane etc. as the working medium instead of the steam [28, 29]. The application of the ORC technology is considered technically and economically feasible. The organic fluids utilized by the technology have the higher molecular weight, lower evaporation heat, and lower critical and boiling temperatures when compared to steam. The slope of the saturation curve in the T-s diagram depends on the type of fluid used. A dry fluid has a positive slope; a wet fluid has a negative slope and an isentropic fluid has infinite large slopes. The absence of condensation also reduces the risk of corrosion on the turbine blade and increases its lifetime up to 30 years instead of 15-20 years for steam turbines [30]. These features make the ORC technology very attractive to generate electricity from various low-to-medium temperature resources such as geothermal energy, waste heat, biomass products and solar energy [31-34].

2.1.1. Thermodynamic analysis

The thermodynamic analysis of the cycle is fairly straightforward. The analysis is based on the usual assumptions commonly applied for these kinds of problems [17]:

- Steady State
- Thermodynamic equilibrium at inlet and outlet sections of each component
- Negligibility of kinetic and gravitational terms in the energy balances
- Negligible heat losses toward the environment in heat exchangers, pump, and expander
- One-dimensional flow

The fundamental laws of mass and energy conservation are implemented in each component of the ORC system. Table 2.1 shows all equations of the energy balance and isentropic efficiency for each component in the cycle. h is enthalpy, m is mass flow of work fluid, W and Q are work and heat transfer rate, respectively, U is overall heat transfer coefficient, A is heat transfer area of heat exchanger, ΔT_{lm} is the logarithmic mean temperature difference, and F is the configuration correction factor. The subscripts c, v, s, p and sh refer to condenser, evaporator, preheater and superheating zone, respectively. Two heat exchange zones are available in the evaporator and condenser. The expressions of the energy balance and convection heat transfer for each zone are written separately. Δh_{vap} and Δh_{cond} are the heat of vaporization and condensation, respectively.

Table 2.1: Thermodynamic equations of the ORC cycle.

Component	Inlet State	Outlet State	Energy Transfer [kW]	Energy Balance	Isentropic Efficiency and Convection Heat Transfer
Turbine	1	2	$W_{1\text{-}2}$	$W_{1-2} = \dot{m}(h_1 - h_2)$	$\eta_{1-2} = \frac{h_1 - h_2}{h_1 - h_{2s}}$
Condenser	2	3	$Q_{2\text{-}3}$	$Q_{2-2a} = \dot{m}(h_2 - h_{2a})$ $Q_{2a-3} = \dot{m}\Delta h_{cond}$	$Q_{2-2a} = U_{sh}A_{sh}\mathrm{F}\Delta T_{lm2-2a}$ $Q_{2a-3} = U_cA_c\mathrm{F}\Delta T_{lm2a-3}$
Pump	3	4	$W_{3\text{-}4}$	$W_{3-4} = \dot{m}(h_4 - h_3)$	$\eta_{3-4} = \frac{h_3 - h_{4s}}{h_3 - h_4}$
Evaporator	4	1	$Q_{4\text{-}1}$	$Q_{4-4a} = \dot{m}(h_4 - h_1)$ $Q_{4a-1} = \dot{m}\Delta h_{vap}$	$Q_{4-4a} = U_pA_p\mathrm{F}\Delta T_{lm4-4a}$ $Q_{4a-1} = U_vA_v\mathrm{F}\Delta T_{lm4a-1}$

2.1.2. Overall cycle analysis

The cycle of the plant is now summed up by looking at the cycle as a whole. The cycle performance can be assessed by the First Law of Thermodynamic using thermal efficiency. The thermal efficiency of the ORC plant is defined as follow [35, 36]:

$$\eta_{\mathrm{th}} = \frac{Wnet}{\mathrm{Q}} \tag{2.1}$$

where Wnet and Q are net electrical power output and heat transferred from the heat resource to working fluid, respectively.

Another measure of cycle performance can be obtained using the Second Law of Thermodynamic in the form of the overall exergy efficiency, η_e, which is defined as the ratio of the actual net electrical power output to the maximum theoretical power obtainable from the brine fluid in the reservoir state [9]:

$$\eta_{\mathrm{e}} = \frac{Wnet}{E_{in}} = \frac{Wnet}{\dot{\mathrm{m}}[(\mathrm{h_{in}}-\mathrm{h_o})-\mathrm{T_o}(\mathrm{s_{in}}-\mathrm{s_o})]} \tag{2.2}$$

where $\dot{m}$, h_{in} and h_o are mass flow rate of the brine and enthalpies at reservoir input state point and the specified dead reference state, T_o is temperature of specified dead

reference state, s_{in} and s_o are entropies at reservoir input state point and the specified dead reference state.

The net power output of an available heat resource is critical due to economic aspects in geothermal power plants [37]. Therefore, this parameter is used as an objective function in optimizing the design of geothermal power plants. The net power output of the plant (Wnet) of geothermal power plants using an air-cooled condenser is defined as turbine power deducted by pump and fan powers:

$$Wnet = W_T - W_p - W_{fans} \quad (2.3)$$

where Wnet, W_T, W_p and W_{fans} are the net power output, work of turbine, pump and fans, respectively.

2.1.3. Economic analysis

The following methods below are used in the economic analyses in this work. The economic analyses have been performed without considering the taxation of the incomes.

The return on investment (ROI) is defined as the ratio of profit to investment [38]. This is the most common criterion used by most engineering companies to determine if an undertaking is successful. The ROI is expressed as:

$$ROI = \frac{N_p}{T} \quad (2.4)$$

where N_p is annual net profit of the plant and T is the total capital cost of power plant.

When the net present value (NPV) is used for project selection, the following rules apply: the projects with the highest present values are given the highest preference among various alternatives. Bejan and Moran. [21] defined the NPV as the sum of the present values of incoming and outgoing cash flows over a period of time.

$$NPV = \sum_{i=1}^{t} \frac{R_i}{(1+q)^i} - TCI \quad (2.5)$$

where t is the equipment lifespan, q is the discounted rate, TCI is the total capital investment, and R_i is the annual revenues from electricity sales. The discount rate is set by the particular industry and may have the inflation rate. The interest rate that has considered inflation rate (q^*) is calculated as follow [39]:

$$q^* = \frac{1+q}{1+f} - 1 \quad (2.6)$$

where q and f are the discounted rate and inflation rate, respectively.

2.1.4. Subcritical and supercritical ORC systems

ORC can be operated in a subcritical or supercritical (transcritical) cycle. In a subcritical cycle, the working fluid always remains below its critical temperature. In supercritical cycle, the evaporation of the working fluid ends in supercritical area and the heat rejection in condenser occurs in the subcritical area. Preißinger et al. [37] compared the performance of subcritical and supercritical cycles using some working fluids such as R227ea, RC318, R236fa and R236ea. The geothermal fluid has to be $>120^0$C to improve the cycle performance. It was observed that supercritical cycle increase up to 6.2% of the exergy efficiency and 15.4% of the gross power output compared to subcritical cycle. Because the required heat input with the operational pressure $\geq$ the critical pressure (P_{cr}) of a working fluid must achieve at least the critical temperature (T_{cr}) of a working fluid, the supercritical cycle has higher power output, higher thermal efficiency and higher Carnot cycle efficiency than a subcritical cycle [40]. The higher pressures require higher strength of the heat exchanger materials. The expensive capital costs of supercritical cycle is caused by the higher pressure level, higher area of the heat exchangers and higher material strength. The scope of the thesis is to analyse the low temperature heat resources, so that the subcritical cycle is selected.

2.2. Selection of the ORC main components

The characteristic and capability of each main component need to be clearly understood before selecting them for the design of the ORC system. The ORC systems utilizing low temperature heat resources tend to have a low and limited system efficiency [7, 9]. The selection of the turbine is an important decision because it is a critical component in a relatively efficient and cost-effective ORC system [41]. Moreover, the total cost of heat exchangers dominates the total power plant investment cost in a low-temperature geothermal power plant [23]. Hence, the right selection of the turbines and the heat exchangers are very important factor to obtain the optimum ORC design.

2.2.1. Heat exchangers

The classification of heat exchangers is based upon several factors: transfer process, number of fluids, surface compactness, construction, flow arrangements and heat transfer mechanisms [42] to accommodate different fluid properties and operating requirements. According to the construction, they are divided into four categories: tubular, plate, extended surface and regenerative. The diagram is showed as follow:

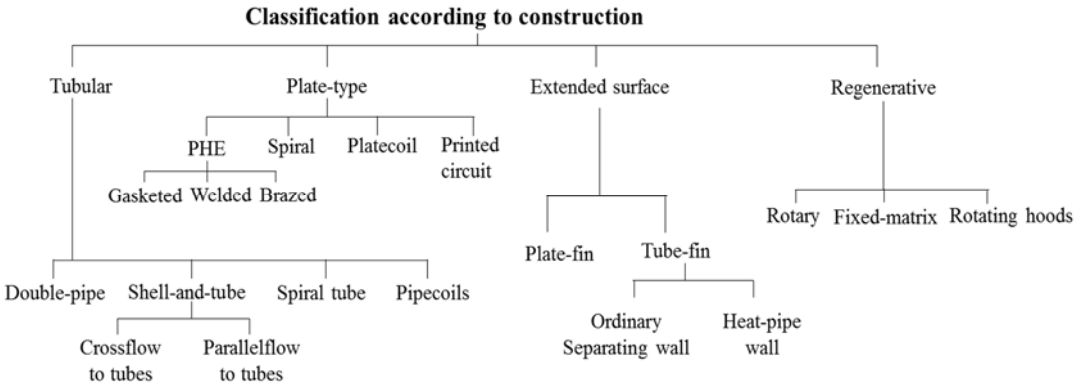

Figure 2.2: Classification of heat exchanger according to construction [42].

The basic ORC system uses the two heat exchangers for evaporator and condenser. In some cases, a recuperator is used to improve thermal efficiency of the ORC system for higher temperature waste heat streams after the turbines. Three common heat exchanger types used in the ORC system are shell-tube exchanger, plate exchanger and air-cooled condenser. The larger-scale ORC systems commonly use shell and tube heat exchangers and the small-scale systems use plate heat exchangers due to their compactness [7, 43]. Table 2.2 shows brief summaries of key criteria for preliminary a selection of the heat exchanger types [44]. The table provides information on pressure and temperature limits of three heat exchanger types that are usually be used in the geothermal field. Note that the material of construction used in many types of the heat exchanger is the only limitation in the heating or cooling of many fluids. However, when seals or gaskets are used to maintain separation between the two fluids in the plate exchanger type, it is the major fluid limitation due to the nature of the seal or gaskets. Because the geothermal fluid has a known fouling characteristic [45], heat exchangers that have limited accessibility, such as welded plate exchangers and compact heat exchangers should not be used.

The main factor of preliminary selection of the type of heat-transfer equipment is recommended based on economics considering the same thermal and hydraulic requirement among the available types of the heat exchangers [38]. Moreover, maintenance, safety, health, and protection of the environment have to be considered as well during the selection to ensure no serious problem due to these aspects.

Table 2.2: Criteria for the preliminary selection of the appropriate heat exchanger type.

Exchanger type	Max. Pressure approx. range (Mpa)	Temperature approx. range (C)	Normal area, approx. range (m^2)	Fluid velocities (shell/tube) m/s	Fluid Limitations	Key features
Shell-and-tube	30	-200-600+	2-1000	Liq. (1-1)/(2-3) Gas (5-10)/(10-20)	Materials of construction	Very adaptable, many types
Gasketed plate	0.1-2.5	-25-175	1-2500	Liq. (1-2)/(1-2) Gas (5-10)/(5-10)	Limited to gasket material, avoid gas flow	Modular construction, minimal $/area cost
Air-cooled	Variable in tube side	Variable on tube side	6-20,000	Liq. (NA)/(2-3) Gas (3-6/(10-20)	Material construction	Use for heat rejection, standardized design

The main advantages of plate exchanger are the minimal risk of internal leakage, compact design, efficient heat transfers, cheaper material, ease of control over pressure drops and ease of maintenance [46] as well as availability in a small scale. [23] designed 90 MWe of the ORC system for low-temperature geothermal heat sources by using plate type due to its compactness and high heat transfer coefficients which result less heat transfer area than would be needed for the same duty as using shell and tube heat exchanger. A small scale of ORC plants [19, 43, 47, 48] use the plate type, because the plate type is available with more competitive prices in the markets than shell and tube type.

The shell and tube exchanger is the most commonly used type of heat exchanger in the process industry for at least 60 percent of all heat exchangers in use today [38]. There are well-established codes and standards prepared by TEMA (Tubular Exchanger Manufacturers Association) and ASME (American Society for Mechanical Engineers) for this type. Many ORC power plants use shell-tube heat exchangers because these types provide relatively large ratios of heat transfer area to volume and weight and they can be easily cleaned. They offer great flexibility to meet almost to

meet almost any service requirement as well as they can be designed for high pressure relative to the environment and high-pressure differences between the fluid streams [49]. Many studies on ORC plants are using these types in their systems.

The lack of cooling water supply that occurs in a geothermal site, air-cooled condenser is the solution. The air is used for cooling and condensing liquid streams in fin-fan heat exchangers. The tubes are arranged in banks, with the air forced across the tubes in cross flow by fans. Therefore, no shell is needed, fouling on the outside of the tubes does not occur. However, the cost of air-cooled condenser is very expensive, because the exchanger type requires the largest area of condenser options. This is because air has significantly less favourable properties of heat transfer than water such as water has over 4 times higher specific heat ($c_{p,water}$ = 4.19 kJ/kg^{0}C and $c_{p,air}$ = 1,0 kJ/kg^{0}C) and water is 830 times more dense than air (density water and air at 15 ^{0}C is 999 kg/m^3 and 1,2 kg/m^3).

Selection process normally includes a number of factors as follow [38]:

1. Thermal and hydraulic requirement
2. Material compatibility
3. Operational maintenance
4. Environmental, health, and safety considerations and regulations
5. Availability
6. Cost

If two specified streams are introduced into an essentially completely defined heat exchanger, thermal performance and pressure drops can be calculated. The computational process is drawn schematically in figure below:

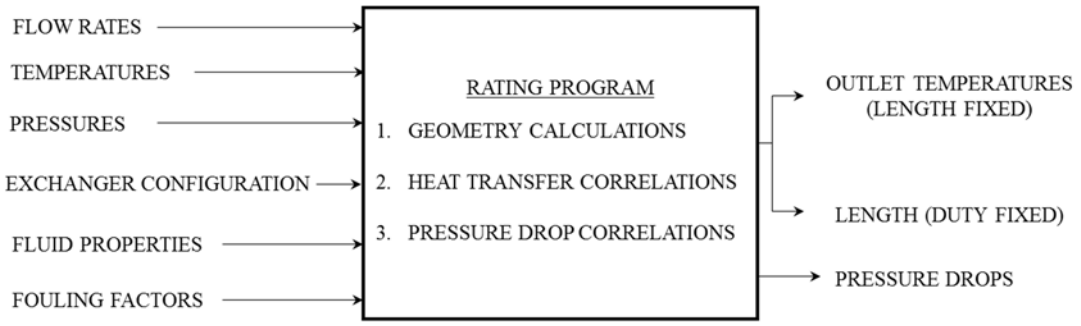

Figure 2.3: Rating program [50].

The rating program takes inlet data such as flow rates, temperatures, the fluid properties (including phase equilibrium data, if phase change is involved) and the heat exchanger parameters as input. The rating program calculates either the outlet temperatures and thermal duty (if the exchanger length is specified) or the required length of the heat exchanger to accomplish the thermal change. In either case, pressure drop of each stream is calculated. A common procedure for design of heat exchanger is showed in Figure 2.4. If the design does not meet the requirements, various modifications are made to until a suitable design is achieved.

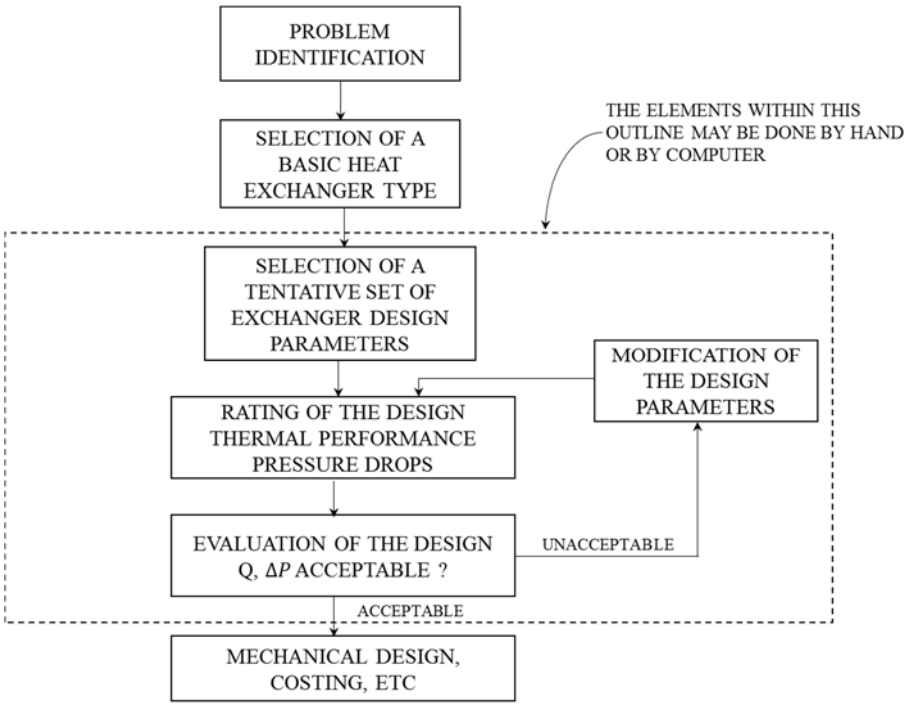

Figure 2.4: Logic Flow chart for heat exchanger design [38]

2.2.2. Turbine

Selection of the turbine is an important design decision to determine the performance of ORC system. The selection is based on the operating conditions and on the size of the system. The turbine can be categorized into two main types: the first is the velocity type, such as axial turbines and radial inflow turbine; the second is the volume type, such as scroll expanders, screw expanders, reciprocal piston expanders [51]. The small-scale ORC units are more appropriate to use the volume type because they are characterized by low flow rates, high pressure ratios, and much lower rotational speeds than velocity types. According to Vanslambrouck et al. [52] expanders are classified based on power range: micro system (0.5 - 10 kW_e), small system (10 - 100kW_e), medium system (100 – 300 kW_e) and large systems (300 kW_e - 3 MW_e).

Table 2.3: The comparison of various types of expanders used in ORC system [41, 53].

Type	Cost	Advantages	Disadvantages
Radial-inflow turbine	High	High efficiency, mature manufacturability, and light weight	High cost, low efficiency in off-design conditions, cannot bear two-phase
Axial turbine	Medium	High efficiency, mature manufacturability and multi axial stages	Expansion ratio on which can be handled efficiently is lower than radial-inflow turbine
Scroll expander	Low	High efficiency, simple manufacture, light weight, low rotate speed and high efficiency in off-design condition	Low capacity, lubrication, and requiring modification
Screw expander	Medium	Tolerable two-phase, low rotate speed and high efficiency in off-design condition	Lubrication requirement, difficult manufacture and seal
Reciprocating piston expander	Medium	High pressure ratio, mature manufacturability, adaptable in variable working condition and tolerable two-phases	Large friction losses, heavy weight, less reliability, and complex device
Rotary vane expander	Low	Tolerate two-phases, torque stable, simple structure, low cost and noise, high volumetric expansion ratios	Lubrication requirement and low capacity

Due to the critical selection of expander in application of ORC system. Quoilin et al. [54] had proposed selection guidance based on allowed power range for each application (low & high temperature waste heat recovery, low temperature solar plant, high temperature combined heat and power) and each type of expansion machine in Figure 2.5. The guidance helps designers easily choosing a suitable type of turbines according to the power range requirement of the systems.

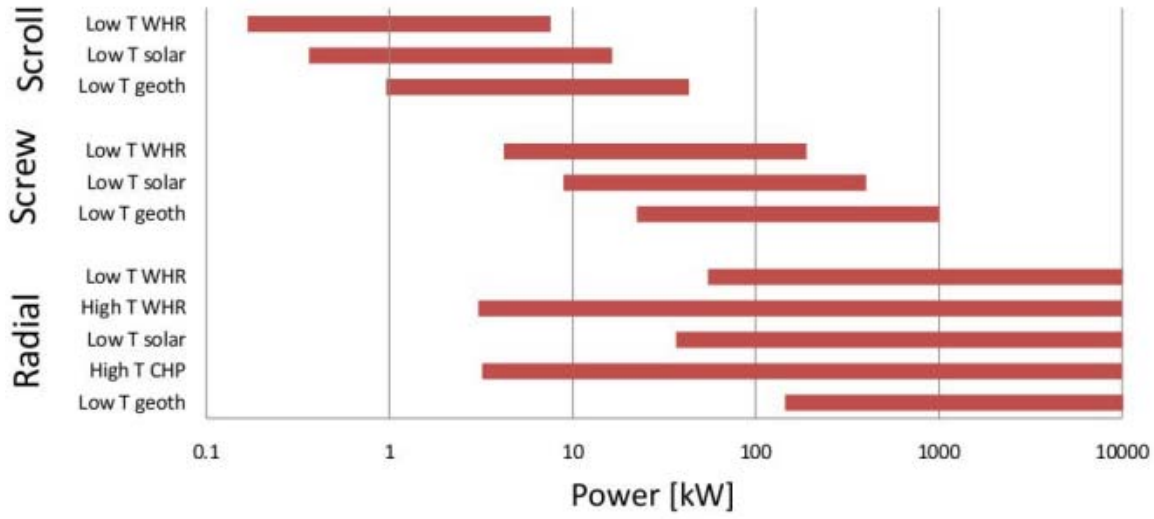

Figure 2.5: Guidance of expansion machine selection based on power range for each application and each type of machine.

Quoilin et al. [54] had also developed operating maps of the expansion machines for some common working fluids at different condensation and evaporation temperatures in three expansion machine categories: scroll, screw and radial (see Figure 2.6).

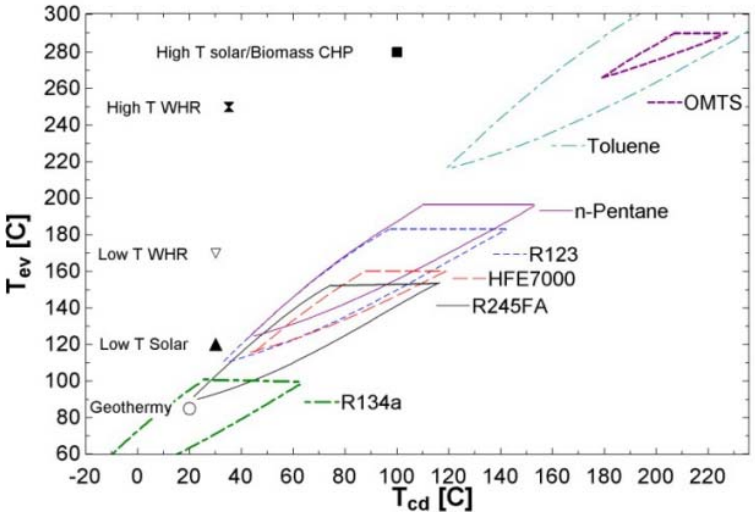
High T solar/Biomass CHP
High T WHR
Low T WHR
Low T Solar
Geothermy
OMTS
Toluene
n-Pentane
R123
HFE7000
R245FA
R134a
T_{ev} [C]
T_{cd} [C]

(a)

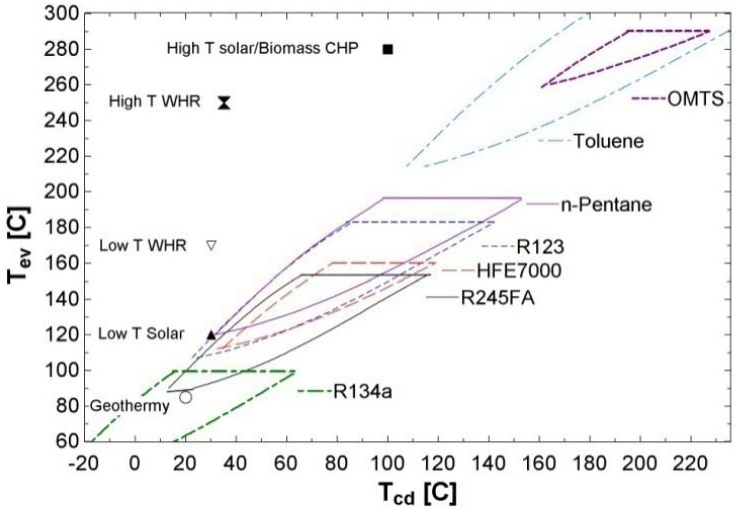
High T solar/Biomass CHP
High T WHR
Low T WHR
Low T Solar
Geothermy
OMTS
Toluene
n-Pentane
R123
HFE7000
R245FA
R134a
T_{ev} [C]
T_{cd} [C]

(b)

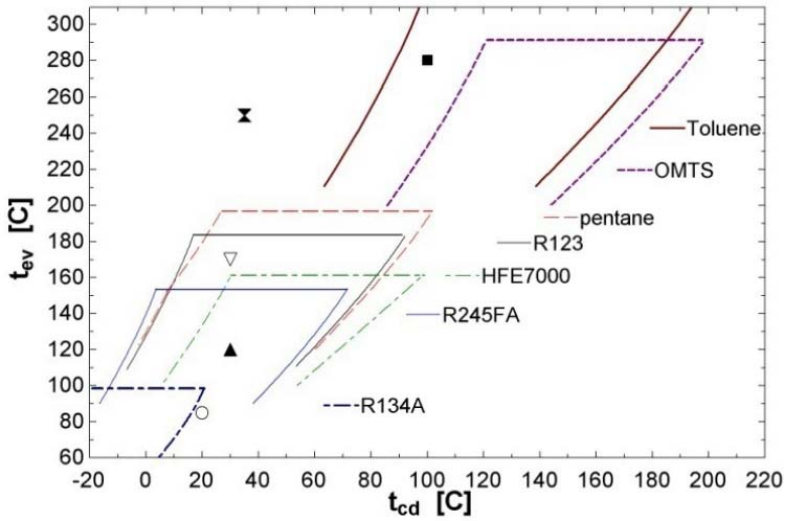

(c)

Figure 2.6: Mapping for scroll (a), screw turbine (b), radial turbine (c).

2.2.3. Pumps

The two main categories of pump according to its basic principle of operation are *dynamic pumps and displacement pumps. Dynamic pumps is* the pumps in which energy is continuously added to increase the fluid velocities within the machine to values greater than those occurring at the discharge, so subsequent velocity reduction within or beyond the pump produces a pressure increase. D*isplacement pumps* are the pumps in which energy is periodically added by application of force to one or more moveable boundaries of any desired number of enclosed, fluid-containing volumes, resulting in a direct increase in pressure up to the value required to move the fluid through values or ports into the discharge line.

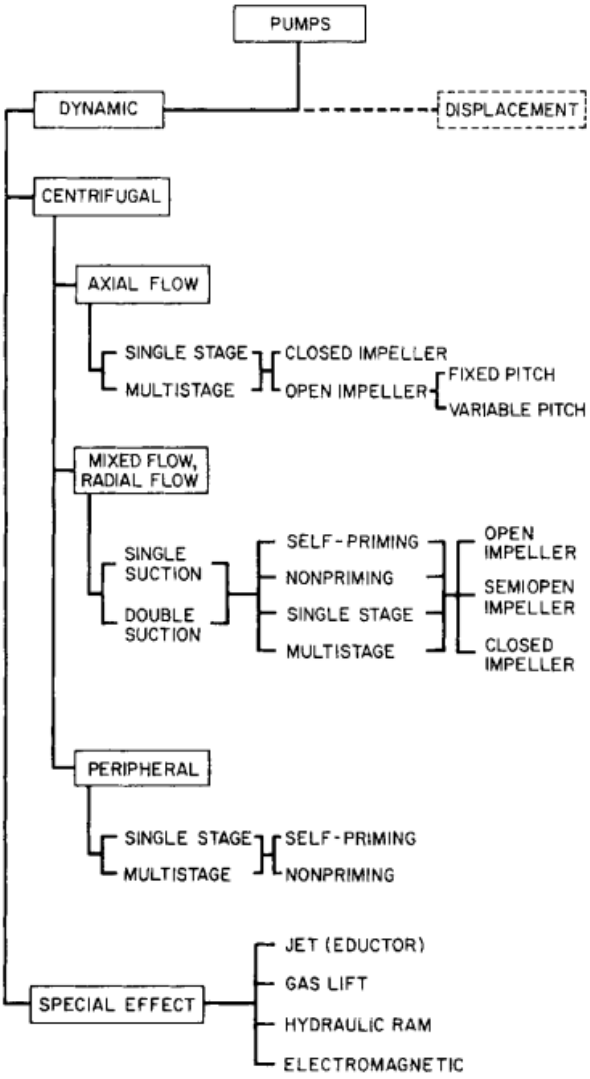

Figure 2.7: Classification of dynamic pump.

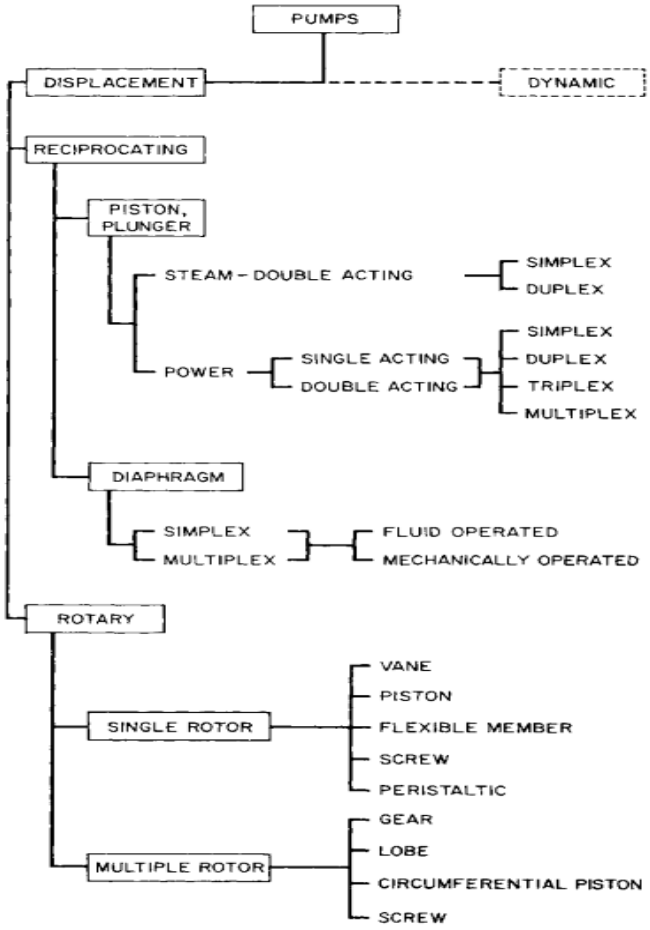

Figure 2.8: Classification of displacement pump.

Five steps in choosing any pump are as follow [55]:

(1) Sketch the pump and piping layout

Single-line diagram is usually satisfactory showing all piping, fittings, valves, equipment and other units in the system. It states the length of pipe runs on the sketch

(2) Determine capacity

The required capacity is calculated based on a given set of conditions. The calculation has to consider safety factor desired, any fluctuation changes that might occur, etc.

(3) Figure total head

ORC system has pipe closed loop, so that the static head is zero. Thus, the friction head = friction head inside pipe + friction heads in fittings + friction heads in the components.

(4) Study liquid conditions

Liquid specific gravity, temperature, vapour pressure, viscosity, chemical characteristics must be carefully considered. The ORC plants use a refrigerant type of various alternatives

(5) Choose class and type

Studying the layout tells what size (capacity and head) pump is needed. This furnishes the first clue as to what class of pump is suitable.

The centrifugal pumps are widely used for industrial applications [21] and a large scale ORC plant [43]. This type may be combined in parallel to deliver greater flow or in series to provide a greater head. A small scale ORC plant requires a much lower flow rate with the same pressure, therefore the plant usually uses the reciprocating pumps. They are used for small quantity with high pressure duties where their efficiency can excess that of a centrifugal pump. The centrifugal pumps have the following advantages compared to the reciprocating pumps [56]:

i) Higher speed resulting in lower size and cost
ii) Continuous delivery free from pressure fluctuations
iii) Absence of vibration and simpler foundation
iv) Applicable to direct drive in almost every case

The ratio of pump consumption to expander production (back work ratio) is higher for organic fluids than for water. Therefore, the low pump efficiency has a dramatic impact on the net power and the cycle efficiency in the ORC systems. The high isentropic efficiency is really required in the ORC systems [53].

2.3. Working Fluid Selection

The selection of working fluids is very important step in the design of ORC systems. Because the selected working fluid influences the efficiency of system, the sizes of the system components, the design of expansion machine, the system

stability, cost, safety and environmental issues. To select the most appropriate working fluid, Drescher et al. [57] and Quoilin et al. [7] proposed some general guidelines that should be taken into account:

a) Thermodynamic cycle performance should be as high as possible for given heat source and heat sink temperatures. The efficiency (η) and/or power output are used to indicate the performance, which depends on a number of interdependent thermodynamic properties of working fluid: critical point, acentric factor, specific heat, density, etc.
b) The density (ρ) of the working fluid should be high either in the liquid or vapour phase. High density leads to increment of mass flow rate and equipment size reduction [29].
c) The viscosity (μ) of the working fluid should be maintained low in both the liquid and vapour phases to result in high heat transfer coefficients and low friction losses in the heat exchangers.
d) The thermal conductivity (λ) must be high to obtain high heat transfer coefficients in the heat exchangers.
e) Higher evaporating pressure leads to higher investment cost and increased complexity.
f) Positive condensing gauge pressure: the condensing pressure should be higher than atmospheric pressure, so that it could avoid air infiltration into the cycle.
g) Stability of the fluid at high temperatures and compatibility with materials in contact.
h) The melting point temperature should be lower than the lowest ambient temperature to ensure that the working fluid remains in the liquid phase.
i) High safety level: the safety factors consist of two main parameters - toxicity and flammability. The ASHRAE standard 34 classifies refrigerants in safety groups and can be used for the evaluation of working fluids.
j) Low environmental level: the environmental factors involve two parameters - ozone depleting potential (ODP) and greenhouse warming potential (GWP).
k) Good availability and low cost of working fluids. The common commercial working fluids are easier to obtain with cheaper price.

Table 2.4: The properties for selecting the most appropriate working fluid.

Process performance	Thermodynamic	Environmental	Safety
Efficiency (η)	Density (ρ)	Ozone depletion potential (ODP)	Toxicity
Power output	Thermal conductivity (λ)	Global warming potential (GWP)	Flammability
	Viscosity (μ)		
	Evaporating pressure		
	Condensing pressure		
	Melting point temperature		

2.3.1. Working fluid categories

The most crucial characteristic of working fluids can be categorized according to the saturation vapour curve. There are three types of working fluids that are shown in vapour saturation curves in temperature-entropy (T-s) diagrams: a dry fluid with the positive slope of saturation curve, a wet fluid with the negative slope of saturation curve and an isentropic fluid with nearly infinitely large slopes [58]. The fluid characteristics influence the fluid capability, cycle efficiency, and equipment arrangement in a power plant system [59]. The examples of wet fluids are water and ammonia. A major problem with the wet fluids is the presence of liquid inside turbine that may damage turbine blades and reduce the isentropic efficiency. This occurs due to the negative slope of the saturation vapour curve for a wet fluid. Therefore, the fluid should be superheated at inlet of the turbine. The superheating apparatus is required impacting the more expensive cost of the evaporator. However, the isentropic and dry fluids do not need the superheating, therefore these fluids are ideal for ORC systems [28, 60] . In addition, Hung et al. [61] reported that isentropic fluids are most suitable for recovering low-temperature waste heat. However, the recent research results from Hung et al. [62] revealed that wet fluids with very steep saturated vapour curves in T-s diagram have a better overall performance in energy conversion efficiencies than dry and isentropic fluids. In other words, wet fluids are also expected to be the promising fluids for ORCs without superheat. Thus, the dry and isentropic

working fluids do not always match to ORC systems when other thermophysical properties are taken into consideration.

According to the structural point of view and type of atoms in fluid molecule, the ORC working fluids can be categorized into seven main classes: hydrocarbons, perfluorocarbons, siloxanes, partially flouro-substituted straight chain hydrocarbons, ethers and fluorinated ether, alcohols and inorganics [41].

Although a broad range of working fluids has been studied in the scientific literature, but only a few fluids are actually used in commercial ORC power plants and the fluids are shown in Table 2.5 [7].

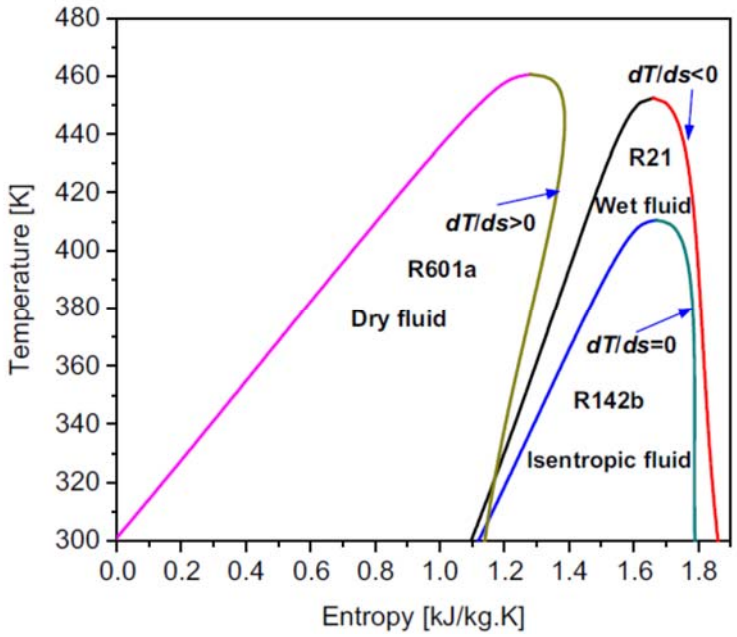

Figure 2.9: Three types of working fluid: dry, isentropic and wet.

Table 2.5: Common working fluids in the commercial ORC units.

	Working fluid	T_c (^{0}C)	Application
1	R134a	101.1	Geothermal power plants or in very low temperature waste heat recovery
2	R245fa	154.0	Waste heat recovery
3	Solkatherm (SES36)	177.5	Waste heat recovery
4	n-pentane	196.5	Waste heat recovery and medium temperature geothermal power plants
5	OMTS (MDM)	290.9	Biomass-CHP power plants
6	Toluene	318.6	Waste heat recovery

2.4. Modelling and simulating the ORC designs

2.4.1. The advantages of thermal simulation models

The numerical modelling is one of the most important elements in the design and optimization of the thermal system [16]. The modelling is expected to represent the behaviour of the actual system. Because experimentation on a test rig of the actual system is generally very expensive and time consuming, the design evaluations have to depend on simulation model to obtain the desired information on the system behaviour of the actual system. The advantages of utilizing simulation models through mathematical and numerical model are that the simulation models can be used to:

- Evaluate different designs to obtain an acceptable design
- Study system behaviour under off-design conditions
- Determine the effects of different design variables for optimization
- Improve or modify existing systems
- Investigate the sensitivity of the design to different variables

2.4.2. The design variables of the ORC designs

Many researchers in this area have reported modelling of steady state ORC systems. The majority of studies focuses on the selection of working fluids (WF) for design optimization especially for specific applications Hong et al., Hung et al., Kuo

et al. Liu et al., Pedro et al., Masheiti et al., Rayegan et al., Roy et al., Saleh et al., and Wang et al. [58, 60, 62-70]. These works discuss a comparison between a set of candidate working fluids in terms of thermodynamic performance and the ORC performances based on thermodynamic models of the cycle. Their results cannot summarise a single fluid that has been identified as optimal for the ORC system. This is because they used different assumptions and hypotheses to conduct the working fluid selections [19, 71]:

- The objective functions of the design optimization are different depending on the target application.
- Different operating conditions (for example the considered temperature ranges) deliver to the different selection results of the optimal fluids.
- Several researchers consider the environmental impact (ODP, GWP), the flammability, and the toxicity of the fluids.

In order to simplify the design problems, this thesis focuses investigations on the common fluids in the commercial ORC power plants. Three working fluids such as R134a, R245fa and n-pentane are selected based on their critical temperature and availability of the fluids in the local New Zealand market.

Another important aspect of the ORC modelling is type of the components (TC). This involves determining the right specifications of the main components for the requirements and constraints of the ORC systems. Two main consideration in selecting main components especially expansion machines are a size of the system and operating conditions [7]. The main components of the ORC system such as turbine, pump and heat exchangers may be selected in the basis of the temperatures in the ambient and heat resource to obtain an initial design. The best possible initial design is important to be employed so that it is either acceptable by itself or iteration

is generally necessary to obtain a satisfactory design. The choice of heat exchanger types guides selection of the heat transfer analysis methods and the equations of heat transfer coefficient in modelling of the heat exchanger design [72]. The selection of expansion machines leads to an accurate calculation of turbine performance as a preliminary turbine design. The turbine performance is very sensitive to the type of machines and the operating condition. The turbine performance especially the radial inflow turbine would be deviated significantly from the actual condition if the constant performance is assumed [73]. Several studies of the thermodynamic cycle optimization have been embedded into turbine modelling approaches, as the following:

- Semi-empirical model of the scroll is incorporated into the ORC model.
- The Stodola's ellipse approach is used to increase the accuracy of turbine performance calculation in the analysis of ORC off-design operation.
- The isentropic efficiency has been modelled as a function of specific speed, volumetric expansion ratio, and the size parameter.

Some other ORC researchers focus their works on type of the cycle configurations (CC). The type of thermodynamic cycle configurations impacts greatly the ORC performance [74]. The basic cycle based on simple Rankine concept can be improved to increase the potential heat recovery. The adoption of strategies such as heat recuperation, heat regeneration, two-pressure level, and supercritical cycles are possible methods. However, few of these methods are already implemented in commercial power plants, while other advanced methods are still under investigation. The exergy analysis of various binary plant types such as standard cycle, recuperative cycle, regenerative cycle and regenerative cycle with recuperator has been conducted by Yari et al. [75]. They concluded that the regenerative cycle with recuperator is a

promising option. Regenerative cycle has been studied and compared to other cycles based on thermodynamic and economic aspects in Meinel et al. [76]. The regenerative cycle has better thermodynamic (higher power output, better match of the temperature profiles) and economic (lower specific investment costs) performance than the standard and recuperative cycles, so that it is a promising alternative for ORC applications. Some researchers have also compared the subcritical and supercritical ORC performances. Both designs were investigated in the term of the comparison performance [77], heat exchanger design [78] and working fluid selection [79-81]. The supercritical process can lead to higher efficiency mainly for low critical temperature fluids for medium and high temperatures of the heat input [79, 82]. However, some disadvantages of the supercritical process have to be considered such as operation at high pressure (e.g. 60-160 bars for CO_2 supercritical cycle), safety concern and expensive investment cost due to special materials of the system. Moreover, Kosmadakis et al. [83] has conducted the experimental investigation of ORC under low-temperature of the heat resource under 100^0C. They concluded that supercritical operation was difficult to be achieved. The supercritical cycle is not discussed in this thesis because this focuses on low-temperature heat resources.

Modelling ORC system requires two categories of design parameters (DP): assumptions and decision parameters. The assumptions are the initial parameters required for creating a cycle of the ORC system. To simplify the model calculations, the efficiencies of pump and turbine are assumed at a constant value. The assumptions are as follow below:

- The isentropic efficiency of turbine is 85% [20, 23, 84-86]
- The mechanical efficiency of turbine is 98% [20]
- The isentropic efficiency of pump is 80% [20]

- Superheat is 5^0C [47, 87]
- Subcooling is 5^0C [47, 87]
- Pinch point is 5^0C [47, 87]

The decision parameters are the variables required to conduct parametric optimization of the ORC design. Four decision parameters are (1) cycle maximum pressure (P_{max}); (2) mass flow of the working fluid ($\dot{m}$); (3) degree of superheat (sh), measured from the specific entropy of the point on saturated vapour curve for subcritical cycles; (4) condensation pressure (P_c) [87]. The assumption of superheat can be changed for the optimization purpose. However, a higher superheated value gives penalties in terms of power and costs, although a few degrees of superheat is required to avoid liquid droplets at the inlet of the turbine although [87].

The sizing of main components (SC) can be carried out in the design optimization or evaluation. The physical size (length, width, height and surface on each side) of the heat exchangers in the ORC system is determined. Inputs to the sizing problem are the fluid inlet and outlet temperatures, flow rates, fouling factors and the pressure drop on each side [72]. The inputs of the sizing problem for heat exchangers are delivered from the ORC system optimization problem and the effects of the optimum component designs (pressure drop, pumping power) are iterated at the system level [6]. The size of main components influences the component costs. The purchased equipment cost in the preliminary design is estimated by considering the optimum results of power of the turbine and pump as well as the heat exchanger area [88].

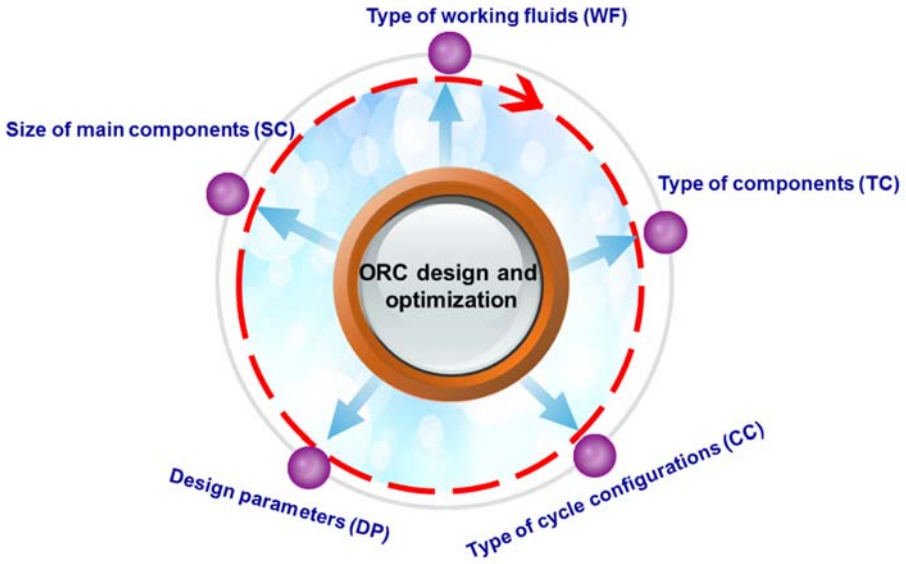

Figure 2.10: Five main design variables of the ORC design and optimization.

Few ORC researchers discussed optimization of the heat exchanger designs and cycle configurations. Most researchers focused on selection of working fluids that has been discussed in above paragraphs. Determining the right size and the best type of heat exchanger in the ORC plants would achieve the most economical design results because total cost of heat exchanger areas dominates greatly to the total plant cost in a low-temperature heat resource [23]. Although some researchers Calise et al., Madhawa et al. and Shenjun et al. [23, 77, 89] discussed optimization of the heat exchanger design, none of the studies discussed about the influence of the heat exchanger design on the ROI of plant investments considering the type and size. Moreover, Branchini et al. [74] mentioned that cycle configurations or designs directly impacts the ORC system performance. Currently, none of them discussed about one and two-stage ORC configurations with cycle enhancements of either recuperator or regenerator based on thermodynamics and economic analyses. Hence, the first contribution of this thesis is to fill this gap by investigating the heat exchanger designs considering the type and size and the type of cycle configurations

based on thermodynamic and economic analyses. Both heat exchanger designs and type of cycle configurations are a member of the main design variables that greatly influences design performance of the ORC plants. These are discusses in detail in Chapter 3 and 4. The investigation results are intended to be used as a useful reference for designing the ORC plant.

2.4.3. State of Art of ORC modelling

Table 2.6 shows the current state-of-art of modelling and simulating the ORC designs. The researchers who focused only on the selection of working fluid in their investigation are excluded in the Table 2.6. To compare the different papers, three characteristics are taken into account: design variables, target application and purpose of the work. According to this literature review, the main design variables of the ORC development include type of working fluid (WF), type of main components (TC), type of cycle configurations or designs (CC), design parameters (DP) and size of main components (SC). These design variables have to be used in design optimization because all parameters can greatly affect to the ORC performance. Some researchers have combined these variables in their investigation. However, none of the current researches considers all these main parameters in a design guideline of the ORC development. Hence, the second contribution of this thesis is to fill this gap by presenting new design methodologies. The design methodologies improves the current approach of the ORC methodology by considering all five main variables to achieve the most optimal design. Both new methodologies are presented in Chapter 5 and 6.

2.4.4. Off-design analysis

The off-design analysis is another important use of simulation models that has been explained in the above section. This analysis has to be considered in designing

the ORC system especially for the ORC system utilizing the geothermal resource. The systems operate in off-design conditions [20]. Some reasons that cause the deviation from design conditions are variation in energy input, differences in raw materials fed into the system, changes in the characteristics of the components with time, changes in environmental conditions, or shifts in energy load on the system [16]. The exploitation of geothermal resources involves the period where the thermodynamic properties of the resource decline under continued exploitation [9], so that the variation in energy input is the main factor affecting off-design operation of ORC binary plants. The thermodynamic properties of the resource degradation is also appeared in the data of 40 years of production of Wairakei geothermal reservoir, New Zealand [90]. This will be explained in more detail in Chapter 7.

Several authors have discussed the effect of part-load and system off-design conditions on the performance of the ORC geothermal power plants. Table 2.7 summarises the current research into off-design investigation. While the literature review reveals that the geothermal resource decreases over the whole life of the exploitation, none of the current research proposes a novel lifetime strategy to design the optimum binary geothermal power plant which takes into account a degradation of thermal input over the whole life of the plant. The strategy investigates and selects the most profitable design among design alternatives. The design alternatives are designed based on the points selected between the lowest and the highest values of the thermodynamic properties of the heat resource over the whole plant life. The analyses consider a decrease of thermal input to the plant. The decrease of the thermal input of the binary plant over the whole plant life is a more realistic to represent the operation of the plant. This work also discusses improvements of the plant performance to overcome the resource degradation. Table 2.8 summaries the current research on the

performance improvements of existing geothermal plants in the off-design operation. None of them discusses an adaptive component design of the plant to overcome the resource degradation over whole plant life. Hence, the third contribution of this thesis is to fill this gap by:

a. Presenting a novel lifetime strategy to mitigate the ORC performance reduction due to resource degradation over whole plant life.
b. Discussing adaptive component designs for improvement of plants to mitigate a performance reduction due to resource degradation.

These contributions are explained in detail in Chapter 7.

Table 2.6: Overview of previous studies in the ORC design and models based on design variables

Design variables	Application	Software	Method	Purpose	Reference
WF, CC, DP	n/a	Matlab	Heatsep	Proposing a method that takes into account several criteria at a time.	Toffolo et al. [87]
WF, DP, SC	Geoth.	Matlab	Thermodynamic and economic	Parameter optimization and performance comparison.	Shengjun et al. [77]
WF, DP, SC	Geoth.	n/a	Thermodynamic	Developing methodology for optimization.	Franco et al. [6]
DP	WHR	n/a	Thermodynamic	A new design method.	Chen et al. [35]
WF, DP, SC	WHR	Matlab	Natural selection with generic algorithm	A generally applicable methodology in marine applications.	Larsen et al. [91]
WF, CC, DP	Multiple	EES	Thermodynamic	Providing optimal design guidelines for a wide range of operating condition.	Maraver et al. [92]
CC, SC	Geoth.	EES	Thermodynamic and economic	Providing the method of the most effective use of the geothermal resource.	Coskun et al. [18]
CC	Geoth.	EES	Exergy	A comparative study of the geothermal concepts for high temperature resources.	Yari et al. [75]
CC	ORC	n/a	Thermodynamic	Presenting the energy and exergy evaluation of three different ORC configurations.	Safarian et al. [93]
WF, CC, DP, SC	Solar	EES	Thermodynamic	Designing a solar Rankine cycle.	Quoilin et al. [94]
WF, CC, DP, SC	WHR	Aspen Plus	Thermodynamic and economic	Providing thermodynamic and economic benefits of the regenerative pre-heating process.	Meinel et al. [76]
WF, DP, SC	Geoth.	Matlab	Thermodynamic	Presenting a cost-effective optimum design criterion for low temperature resources.	Madhawa et al. [23]
WF, CC, DP, SC	WHR	n/a	Thermodynamic and economic	Proposing a design methodology to optimize the ORC considering a wide range of design variables as well as practical aspects such as component limitation and costs.	Amicabile et al. [95]

WF,DP, TC, SC	WHR	Surface V 8.0 and Refprop Nist 7.0	Thermodynamic	Describing a methodology for the optimization of a bottoming cycle as a waste heat recovering system in vehicles.	Macian et al. [96]
WF, DP, SC	WHR	EES	Thermodynamic and economic	Investigating the technical and economic feasibility of converting waste heat from a stream of liquid kerosene.	Jung et al. [97]
WF, CC, DP	Biomass	EES	Thermodynamic and economic	Presenting a technical and economic feasibility assessment of a biomass cogeneration plant	Uris et al. [98]
WF,CC, DP, SC	Oil and gas sector	Aspen Hysys V7.1	Thermodynamic and economic	Performing thermodynamic and economic analyses to utilize the waste heat disposed from an existing Egyptian gas treatment plant.	Khatita et al. [99]
WF, DP	Geoth.	Matlab	A multi-objective particle swarm optimization	Developing a method for determining the optimum use of a superheater and/or recuperator in a binary geothermal power plant.	Clarke et al. [100]
WF, DP	WHR	n/a	Exergy analysis and optimization uses Penalty Function and Golden section Searching algorithm	Performing the exergy analysis of waste heat powered ORC unit and proposing an intuitive approach with simple expressions to calculate the OR performances.	Wang et al. [101]

Table 2.7: Overview of previous studies in off-design analysis of the ORC system

Reference	ORC Application	Purpose	Main varied parameters impacting to off-design	Consideration	Results
Calise et al. [89]	Solar	To evaluate the off-design performance of ORC plant	Mass flow rate of thermal oil, temperature of thermal oil	Varying thermal input of heat source	Mass flow rate is a key variable
Song et al. [102]	WHR	To simulate and consider the system performance under off-design conditions	Heat source inlet temperature,	The one-dimensional aerodynamic analysis model of turbine and the performance prediction model of heat exchanger	Inlet temperature of the heat source and the cooling water have a significant influence on the performance
Wang et al. [103]	Solar	To carry out the off-design performance of a solar powered ORC	The environmental temperature, thermal oil mass flow rates of vapor generator and compound parabolic collection (CPC)	A solar-powered ORC with CPC to collect the solar radiation and thermal storage unit to achieve the continuous operation of the overall system	The decrease of environmental temperature or the increase of mass flow rate of thermal oil of vapor and CPC could improve the performance
Carcasci et al. [104]	WHR	To illustrate the off-design results of an ORC by varying the temperature of the air condenser.	The ambient air temperature	The behavior of the condenser	The ORC is very sensitive to the variation of the ambient temperature
Gabbrielli et al. [20]	Geoth.	To select the optimal design point of the power plant	Mass flow rate and temperature of geothermal fluid and ambient temperature	A constant thermal input to the ORC system	The lowest temperature of the geothermal resource results the best option
Fu et al. [105]	n/a	To analyse the effect of the heat source flow rate on the heat transfer characteristics	Heat source flow rate	A heat source flow rate is varied by -39% to +78% from the designed rate	The operating pressure, the net power output and system thermal efficiency significantly increase with increasing the flow rate of heat source.
Savola et al. [106]	CHP	To analyze the part load behavior of the small-scale CHP plants	The district heating load and the temperature	Two and three line regression models were developed to increase the accuracy of the models	There is a nonlinear reduction of the net power at the partial district heat loads due to decreasing isentropic efficiency of the turbine

Wendt et al. [107]	Geoth.	To determine the plant design specifications and performance characteristics both design and off-design ambient and resource conditions	Ambient temperature, ambient pressure, temperature and flow rate of the resource	Resource and ambient conditions	Simulation results may be used to evaluate net power during a specified time period having defined ambient and resource conditions
Manente et al. [108]	Geoth.	To find the optimal control strategy	Ambient temperature and geofluid temperature	Operation of the plant in subcritical and supercritical	The ambient and geofluid temperatures greatly influences the power output. The optimal operation strategy is different for subcritical and supercritical cycles.
Walnum et al. [109]	n/a	To compare how an ORC and a transcritical CO_2 Rankine cycle responds to off-design operation	Air temperature and air mass flow rate	Superheating in the ORC operation	The CO_2 cycle seems to have a marginally better response without control of the process, and it is more robust and less in need of detailed control. However, the optimization of the CO_2 cycle is more complex than the R123 cycle

Table 2.8: Overview of previous studies in performance improvement of an existing geothermal power plant

Reference	Application	Considering factors in off-design operation	Improvement	Results
Sohel et al. [110]	Binary plant	Resource characteristic	Four adaptive designs of the hypothetical power plant are provided depending on the changes in resource characteristic.	The modification increases an initial investment cost, but the total benefit may be greater over the life span of the plant
Pambudi et al.[111]	Single flash plant	Resource characteristic	Single flash design is combined with a binary cycle	The combined cycle increases the power output by 17.16%
Pambudi et al. [112]	Single flash plant	Resource characteristic	Single flash design is changed into double flash design	The double flash design increases the power output by 19.97%
Mines et al. [113]	Air-cooled binary plant	Resource characteristic and ambient conditions	Some modification options are the evaporative pre-cooling of the air, the hybrid heat rejection system, and the use of variable frequency drives on the plant motors	All options give an increase of the power output in off-design conditions. The increase of output result depends on type of modifications and operational parameter assumptions
Kanoglu et al. [114]	Air-cooled binary plant	Ambient conditions	The temperature of cooling air is decreased by evaporative cooling and optimizing the maximum pressure in the cycle.	The evaporative cooling can increase the power output by up to 29%. The net power output of the plant can be increased by 2.8%
Wendt et al. [115]	Air-cooled binary plant	Resource characteristic and ambient conditions	Three concepts are evaluated the use of recuperation, the use of turbine reheat, and the non-consumptive use of enhance geothermal system (EGS) make-up water to supplement heat.	Recuperator increases power output by 7-8% and suitable for the plant with limit of geothermal outlet temperature, while the use of turbine reheat gives no performance advantage. The EGS make up water provides a small increase in the net power output.

2.5. Nomenclature

A	Heat transfer area of heat exchanger (m^2)
F	The correction factor of heat exchanger configuration
h	Specific enthalpy (kJ/kg)
$\dot{m}$	Mass flow rate (kg/s)
P	Pressure (bar)
P_{cr}	Critical pressure of a working fluid (bar)
Q	Heat transfer rate (kW)
s	Specific entropy (kJ/(kg^{0}C))
sh	Degree of superheating (^{0}C)
T_{cr}	Critical temperature of a working fluid (^{0}C)
T_o	The temperature of specific dead reference state (^{0}C)
U	Overall heat transfer coefficient (W/m^2 C)
W	Work (kW)
Wnet	The net power output (kW)
W_t	Net power of turbine (kW)
W_p	Net power of pump (kW)

Acronyms

CC	Type of cycle configurations or designs
CHP	Combined heat and power system
DP	Design parameters
EGS	Enhance geothermal system
Geoth.	Geothermal
ORC	Organic Rankine Cycle
SC	Size of main component
TC	Type of main components
WF	Type of working fluid
WHR	Waste heat recover

Greek symbols

η_e	The overall exergy efficiency (%)
ΔT_{lm}	The logarithmic mean temperature difference (^{0}C)

Subscripts

1,2,3,4	State points
c	Condenser
o	The dead reference state
in	Reservoir input state point
v	Evaporator
max	Maximum

Chapter 3 – The effect of Heat Exchanger Design on Return on Investment (ROI) of The Binary Geothermal Power Plant

The aim of this thesis is to develop an approach for a feasibility study for flexible design (FSFFD) for the ORC development, which includes thermodynamic, component, resource, and cost considerations. It has been identified that the heat exchanger cost is the most expensive cost of the plant investment; therefore this chapter discusses the effect of heat exchanger design on return on investment (ROI) of the real binary geothermal plant. The heat exchanger design includes type and size of the heat exchangers. The effect of adding a recuperator in the system on the ROI of the plant is also analysed. The Chena binary geothermal power plant is used as a case study for implementing the investigations. The real data from the Chena geothermal power plant is used to validate the models. Chapter 2 discussed the ORC technology and the procedure for selecting heat exchangers.

3.1. Introduction to basic ideas

The design of heat exchangers for the geothermal plants utilizing low-temperature geothermal resources deals to an expensive cost of heat exchangers. The costs contribute a major cost of the total plant cost [23]. The choice of heat exchanger type impacts the values of heat transfer coefficient. The required heat transfer area is inversely proportional to its heat transfer coefficients of heat exchanger [116]. As a result, the higher heat transfer coefficients give a cheaper cost of heat exchangers in the system. For example, Madhawa et al. [23] mentioned that plate heat exchangers have the higher heat transfer coefficients than shell and tube heat exchangers. As a result, the plate heat exchangers require a less heat transfer area than the area required

by the shell and tube heat exchangers with the same heat duty. Note that every type of heat exchanger has key limitation criteria that the design engineer needs to consider when making preliminary selection of heat exchanger such as pressure and temperature limits [42]. This is explained in detail in Table 2.2.

The heat transfer rate ($\dot{q}$) of the heat exchanger is equivalent to the size of heat exchanger (A). The equation 3.1 shows correlation between both parameters based on energy conservation equation for a heat exchanger with an arbitrary flow arrangement [72]:

$$\dot{q} \propto A \tag{3.1}$$

The various sizes of exchanger are analysed based on the given initial conditions (process-fluid flowrate, inlet temperature of utility fluid for cooling or heating and allowed temperature difference of process fluid and allowable maximum pressure drops) [38]. Afterward, an engineer is able to ultimately obtain a final design that will meet the required process conditions (outlet temperature, flow rate and pressure drop for the hot and cold fluids).

An additional recuperator in the binary plant can reduce heat exchanger surface area required for cooling system. The recuperator utilizes the remaining vapour at the turbine outlet to preheat the fluid before flowing to evaporator. This binary plant using an additional recuperator has been used by some manufacturers like Ormat in geothermal projects all over the world [117]. The additional recuperator in the plant cycle increases the thermal efficiency because less heat input from the geothermal fluid is needed to produce the same power output [118]. Therefore, the influence of an additional recuperator on the success of plant investment needs to be investigated.

3.2. The Chena geothermal power plant

The geothermal source is located in Chena in Alaska, USA approximately 96.6 kilometres east-northeast of Fairbanks, at an elevation of 367 meters. The plant was designed using the basic ORC system consisting of an expander, condenser, pump and vaporizer. The plant uses a water-cooled condenser. The process diagram is the same process flow as in Figure 2.1. The plant has been run at the following operating conditions [119]:

- Water design points:

  Heat source:

Inlet temperature:	73.33 ^{0}C
Outlet temperature:	54.44 ^{0}C
Mass flow rate:	12.17 kg/s

  Heat sink:

Inlet temperature:	4.44 ^{0}C
Outlet temperature:	10 ^{0}C
Mass flow rate:	101.68 kg/s

- Refrigerant design points:

Mass flow rate:	12.16 kg/s
Evaporator/turbine inlet pressure:	16 bar
Condenser/turbine exit pressure:	4.38 bar
Turbine gross power:	250 kW
Pump power:	40 kW
Net power output:	210 kW
Vaporizer heat transfer rate:	2580 kW
Condenser heat transfer rate:	2360 kW

The working fluid used in the real plant is R134a. Figure 3.1 shows a representation of thermodynamic cycle of the system under investigation in the pressure-enthalpy diagram.

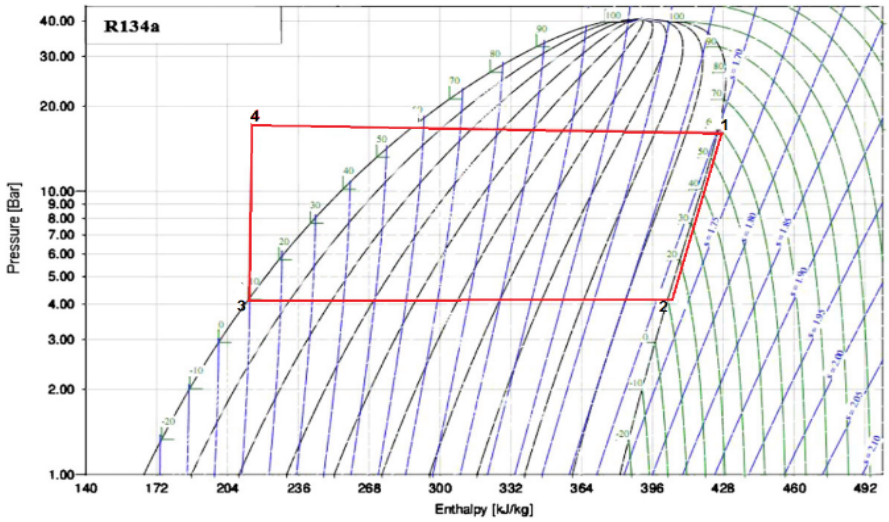

Figure 3.1: Pressure–enthalpy diagram of thermodynamic cycle (R134A).

3.3. Modelling using Aspen

The simulation models of the geothermal ORC power plant have been developed by an integration between Aspen plus process modelling and Aspen Exchanger Design and Rating (EDR). The Aspen Plus is used to simulate overall system while the detail models of heat exchangers use Aspen EDR. The models are used to calculate the plant performance and heat exchanger costs.

3.3.1. Primary Equations

The models apply mass and energy balances to each of the four ORC cycle components and use the primary equations of energy balance and isentropic/transfer efficiency listed in the Table 2.1. The heat exchanger calculations are based on the Log-mean temperature difference (LMTD) method. The pump and expander are modelled from a thermodynamic point of view. They are considered adiabatic and their isentropic efficiencies are calculated using isentropic efficiency equations in Table 2.1. It is assumed that isentropic efficiencies of the pump and expander remain constant at the values found in Table 3.1.

Here a correction factor (F) for multiple tube-side and/or shell side passes, derived through the work of Nagle (1933) and Underwood (1934), can be calculated as [120]:

$$F = \frac{\sqrt{R^2+1}\,ln[(1-S)/(1-RS)]}{(R-1)Ln\frac{2-S\left(R+1-\sqrt{R^2+1}\right)}{2-S\left(R+1+\sqrt{R^2+1}\right)}} \tag{3.2}$$

where

$$R = \frac{T_{in}^{hot}-T_{out}^{hot}}{T_{out}^{cold}-T_{in}^{cold}} \tag{3.3}$$

$$S = \frac{T_{out}^{cold}-T_{in}^{cold}}{T_{in}^{hot}-T_{in}^{cold}} \tag{3.4}$$

ΔT_{lm} can be calculated as

$$\Delta T_{lm} = \frac{\Delta T_1-\Delta T_2}{Ln\left({}^{\Delta T_1}/_{\Delta T_2}\right)} \tag{3.5}$$

The ROI is calculated from Equation 2.4 where the annual net profit is calculated based on the net electrical power output calculated by Aspen plus. The total capital cost of plant is assumed from heat exchanger costs. Aspen EDR generates calculation costs of the heat exchangers once all the geometry of each component part of the heat exchanger has been calculated. The cost is calculated according to the three elements of the exchanger cost: the material cost, the labour cost and the mark-ups on material and labour. The default cost database from the Aspen EDR version 8.4 has been used in the analysis [25]. The thermal efficiency of the ORC is calculated based on Equation 2.1. The net electrical power output is calculated as follow below:

$$Wnet = W_T - W_p \tag{3.6}$$

where W_T and W_p are the work of turbine and pump, respectively.

3.3.2. Property Methods

The accuracy of the model results depends strongly on a suitable prediction of the working fluid's thermodynamic properties. The cubic Peng-Robinson equation of state (EOS) has been adopted to calculate the thermodynamic and thermophysical characteristics of R134 working fluid and geothermal brine. This thermodynamic properties model is recommended for hydrocarbons by Aspen [25]. The geothermal brine has been assumed equal to thermodynamic and thermophysical characteristic of pure water. The validity of this EOS for simulation has been confirmed by comparing the data obtained from software with those available from the website of NIST [121]. For every case that has been compared, the errors concerning the most important thermodynamic and thermophysical data between the simulated and the actual data resulted lower than 2%.

3.4. Results and Discussion

3.4.1. Model validation

The simulation results were validated with the real operational data from Chena Geothermal power plant that has been discussed in Section 3.2. Table 3.1 shows that the comparison between both data is very good with a maximum deviation of 3.56%. Thus, this model can be used to represent the real plant. In addition, Figure. 3.2 shows the model of the plant at the nominal design points.

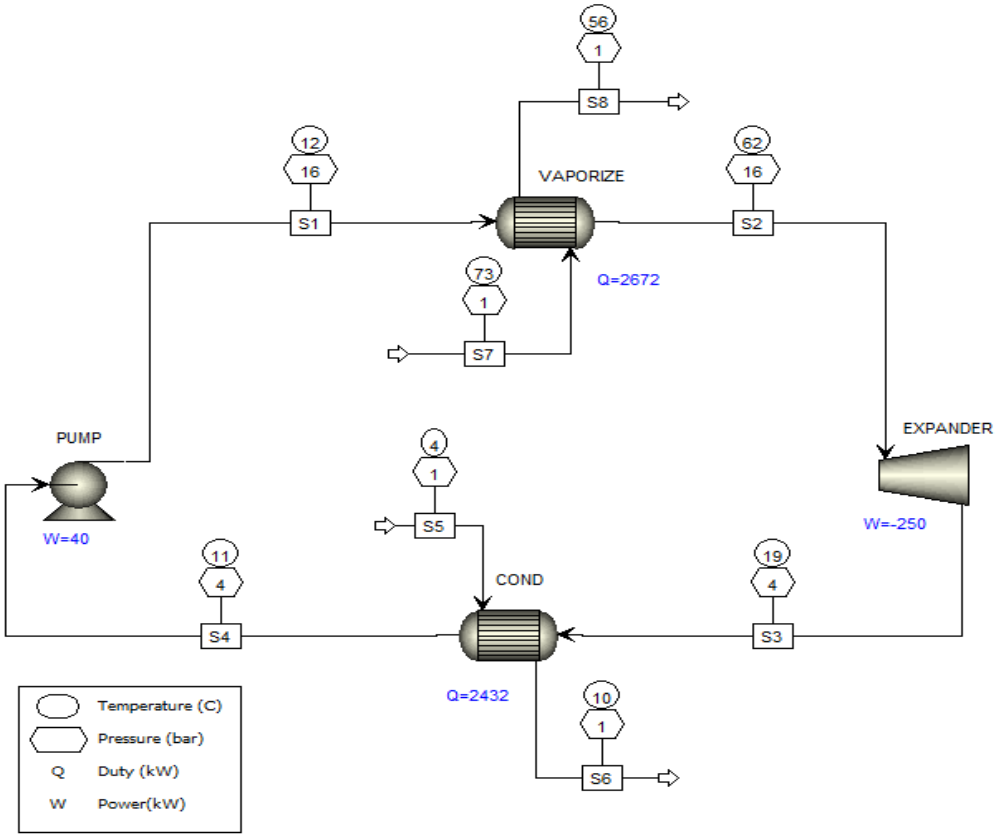

Figure 3.2: Aspen model of the Chena Power Plant at the real plant design condition.

Table 3.1: Validation of the numerical model with real plant design data.

Parameters	Real power plant data	Simulation Result	% Relative error (| ΔX | *100)/X
Geothermal fluid masss flowrate [kg/s]	33.39	33.39 [a]	0.00
Geothermal fluid temperature [^{0}C]	73.33	73.33 [a]	0.00
Cooling water mass flowrate [kg/s]	101.68	101.68 [a]	0.00
Cooling water source temperature [^{0}C]	4.44	4.44 [a]	0.00
Working fluid type	R 134	R 134 [a]	0.00
Expander effciency	0.80	0.8 [a]	0.00
Expander mechanical efficiency	-	0.958 [b]	0.00
Expander inlet pressure [bar]	16.00	16.00 [a]	0.06
Expander outlet pressure [bar]	4.39	4.39 [a]	0.00
Gross power output [kW]	250.00	250 [b]	0.00
Pump Power [kW]	40.00	40.00 [b]	0.00
Pump efficiency	-	0.56 [b]	0.00
Driver efficiency	-	0.51 [b]	0.00
Geothermal exit temperature [^{0}C]	54.44	55.70 [b]	0.48
Cooling water exit temperature [^{0}C]	10.00	9.70 [b]	3.00
Working fluid mass flowrate [kg/s]	12.17	12.17 [a]	0.00
Net plant power [kW]	210.00	210.00 [b]	0.00
Thermal efficiency	0.08	0.08 [b]	0.00
Vaporizer heat transfer rate [kW]	2580.00	2680.00 [b]	3.56
Condenser heat transfer rate [kW]	2360.00	2432.00 [b]	3.05

[a] Set variables
[b] Calculated variables from the Aspen simulation

3.4.2. Design analysis of the Chena geothermal ORC power plant using the validated models

This study analyses the influence of heat exchanger design to ROI of plant investment. In order to conduct this case study so that it will represent a real plant condition, some assumptions used in simulation analyses are:

- The turbine and pump are simulated with fixed values of mass flow rate, working pressures and efficiency according to the real plant design data in Table 3.1 in order to avoid failure in the real operation.
- The heat duty for each type of the heat exchanger is equal to heat duty from the real plant design data.

- The sizing heat exchanger analysis includes three limitation parameters of the plant operation:
    a. Chena geothermal plant, like most other geothermal power plants, makes use of re-injection of the used geothermal fluid into the re-injection wells in order to improve the pressure on the production wells. Table 3.1 displays that the geothermal exit temperature from real plant data and the simulation model is 54.44 ^{0}C and 55.70 ^{0}C, respectively. The temperature has to be maintained in order to avoid salt precipitation and the cooling of the geothermal fluid. Based on this argument, the maximum reduction of exit temperature of the geothermal fluid is assumed around 1^{0}C in order to obtain more heat into the system with a larger size of the heat exchangers.
    b. Minimization of heat exchanger size has to consider the moist condition. Moisture inside the expander can cause severe mechanical damage to the rotor and stator, that have been designed for dry steam [20].
    c. The sizing of heat exchanger has to avoid temperature crossovers of hot and cold streams through the exchanger unit during heat transfer process (the basic principle of the pinch point).

3.4.3. Effect of the type and the size of heat exchanger design on ROI

In this study, the evaluation of investment is analysed by ROI method where this profitability measure is defined in Equation 2.4. The annual net profit is calculated with data given in Table 3.2. The total capital investment is counted according to the total cost of heat exchangers and it neglects the cost of the pump and turbine because their costs are set to be fixed.

Table 3.2: Data for calculating annual net profit.

DATA	VALUE
Price of electricity in Alaska 2007 **[122]**	USD 0.13/kWh
Capacity factor of the plant **[123]**	0.9
Operating hour per year	8760 hours
Cost of production [119]	USD 0.05 / kWh
Cost of maintenance [119]	USD 0.01 / kWh

3.4.3.1 Effect of the type of heat exchanger design on ROI

The costs of heat exchangers dominate the total cost of ORC plants especially in plants driven by a low temperature geothermal resource. The brine of geothermal resources has known fouling and unique characteristics that influence the plant design. Holdmann et al. [119] reported that Chena water analysis results show both geothermal water quality and the surface water are soft and have low ammonium, so all possible types of heat exchanger may be selected as long as they meet the thermal and hydraulic requirements. The plant base case of analyses used shell and tube (S&T) type because the type is installed in the real plant for the vaporizer and condenser [119].

Figure 3.3: Heat exchanger cost and ROI of six different plants.

Figure 3.3 shows the comparison of heat exchanger cost and ROI in six plants with different types of heat exchangers in the vaporizers and condensers. The ROI of plant base case is 0.737. The usage of plate (PL) type increases the ROI and reaches a maximum ROI at 1.107 when PL type is used in both vaporizer and condenser. However, the air cooled condenser (ACC) type decreases the ROI significantly, since the price is 4 – 6 times that of S&T and PL type and it needs an additional load of electricity in order to operate air condenser fans. The ROI reaches the lowest value of 0.234 when the system is designed to use S&T vaporizer and ACC. The main characteristics of the different types of vaporizer and condenser are given in Table 3.3. The values of heat duty in each type of heat exchangers are not be exactly the same value as the heat duty of real plant design for the vaporizer and condenser, because the calculation of heat duty takes into consideration of the heat exchanger geometry of different types. However, the plant models must produce the same net power output of the plant design at 210 kW. Comparison of the required heat transfer area between PL and S&T types shows the PL type needs larger area than S&T type, but the price of PL type is cheaper than S&T, so it means that price per unit area of PL type is lower than S&T type.

In addition, ACC type requires the largest area of condenser options. This is because air has significantly less favourable properties of heat transfer than water such as water has over 4 times higher specific heat ($c_{p,water}$ = 4.19 kJ/kg^{0}C and $c_{p,air}$ = 1,0 kJ/kg^{0}C) and water is 830 times more dense than air (density water and air at 15 ^{0}C is 999kg/m^3 and 1,2 kg/m^3)

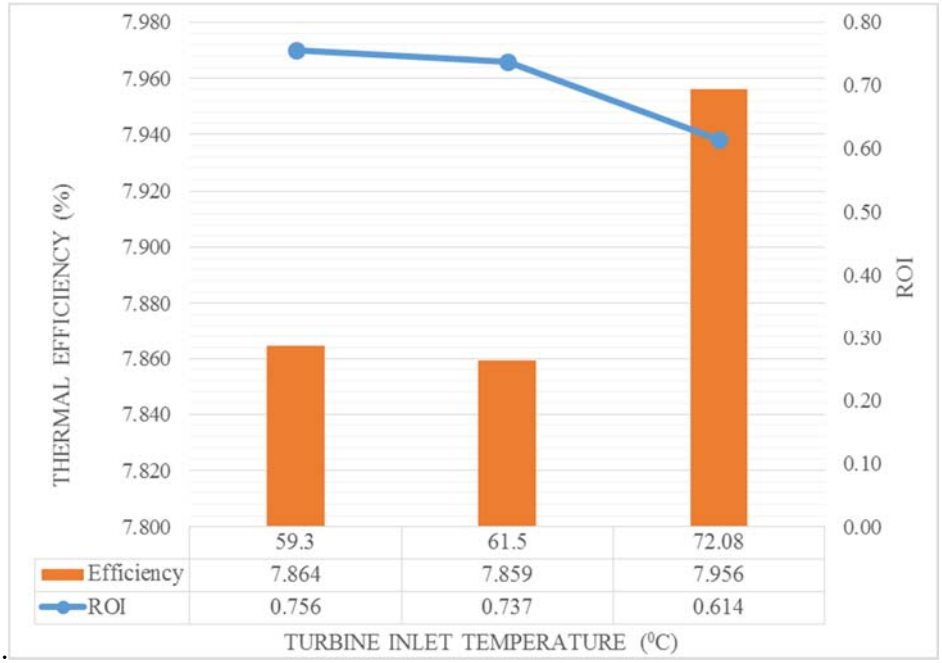

Figure 3.4: Thermal efficiency and ROI of possible size of heat exchangers in the plant

Table 3.3 shows that heat transfer coefficient of air is 1018 W/m^{2}K which is significantly lower than the heat transfer coefficient of water in S&T and PL type at 5135 W/m^{2}K and 2098 W/m^{2}K, respectively. The poor heat transfer of air necessitates a significantly higher surface area for heat transfer, so the equipment is very expensive. However, in case no cooling water is available on the site, ACC must to be selected. In addition, the fans of ACC consume a lot of electricity that causes a reduction of the net power plant output.

For a special case where the ambient temperature is usually subzero during several months in the winter causing a freeze, like in Chena, ACC type is the solution of the operational problem. The Chena geothermal power plant experienced a failure of the operation due to a frozen cold water supply during the late winter and early spring months, because the temperature dropped to -10 ^{0}C and hampered the operations of the plant [119]. The ACC becomes a good solution during the winter in

order to maintain a sustainable plant operation. Seasonal temperature variation is not taken in consideration of the analysis

Table 3.3: The main characteristic of vaporizer and condenser.

Vaporizer Parameters	Heat Exchanger Type	
	S&T	PL
Cold side temperature (in/out) (^{0}C)	12.46 / 62.77	10.63 / 62.87
Hot side temperature (in/out) (^{0}C)	73.33 / 55.65	73.33 / 55.84
Cold/hot side pressure drop (bar)	0.087 / 0.047	0.00247 / 0.00463
Cold/hot side heat transfer coefficient (mean) (W/m^{2}K)	1695 / 2934	857.5 / 1853.6
Overall coefficient (W/m^{2}K)	1023	569.6
Heat duty [124]	2680	2710.5
Required exchanger area (m^2)	278.7	503

Condenser Parameters	Heat Exchanger Type		
	S&T	PL	ACC
Cold side temperature (in/out) (^{0}C)	4.44 / 9.71	4.44 / 9.77	4.44 / 10.64
Hot side temperature (in/out) (^{0}C)	19.52 / 11.31	19.38 / 9.49	20 / 8.1
Cold/hot side pressure drop (bar)	0.173 / 0.0553	0.031 / 0.0061	0.00192 / 0.07429
Cold/hot side heat transfer coefficient (mean) (W/m^{2}K)	5135 / 2071	2098 / 1227	1018 / 2240
Overall coefficient (W/m^{2}K)	1382	761.6	686.2
Heat duty [124]	2436	2465	2500
Required exchanger area (m^2)	429	761.6	26623.2

3.4.3.2. Effect the size of heat exchanger design on ROI

The sizing analysis is conducted to evaluate the size of the current heat exchangers (the plant base case) in comparison to possible minimum and maximum sizes of the heat exchanger design for the Chena plant. Because the real heat exchangers have been optimized, the variable used in this analysis is only the degree of superheating. Other decision variables of the ORC optimization (cycle maximum pressure (P_{max}), mass flow of the working fluid (m_{WF}), and condensation pressure (P_{cond}) are set to be fixed. The detail explanation of the parametric optimization is discussed in the Chapter 5. Figure 3.4 shows the thermal efficiency and the ROI of the

minimum and maximum sizes of the heat exchanger design compared to the plant base case. The minimum size of the heat exchangers with the inlet turbine temperature at 59.3^{0}C increases the ROI of the plant base case at 2.59% from 0.737 to 0.756, but reduces the net power output from 210 kW to 203.9 kW with an almost constant level of thermal efficiency around 7.8%. However, a maximum size of heat exchangers reduces the ROI dramatically by 17% (from 0.737 to 0.614). The net power output increases from 210 kW to 220.3 kW while increasing the thermal efficiency about 1.2% from 7.859% to 7.956%. The maximum size of the heat exchanger design is limited by the geothermal exit temperature. The temperature reduces from 55.7^{0}C to 54.7^{0}C which is still within the limited range of the geothermal outlet temperature that has been explained in section 3.4.2. The minimum size of heat exchanger design is limited by a few degrees of superheat at 1.9^{0}C that is required to avoid liquid droplets at the inlet of the turbine. The superheat of the heat exchanger design for the plant base case is 5^{0}C, which is the same superheat as used by the most ORC researchers [125]. The maximum size of heat exchanger designs uses the superheat at 15.3^{0}C.

3.4.4. Effect of recuperator on ROI

A proposed investment of a recuperator must be evaluated for its economic feasibility. The system with a high remaining energy after expansion of the expander is more reasonable to be analysed. The maximum size of the heat exchanger design that has been discussed in section 3.4.3.2 is used to analyse the effect of recuperator on ROI. The plant has the turbine inlet temperature at 72.08^{0}C shown in Figure 3.4, therefore it has a higher heat for preheating the fluid after the pump. The simulation results indicate that installing recuperator increases the net power output from 220.3 kW to 221.3 kW with an incrementally higher thermal efficiency from 7.956% to

8.417%. However, the ROI reduces significantly from 0.614 to 0.409. Although a recuperator has used PL type which is more cost-effective than S&T type.

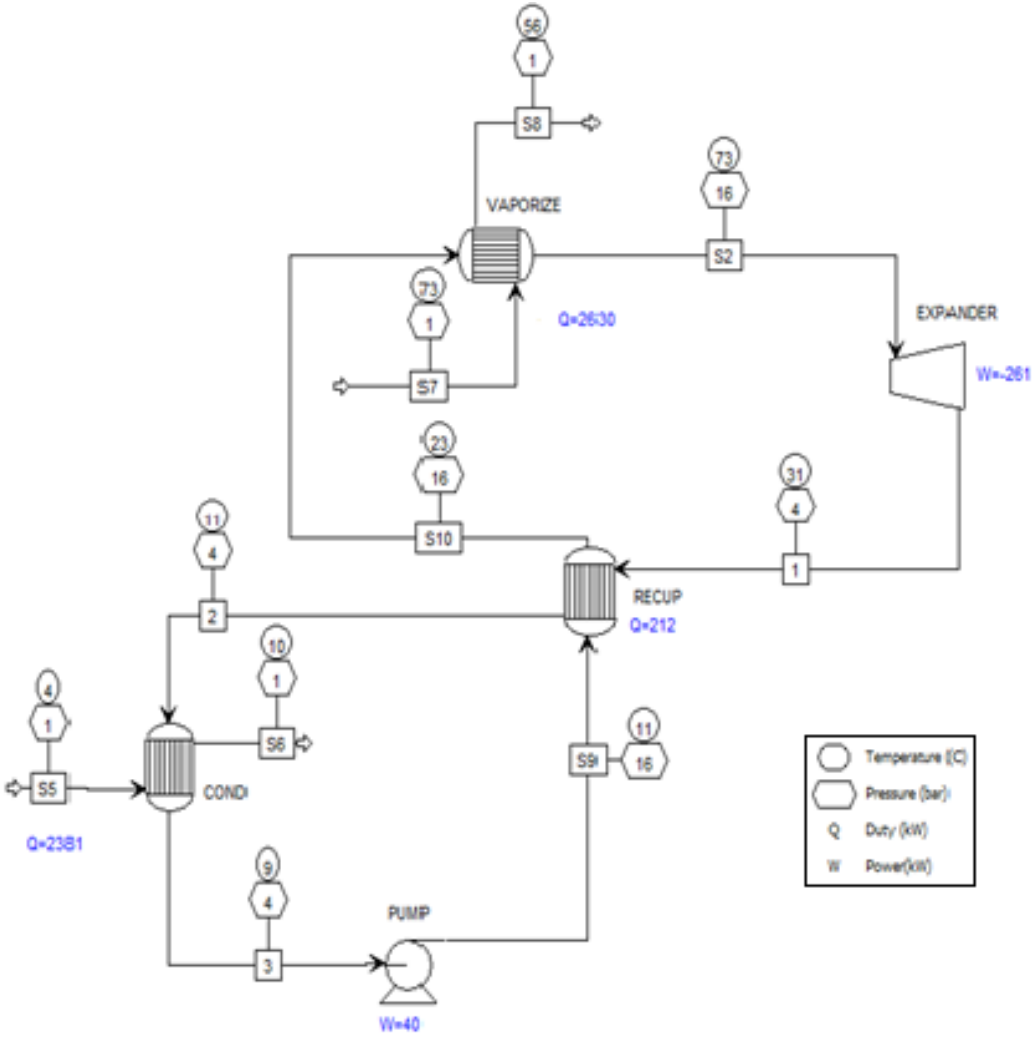

Figure 3.5: Process flow of the plant using a recuperator.

3.5. Conclusion

The effect of heat exchanger design on ROI has been examined by the simulation models. The simulation models have been validated with the real plant design data from the Chena geothermal power generation plant. The simulation results show that the selection of heat exchanger type significantly influences on the ROI of the plant. The model indicates that the ROI of the Chena geothermal power plant is able to be increased from 0.737 to 1.107 by changing from S&T type to PL type for both heat exchangers.

Based on the sizing analysis of the heat exchanger design, the current sizes of the heat exchanger design have given an optimal ROI of the plant at 0.737 with the net power output of 210 kW. The minimum size of the heat exchanger design can increase the ROI of the plant base case at 2.59%, but reduces the net power output from 210 kW to 203.9 kW. However, this option has a higher risk of wet fluid inside the expander due to less superheat to buffer fluctuation in the real operation, which is not feasible and causes severe mechanical damages to the rotor and stator of the turbine. The maximum size of the heat exchanger design has a 17% lower ROI at 0.614. Although an additional recuperator in the maximum design of heat exchanger size increases a net power output and thermal efficiency, but the plant ROI reduces significantly. As a result, the design without a recuperator is preferable.

3.6. Nomenclature

ACC Air Cooled Condenser
EDR Exchanger Design & Rating
EOS Equation of state
F Correction factor
LMTD Log-mean temperature difference method
N_p The annual net profit (USD)
ORC Organic Rankine cycle
PL Plate heat exchanger
Q Heat transfer rate (kW)
ROI Return on investment expressed as a fraction per year
S&T Shell and tube heat exchanger
T The total capital investment (USD)
Temp Temperature (^{0}C)
W Work (kW)
ΔT The temperature difference at an end of the exchanger

Greek symbols
η Efficiency (-)

Subscripts
1,2,3,4 State points
In Input
Out Output

Chapter 4 - Feasibility Study of a Binary Geothermal Power Plant Design using Thermodynamic and Economic Analyses

The aim of this thesis is to develop an approach for a feasibility study for flexible design (FSFFD) for the ORC development, which includes thermodynamic, component, resource, and cost considerations. This chapter presents the feasibility study for designing a binary geothermal power plant that utilizes a potential geothermal resource based on thermodynamic and economic methods. The main objective of this chapter is to perform comparative thermodynamic and economic analyses of the different binary geothermal power plant configurations. A realistic constant pressure ratio and an absolute pressure level consistent with known turbines were used to improve the accuracy of the turbine models, which is one of the contributions of this thesis. Thus, this chapter investigates the influence of cycle configuration types on design optimization and selection. Chapter 3 investigated another of the main design variables, which is the heat exchanger design. The simulation models for the analyses were developed using Aspen plus. A case study is presented, in which a binary geothermal power plant is designed using the real potential geothermal well located in Taupo Volcanic Zone (TVZ), New Zealand.

4.1. Introduction

The feasibility study is a process during which the plant design's viability is tested. The results obtained from this study strongly influence to determine if the design is feasible to be further investigated for the project investment. Designing a binary geothermal power plant involves five design variables that may be varied in the system in order to satisfy an objective function and the given requirements. The feasibility study should only focus on the main design variables to avoid the complexity of design analyses. This chapter aims to analyses different plant configurations on the plant performance using thermodynamic and economic analyses. It presents a thermo-economic approach to cycle and component designs and co-optimization for the plant performance and costs. The configurations consist of one and two-stage designs with cycle enhancements of either recuperator or regenerator.

In order to improve the accuracy of the turbine models, a constant pressure ratio and an absolute pressure level consistent with known turbines were used for every design configuration and every working fluid. According to Moustapha et al. [126], the pressure ratio, actual inlet and exit pressures expected must be matched to accurate the turbine models. When the turbine runs at off-design absolute pressure, there will be a difference in Reynold numbers that might impact on its performance to varying degrees, depending on the type and design of the turbine. Most of the investigations reported in the literature do not consider realistic absolute pressure levels as a constraint when calculating the turbine performance during the thermodynamic analysis.

4.2. Type of cycle configurations and potential heat resource

Figure 4.1 gives the basic ORC plant schematic diagram and TS diagram for 1-stage turbines, and Figure 4.2 gives the different cycle configurations for 2-stage ORC plants.

A case study was implemented for the feasibility study using an actual geothermal well and the cooling water data from a location in the Taupo Volcanic Zone (TVZ) in New Zealand, as shown in Table 4.1. The geothermal outlet temperature is constrained to be > 45°C to avoid silica precipitation in the reinjection wells (note that the temperature is valid for the specific site and may be different for other geographic boundary conditions).

Table 4.1: Geothermal and cooling water source data.

Parameter	Nominal Value
Geothermal source temperature (^{0}C)	173
Geothermal source pressure (bar)	9
Geothermal mass flow (kg/s)	8
Cooling water source temperature (^{0}C)	20
Cooling water source pressure (bar)	1.53
Cooling water source mass flow (kg/s)	90

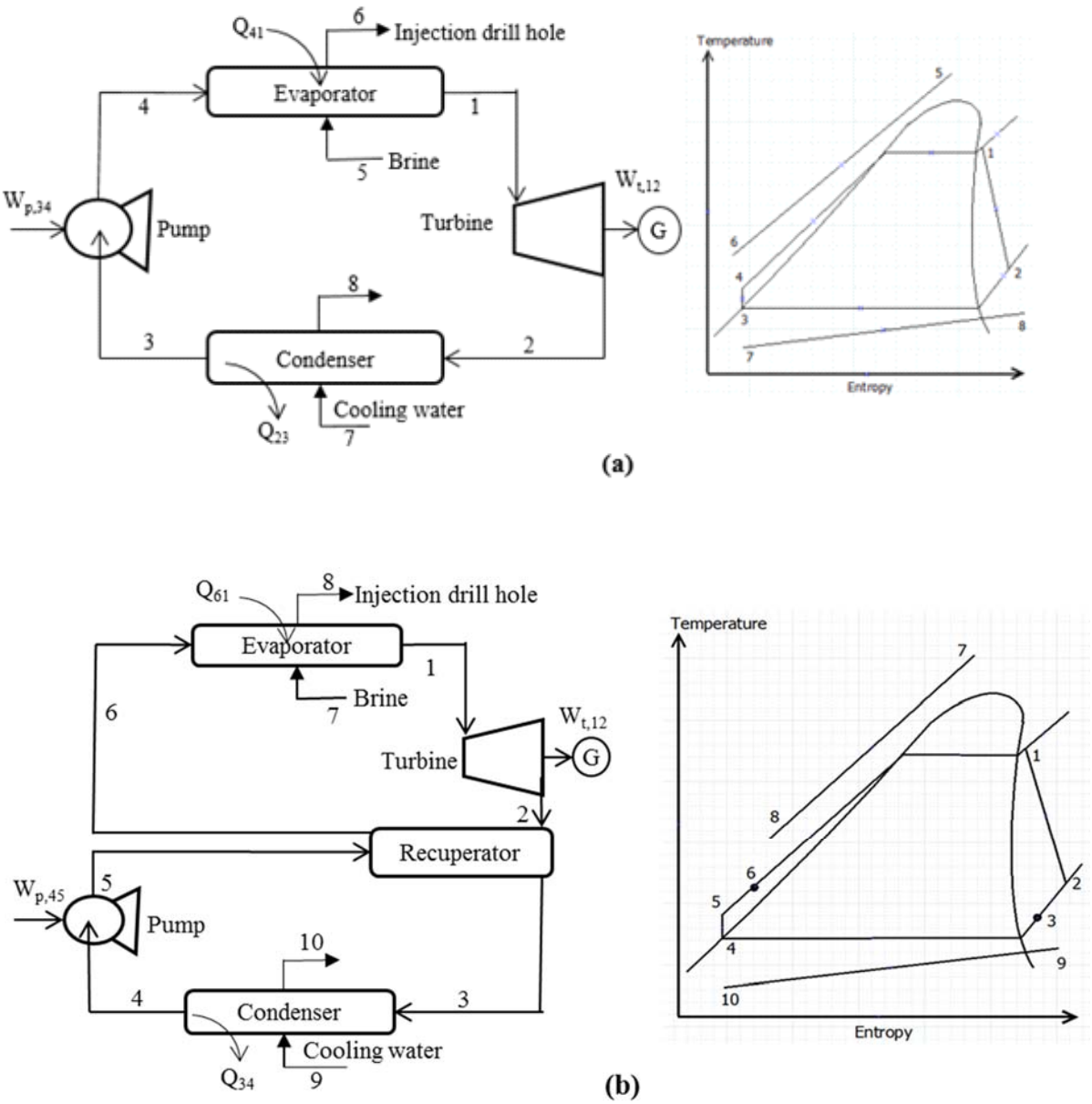

Figure 4.1: The 1-stage turbine: (a) standard cycle (b) recuperative cycle.

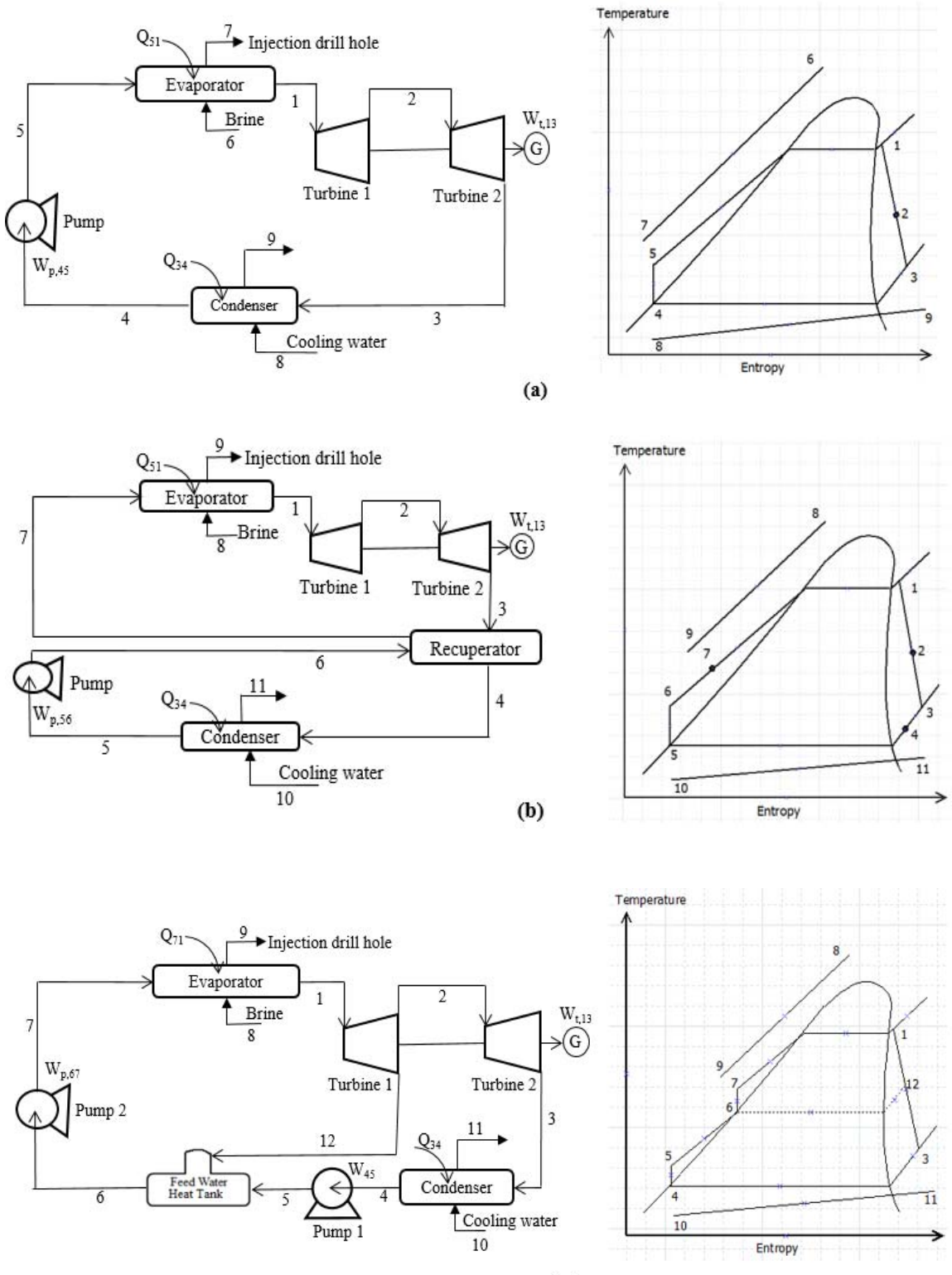

Figure 4.2: The 2-stage turbine (a) standard cycle (b) recuperative cycle (c) regenerative cycle.

4.3. Methodology of investigation

The working fluids considered in this feasibility study are R245fa, n-pentane and R134a as these are most commonly used in the commercial ORC units. The thermodynamics cycle design parameters are based on standard assumptions for superheat, subcooling, pinch point for heat exchangers and nominal performance for components as shown in Table 4.2. These values are commonly used by ORC researchers. The pressure ratio of 3.5 is based on the literature study conducted by Bao et al. [41]. They summarised that the range of this value for Radial-inflow turbine is between 1.1 and 6.3. Furthermore, the pressure ratio of the Chena hot spring 400 kW geothermal power plant [119] is fairly close at 3.65. The net electrical power output (Wnet) was used as an objective function for optimization for the feasibility study. This measure of performance is more relevant than thermal and exergy efficiencies in designing real geothermal power plants [37]. Firstly, thermodynamic analysis was conducted for each cycle, and Wnet calculated. Secondly, the cycle and component designs were further compared by estimating the purchased equipment costs (PEC). The ratio of net electrical power output (Wnet) to indicative capital cost (γ = Wnet/PEC) was used as an indicator to select the most economical designs among design alternatives. Finally, profitability analysis of top four economical designs was conducted to compare their economic performance.

Table 4.2: Assumption parameters for creating thermodynamics cycles.

Parameter	Value
Superheat (^{0}C)	5
Subcooling (^{0}C)	5
Minimum temperature approach (^{0}C)	5
Expander isentropic efficiency (%)	85
Expander mechanical efficiency (%)	98
Pump isentropic efficiency (%)	80
Pressure ratio	3.5

4.3.1 The thermodynamic cycles

The thermodynamic configurations modelled are as shown in Figures 4.1 and 4.2. The standard cycle configurations shown in Figures 4.1a & Figure 4.1b are typically used in reported ORC research. In the standard ORC cycle, the vapour is expanded through a turbine which drives an electric a generator. After expansion, the vapour is condensed, pressurized by pump, flows to the evaporator, vaporized to a superheated state which is the inlet to the turbine (Figure 4.1a). The recuperative cycle recovers some heat from the fluid at the turbine outlet by addition of heat exchanger (the recuperator) which preheats the high pressure liquid after the pump and before the evaporator (Figure 4.1b). The two stage standard cycle (2-stage std.) uses either axial turbine with two stages or two radial turbines with different operating pressures (Figure 4.2a). A 2-stage turbine allows a wider cycle pressure ratio to be used. All 2-stage turbines are assumed to be co-axial, driving one generator. The recuperative cycle in the 2-stage is the same principle as for the 1-stage cycle (Figure 4.2b), but the regenerative cycle uses a portion of the exhaust from the first turbine stage to pre-heat the working fluid prior to the evaporator (Figure 4.2c).

4.3.2 Modelling Description

4.3.2.1 Thermodynamic modelling

Standard adiabatic models of the components, first law energy balance, and second law efficiency are used in the feasibility study according to the assumptions explained in Section 2.1.1 and the following assumptions:

- Fouling in the heat exchangers and pressure drop along pipelines are neglected
- The turbines and pumps have constant isentropic efficiencies
- Geothermal brine is modelled as water
- Dead state temperature and pressure for the cycles are 20°C and 1 bar, respectively.

The first-law thermal efficiency of the ORC is calculated using equation 2.1 and the overall exergy efficiency of a geothermal plant is calculated using equation 2.2. The fraction of the flow rate flowing to the feed water heater tank in a regenerative cycle configuration (Figure 4.2c) is calculated by an equation from Mago, et al. [127]:

$$X = \frac{h_6 - h_5}{h_{12} - h_5} \tag{4.1}$$

4.3.2.2 Economic Modelling

Purchased equipment cost (PEC) of pumps and turbines are estimated using the correlation from Turton et al. [128]:

$$\log_{10} PEC = K_1 + K_2 \log_{10} Y + K_3 (\log_{10} Y)^2 \tag{4.2}$$

where the value of K_1, K_2 and K_3, along with the maximum and minimum values used in the correlation are given in Table 4.3 and Y is the power transferred in kW.

Table 4.3: Parameters for the calculation of purchased equipment costs in Equation (4.2).

Component	Y	K_1	K_2	K_3	Range
Pumps	Power (kW)	3.3892	0.0536	0.1538	1-300
Axial turbines	Power (kW)	2.7051	1.4398	-0.1776	100-4000

The regenerative cycle uses a stainless steel storage tank for direct liquid contact heat exchange to pre-heat the working fluid. The PEC of a tank is estimated as [44]:

$$PEC = 2.48\ x\ 10^3\ V^{0.597} \tag{4.3}$$

where V is tank volume.

The equation for updating PEC due to changing economic conditions and inflation [88] is:

$$C_{\text{new}} = C_{old}\left(\frac{I_{\text{new}}}{I_{\text{old}}}\right) \tag{4.4}$$

where C is the cost (referring to PEC) and I is the cost index. Subscripts *old* and *new* refer to the base time when the cost is known and to time when cost is desired, respectively. The data for the cost index is taken from infoshare of New Zealand statistics [129] in Table 4.4.

Table 4.4: Capital goods price index for the calculation of updated PEC prices in equation (4.4).

Components	Quarter 2-3 (2001)	Quarter 3-4 (2004)	Quarter 1-2 (2014)
Pump	1047	-	1390
Axial turbine	1064	-	1088
Tank	-	1143	1685

The ratio of net electrical power output to total purchase equipment costs is used to compare the investment options. The investment ratio, γ, is similar to levelized cost that does not consider time value of money.

$$\gamma = \frac{Wnet}{\sum_{i=1}^{n} Purchased\ Equipment\ Cost_i} \quad (4.5)$$

where *n* is an index number for the main components in the cycle configuration.

The investment cost of the ORC plant can be evaluated by direct and indirect costs as listed in Table 4.5, according to Bejan and Moran [21].

Table 4.5: Estimation of total capital investment from direct and indirect costs [21].

Total Plant Cost (TPC) in ORC Plant	
A. Direct costs	**B. Indirect costs**
1. Onsite costs	1. Engineering + supervision: 6% DC
1. Purchased equipment costs (PEC)	2. Construction costs + construction profit: 15% DC
2. Piping: 35% PEC	3. Contingency: 8% (of the sum of the above costs)
3. Purchased equipment installation: 20% PEC	
4. Instrumentation + controls: 6% PEC	
5. Electrical equipment +materials: 11% PEC	
2. Offsite costs	
6. Civil, structural + architectural work: 15% PEC	
7. Service facilities: 30% PEC	

Two decision variables are used to evaluate profitability of the projects: Net Present Value (NPV) and Discounted Payback Period (DPB). The NPV is calculated based on Equation 2.5. The discount rate is usually set by the particular industry and may have the inflation rate [39]. The DPB estimates the years to recover the initial capital investment.

4.3.3 Modelling using Aspen Plus

The processes are simulated in Aspen Plus using the cubic Peng-Robinson equation of state (EOS) that has been adopted to calculate the thermodynamic and thermophysical characteristics for working fluids [25]. The newest version 8.4 of Aspen Exchanger Design and Rating (EDR) was used to calculate the heat exchanger

sizes and costs. The program can perform the costing calculation once all the geometry of each component part of the heat exchanger has been calculated. The program needs material and labour costs. Both of these data will vary from fabricator to fabricator, but Aspen EDR supplies a standard database with each version of the program that is updated every year. The three elements of the heat exchanger costs are the material and the labour costs, and the mark – ups on materials and labours. The material costs are determined by material prices of the components from material database and rough dimensions calculated as part of the mechanical design. The labour costs are determined from the labour rate (hourly rate) and the labour hours required to fabricate and assemble each component within the heat exchanger. The labour hours are from correlations that have been developed from several hundred labour estimates for a wide variety of the heat exchanger types and design conditions. These correlations are a function of design pressure, weight, tube length, and material. The mark-ups are a quick way of customizing the answers as these can be used to increase or decrease the calculated exchanger cost. The authors used the original three elements of the heat exchanger costs provided by Aspen EDR version 8.4.

4.4. Results and Discussion

4.4.1. Thermodynamic analysis

Thermodynamic cycles were constructed according to the assumptions and data in Table 4.1 and 4.2 for each working fluid and each cycle configuration in Figure 4.1 and Figure 4.2. The turbine inlet pressure and the working fluid mass flow rate have a range of possible values for each cycle configuration.

4.4.1.1. Influence of turbine inlet pressure and mass flow

A sensitivity analysis was conducted to measure how the changes in turbine inlet pressure and mass flow of working fluid affect the Wnet**.** Figure 4.3 shows modelling results of the possible maximum of the Wnet in different turbine inlet pressures for the standard-cycle with the three working fluids. In 1-stage designs (Figure 4.3a), the cycles with n-pentane and R245fa achieve maximum Wnet between 400-410 kW at the highest mass flow rate, but at the lowest turbine inlet pressure for n-pentane and at the second lowest turbine inlet pressure for R245fa. The minimum temperature approach in the evaporator and the constraint of geothermal outlet temperature limit the mass flow rate in each level of the turbine inlet pressure. The optimal mass flow rate decreases with a higher turbine inlet pressure. This result is expected when a reasonable pressure ratio is required for the turbine, but the turbine radius can be increased to accommodate more fluid flow. The optimal mass flow rates at the lowest turbine inlet pressure are constrained by the geothermal outlet temperature, while the optimal mass flow rates at other turbine inlet pressures are constrained by the minimum temperature approach in the evaporator. The bending of the curves in a continuous drop is created by these different constraints. R134a performs differently from other working fluids, achieving the maximum Wnet of around 398.4 kW at a very high pressure of 31 bar and 22.8 kg/s of mass flow. The very high pressure and mass flow are not considered a feasible design range for the vaporizer and turbine. Increasing turbine inlet pressure after the optimal pressure point is reached will produce designs that have the turbine outlet condition in two-phase areas (the vapour fraction is less than 1). These designs are not feasible because

they cause mechanical damage to the turbine. This occurs because the outlet turbine pressure increases by a higher turbine inlet pressure due to the constant pressure ratio.

In the 2-stage designs (Figure 4.3b), the cycles using R245fa and n-pentane reach the maximum Wnet at 22 bar and 10 bar and mass flow of working fluid at 16.3 kg/s and 6.5 kg/s, respectively. The 2-stage designs would naturally have a lower condenser pressure and a higher turbine inlet pressure than 1-stage designs. The values of optimum turbine inlet pressure and mass flow rate at maximum Wnet from the analysis are used in recuperative-cycle and regenerative-cycle for further investigation. R134a cannot be used in 2-stage designs, because the required condenser pressure could lead to condensation in the turbine.

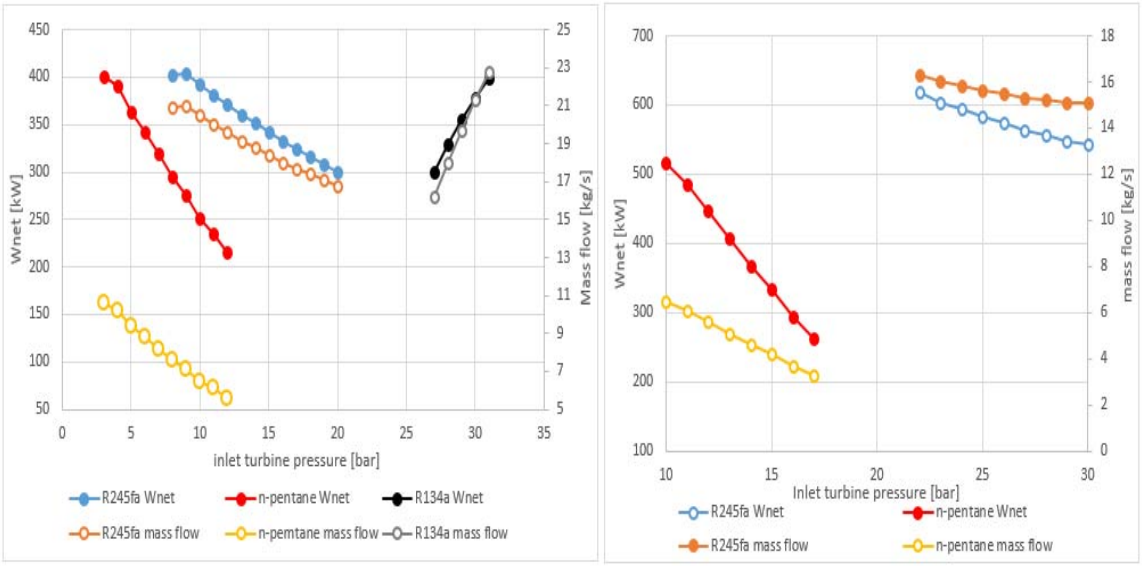

(a) **(b)**

Figure 4.3: Net electrical power output (Wnet) is maximized with higher mass flow rate and lower turbine inlet pressure for different working fluids and (a) 1-stage designs (b) 2-stage designs.

4.4.1.2. The influence of cycle configuration on the plant performance

Figure 4.4 shows model results for maximum Wnet from different cycle configurations using the optimum turbine inlet pressure and maximum working fluid mass flow rate. The maximum Wnet at 619 kW is produced by two stage with standard cycle (2-Stage_Std) and two stages with recuperative cycle (2-Stage_Rec) using R245fa.

The results illustrate the benefits of using multistage turbines designed to best fit the heat and cooling resource. The Wnet is consistently higher for R245fa than for n-pentane, except when using one stage, recuperative cycle (1-Stage_Rec) designs. Large-scale commercial geothermal power generators typically use n-pentane in the binary ORC plant. R245fa is a manufactured compound, whereas n-pentane is refined from petroleum. As a result, R245fa is more expensive and may not be considered feasible in multi-megawatt ORC plant. However, the improved power generation performance for lower temperature resources such as this case study may offset the higher material cost.

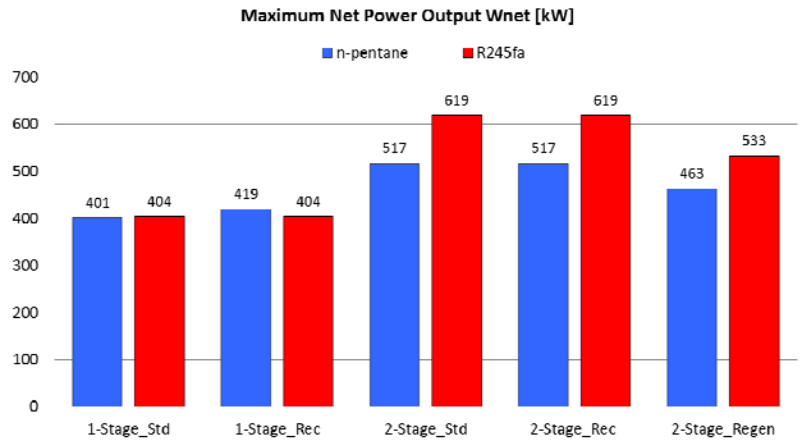

Figure 4.4: Maximum net electrical power output (Wnet) for different thermodynamics cycles showing the benefit of multi-stage turbines.

Figure 4.5 presents the comparison of thermal and exergy efficiencies for the R245fa and n-pentane cycle configurations using the maximum power output conditions. The recuperative and regenerative cycles have higher thermal efficiency than the standard cycles for both 1-stage and 2-stage standard cycles. The exergy efficiency is the same for the standard and recuperative cycles except when using 1-Stage_Rec designs with n-pentane, but lower for regenerative cycles. The exergy efficiency is influenced by the value of Wnet according to Equation 2.2. The regenerator increases the inlet temperature of the working fluid at the evaporator entry, and leads to higher outlet temperature of the geothermal fluid from the evaporator. Thus, the heat removal from the geothermal fluid is partly replaced by the recovered heat from the recuperator. The increase of mass flow of the working fluid in the cycle using a recuperator is not possible due to a constraint of the minimum temperature approach between hot and cold fluids in the evaporator, therefore it does not increase the produced power output except for the case of 1-Stage_Rec designs with n-pentane. The Wnet is the same for standard and recuperative cycles but lower for regenerative cycles. The lower Wnet of the regenerative cycles occurs because a part of the exhaust mass flow rate from the first turbine stage is used to preheat the working fluid prior to the evaporator, therefore second turbine stage has a lower mass flow rate. In general, the comparison between 1-stage and 2-stage designs shows that 2-stage designs have significantly higher thermal and exergy efficiencies than 1-stage designs.

It is theoretically possible to have an additional recuperator in the two stage with regenerative cycle (2-Stage_Regen) in order to increase the cycle performance [75]. However, this cannot be implemented in this case study because the temperature

of working fluids at the point after feed water heater tank in regenerative cycle (Figure 4.2c) is near the boiling temperature. Thus, a two regenerator design is not feasible for this case study due to the high risk of causing a malfunction of pump 2 due to vaporization inside the pump. It is also interesting to note that the 1-stage thermal efficiency (8.83%) and exergy efficiency (37.91%) would be high for the un-feasible R134a working fluid, demonstrating that thermodynamic analysis alone is not ideal for a feasibility study.

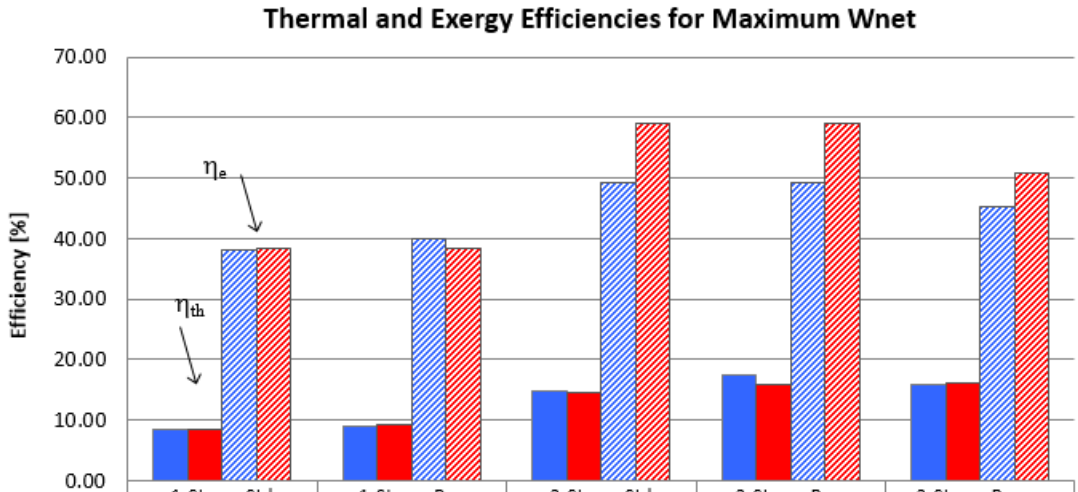

	1-Stage_Std	1-Stage_Rec	2-Stage_Std	2-Stage_Rec	2-Stage_Regen
n-pentane (th)	8.41	8.99	14.80	17.40	15.86
R245fa (th)	8.49	9.21	14.43	15.90	16.21
n-pentane (e)	38.12	39.92	49.15	49.15	45.35
R245fa (e)	38.40	38.40	58.90	58.90	50.69

Figure 4.5: Thermal and exergy efficiency of different cycle configurations and working fluids for the maximum power output conditions.

4.4.2. Economic analysis

4.4.2.1. Purchased equipment costs (PEC)

Figure 4.6 shows purchased equipment cost in each configuration of the plants with different working fluids. This PEC includes turbine, pump, heat exchanger and an additional tank for the regenerative designs. The working fluid cost is not included as the estimate of the volume of fluid needed for each design would depend on site

variables and design details not available at the feasibility analysis stage. Note that the costs for feed water heat tank of the regenerative cycle are calculated using Equation 7 assuming a capacity of 6 m^3 for design using n-pentane and 8 m^3 for designs using R245fa. The tank capacity is based on the assumption that the tank can retain a working fluid flow for 10 minutes. The different tank capacity is used because these designs have different total working fluid flows. The designs with R245fa have significantly higher PEC than designs with n-pentane. The main difference in PEC is due to the much larger heat exchangers needed for R245fa due to the much higher working fluid flow rate required.

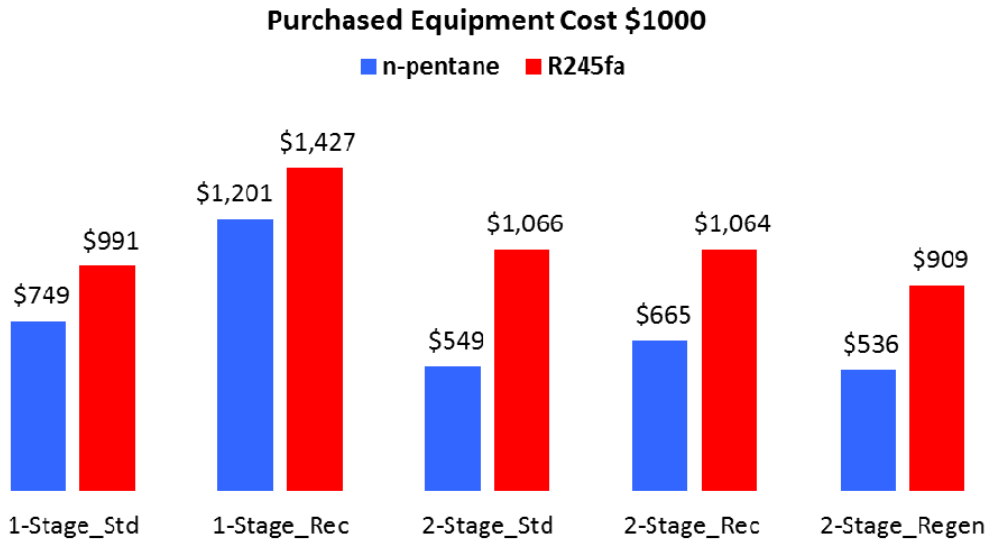

Figure 4.6: Total purchased equipment cost (PEC) estimated in 2014 USD.

Heat exchanger and turbine costs are the main equipment costs of PEC. The heat exchanger and turbine costs for the n-pentane and R245fa designs comprise 46% - 73.6% and 26% - 53% of the total PEC, respectively. The turbine cost is related to the design capacity of the turbine and the heat exchanger costs are directly related to the required heat transfer areas. Figure 4.7 shows the required heat transfer area of

every heat exchanger in the system. The designs using n-pentane need smaller heat exchangers than the designs using R245fa. The difference of the heat transfer areas occurs because these cycle configurations need different heat duty of the heat exchangers. Each heat exchanger design has a different overall heat transfer coefficient and logarithmic mean temperature difference (LMTD), which are the main factors affecting the heat exchanger size. The recuperative and regenerative cycles require smaller sized evaporator and condenser, therefore the costs of heat exchangers can be minimized. However, if the cost of the recuperator is higher than the reduction costs of evaporator and condenser, the total investment cost will be higher than designs without a recuperator. The two stage regenerative cycle (2-Stage_Regen) has lower total cost of heat exchangers because a feed heater tank has significantly lower cost than a recuperator heat exchanger. However, Wnet of this design is lower than other 2-stage designs.

R134a has already been eliminated as not being technically feasible for this resource. However, it is interesting that the one stage standard cycle configuration has heat exchange total area of only 724 m^2, and the lowest PEC of $ 406,229.

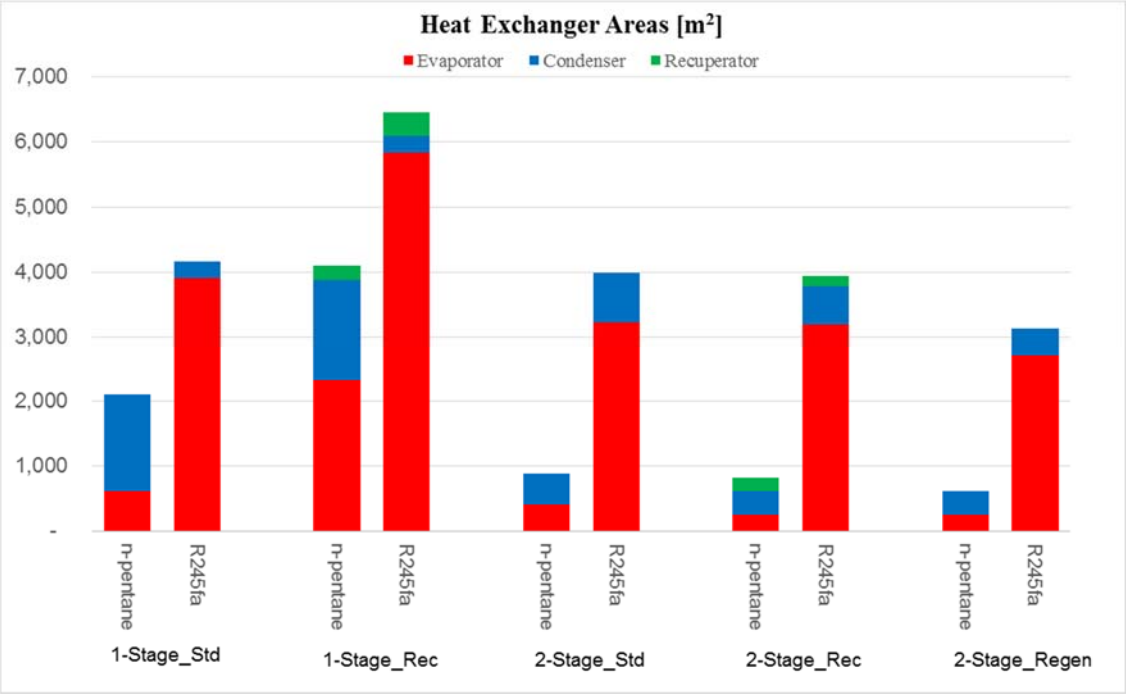

Figure 4.7: Required areas of heat exchanger from different cycle configurations.

4.4.2.2. Investment ratio (γ)

Table 4.6 shows the power/cost ratio for the technically feasible cycle configurations. The highest ratio is 0.942 for the two stage, standard cycle (2-Stage_Std) with n-pentane working fluid. The highest ratio for R245fa is 0.586 for the two stage, regenerative cycle (2-Stage-Regen) design. The power/cost ratio is not really sensitive to thermodynamic improvements of adding recuperator or regenerator for a given turbine configuration. However, there is a marked difference between two stage and one stage designs for each of the working fluids. This result highlights that the choice of the working fluid can greatly affect the power generation economics due to expensive heat exchangers even though the power production may be quite favourable. For example, two stage R245fa designs have a low power/cost ratio, even though they produce the highest Wnet at 619 kW.

The importance of technical, thermodynamic, and economic analyses at the feasibility stage is highlighted by the fact that the technically non-feasible 1-stage cycle using R134a would have the first highest investment ratio of 0.980

Table 4.6: Investment ratio of Wnet to purchased equipment costs (PEC).

γ	1-Stage_Std	1-Stage_Rec	2-Stage_Std	2-Stage_Rec	2-Stage_Regen
n-pentane	0.535	0.349	0.942	0.778	0.865
R245fa	0.408	0.283	0.580	0.581	0.586

4.4.2.3. Air-cooled condensers and water-cooled condensers

The designs so far have all used water-cooled condensers. When no cooling water is available on the site, air-cooled condensers must be selected although they are more expensive than shell and tube condensers. Most commercial geothermal binary power plants use air-cooled condensers because of the issues of resourcing and pumping cooling water. The recuperative and regenerative cycles using n-pentane have the smallest heat transfer area requirement, but the investment ratio is reduced due to more expensive of condenser prices. For example the investment ratio drops from 0.942 to 0.636 for the two stage n-pentane standard cycle, and from 0.865 to 0.562 for two stage n-pentane regenerative cycle when air cooled condensers are used. These results assume that the specific power consumed by fans of the air-cooled condenser is 0.15 kW per kg/s of air flow [87].

4.4.2.4. Total plant cost (TPC)

The TPC for each design is calculated based on direct and indirect costs given in Table 4.5. The specific investment costs (SIC) is calculated by dividing TPC with the optimal Wnet. The results for the thermodynamic-economic analysis of the three best

options are shown in Table 4.7. The specific investment costs (SIC) of the three designs with the three highest investment ratios ranges from $3,011 USD/kW to $3,646 USD/kW. These values are within the range of 2,000 €/kW to 4000 €/kW (about $2,500 USD/kW and $5,000 USD/kW) reported by Gawlik et al.[130], and this value can be higher if exploration and drilling costs are considered. Roos et al. [131] reported that ORC manufacturers produced the typical ORC systems with SIC ranging from $2,000 USD/kW to $4,000 USD/kW in 2009. Jung et al. Jung, Krumdieck [97] reviewed limited data on small commercial systems using ORC technology and reported SIC of $2000 USD/kW to $3500 USD/kW in 2014.

Table 4.7: Total plant cost (TPC) and specific investment costs (SIC) of the three optimal ORC cycle configurations.

Cycle Configuration		TPC (in $1000)	SIC ($USD/kW)
n-pentane	2-Stage_Std	1,557	3,011
n-pentane	2-Stage_Regen	1,519	3,280
n-pentane	2-Stage_Rec	1,885	3,646

4.4.2.5. Geothermal development costs

The investment in a binary geothermal power plant must necessarily include drilling cost, which has historically been the highest share of total geothermal development. The costs of geothermal development are difficult to estimate because of commercial sensitivity and inherent uncertainly involved in geothermal drilling and reservoir engineering. Drilling costs are reported in only a few sources. Stefansson et al. [132] estimated that drilling cost for a typical geothermal power plant is about 20% – 50% of total plant cost. Drilling and development costs can be as much as 70% of total costs for binary power plants installed in Europe according to Kranz et al. [133].

Kutscher et al. [134] reported that binary geothermal power plants with capacity of 5 MW or larger had installed costs about $500 USD/kW for exploration and drilling in 2000. The Geothermal Energy Association reported in 2006 that geothermal confirmation and site development drilling range from $600 USD/kW to $1,200 USD/kW with an average of $1,000 USD/kW. The US producer cost index for mining services including drilling oil and gas wells increased 77.2 % from 2005 to 2014. Thus, the average drilling and development costs for the economic analysis in this paper are estimated at $1,772 USD/kW in 2014.

4.4.2.6. Profitability analysis

According to the Geothermal Energy Association, the construction time for geothermal power plants is 3 to 5 years. Capital investment is modelled as 20% of TPC in the first two years for exploration and confirmation of resources and the remaining 80% is invested in the third year. The plant starts to produce the electricity in the fourth year at the Wnet rate times the plant availability factor, which for commercial geothermal plants is around 90%. The discount rate is assumed to be 10% [97]. The value of inflation rate was taken from New Zealand Consumer Price Index (CPI) where the inflation rate has averaged around 2.7% since 2000 [135]. The electricity revenue price at the first year of the construction is estimated at 0.083 USD/kW with 3% of electrical price increment per year over the plant lifetime [97]. Average operating and management (O&M) costs were estimated at 0.01 €/kW (about $0.013 USD/kW) for the ORC plant according to David et al. [136]. The estimation of average O&M costs are based on the relatively small size of the ORC plant with capacity less than 1 MW. The parameters used in the economic models are summarised in Table 4.8.

Table 4.8: Assumptions for economic modelling in the profitability analysis.

Plant lifetime	20 years
Plant availability	90%
Electricity revenue unit price at the first year	USD $0.083/kWh
O&M cost	USD $0.013/kWh
Annual electricity price escalation	3.0%
Inflation rate	2.7%
Discount rate	10%

Table 4.9 shows the profitability factors for the three candidate designs. The NPV has a wide range between USD $809,231 and USD $1,082,581, but DPB is more consistent between 12 years and 15 years. The total cost of investment ranges from USD $2,339,119 to USD $2,801,354. These values are consistent with the total investment amount reported for building the 400 kW geothermal power plant at Chena Hot Springs, Alaska, USA at the end of 2006. The actual expense of Chena geothermal plant project was USD $2,007,770 [137]

The profitability analysis for the R134a standard ORC cycle would indicate that it is an appealing option. The technology is simple, R134 is low cost, the heat exchangers are small, and the one stage expansion through a simple turbine is attractive. The total cost is attractive, USD $1,857,222, the NPV is USD $871,890 and the DPB is 12.64 years.

Table 4.9: Profitability analysis from thermodynamic and economic modelling results.

Cycle Configuration		TCI (USD)	NPV (USD)	DPB (Years)
n-pentane	2-Stage_Std	$2,472,648	$1,082,581	12.93
n-pentane	2-Stage_Regen	$2,339,119	$865,777	13.61
n-pentane	2-Stage_Rec	$2,801,354	$809,231	14.55

Figure 4.8 shows the cumulative discounted cash flow against the operating years for the design of the standard 2-stage ORC cycle using n-pentane. Clearly, a longer plant lifetime would increase the cumulative NPV, as would a lower discount rate. A lower discount rate could be inferred if government subsidies or public investment were made in the project.

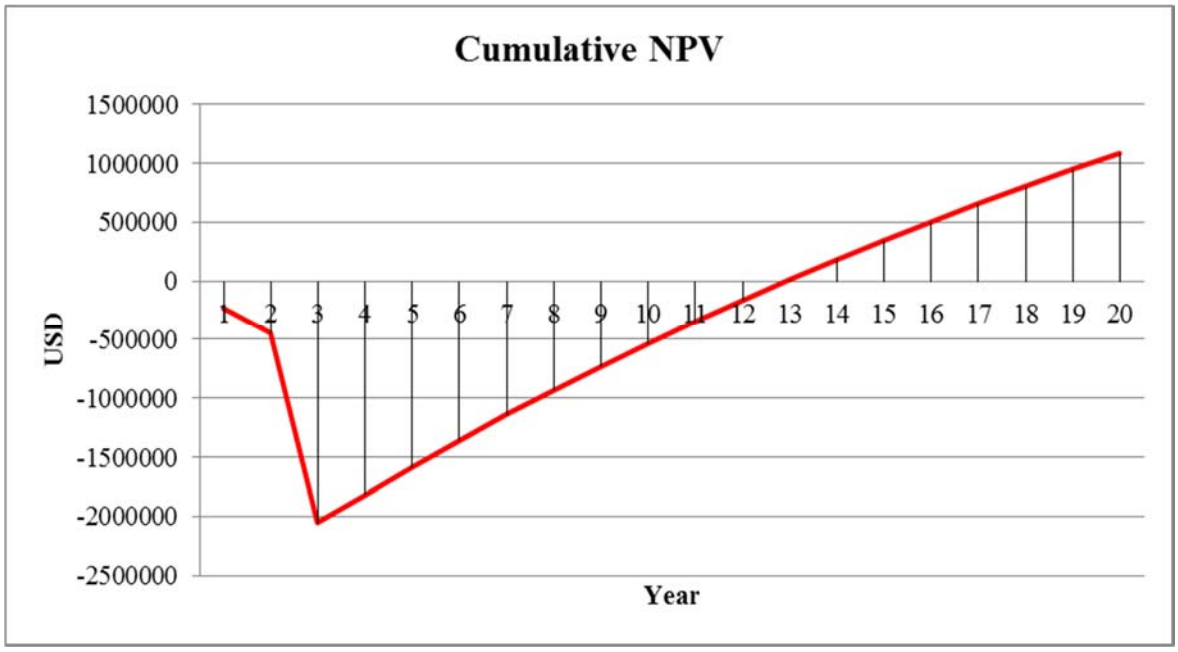

Figure 4.8: Cash flow analysis represented as cumulative NPV for the n-pentane 2-Stage_Std ORC.

4.5. Conclusion

The thermodynamic, technical and economic feasibility were investigated for design of a binary geothermal power plant with different cycle configurations, working fluids and component options. Three working fluids, two expansion stages and five different ORC binary cycle configurations were modelled with the requirement of technically feasible pressure ratio for calculating turbine performance. The analysis used a typical geothermal resource in New Zealand with brine temperature of 173ºC, pressure of 9 bar and flow rate of 8 kg/s. The most technically and economically favourable design for this resource uses n-pentane working fluid, uses a two stage turbine, and does not use a regenerator or recuperator. This design had net power production capacity of 517 kW with NPV for a 20-year plant life of USD $1,082,581 and DPB of about 12.93 years.

The 2-stage expansion in the thermodynamic cycle configuration provides higher net electrical power output, and higher thermal and exergy efficiencies than the 1-stage designs. Thermodynamic analysis alone would indicate the 2-stage system is the optimal design. However, total capital costs and profitability analysis show that the increased cost of larger heat exchangers and the added technical complexity can make the 2-stage designs less feasible than 1-stage designs. Similarly, the added cost of the recuperator heat exchanger and regenerator mixing tank for this lower temperature case study tend to negate the thermodynamic benefits. There may not be a choice to use the lower cost shell and tube water-cooled condenser when the geothermal site has the issues of resource and pumping cooling water. The added cost of the air-cooled condensers may mean the case study would not be economically feasible even though the two condensers are thermodynamically equivalent.

The working fluid type and cycle configuration are the main factors influencing performance and total investment cost of the plant. The cost of the working fluids was not included explicitly in the economic modelling, but it is likely that the lower cost of n-pentane, as well as the substantially lower required mass flow rate would increase the feasibility preference for n-pentane over R245fa. Handling, toxicity and flammability may also be important factors in working fluid selection that were not explicitly considered in this analysis. The contribution of this thesis in this chapter is the exploratory feasibility study using technical, thermodynamic and economic analyses. The most important example of the importance of using the multi-criteria feasibility approach is the lesson learned from modelling the R134a refrigerant. If the technical feasibility limitations of maximum system pressure and realistic turbine expansion ratio were not applied in the analysis, the results of modelling of power generation, efficiency, cost and profitability would lead to the wrong conclusion from the optimization study.

4.6. Nomenclature

1-Stage_Rec One stage, recuperative cycle
1-Stage_Std One stage, standard cycle
2-Stage_Rec Two stages, recuperative cycle
2-Stage_RegenTwo stages, regenerative cycle
2-Stage_Std Two stages, standard cycle

C	Cost ($)
DPB	Discounted Payback (year)
EDR	Exchanger Design & Rating
G	Generator
h	Specific enthalpy (kJ/kg)
I	Cost index
$\dot{m}$	Mass flow rate (kg/s)
N	Lifetime of the plant (year)
NPV	Net Present Value ($)
ORC	Organic Rankine cycle
PEC	Purchase Equipment Cost ($)
Pr	Pressure ratio
Q	Heat transfer rate
q	Discount rate (%)
R	Annual revenues ($)
s	Specific entropy (kJ/kg.K)
SIC	Specific Investment Cost ($)
t	Time (year)
Tank	Feed water heater tank
TCI	Total capital investment ($)
V	Tank volume (m^3)
Wnet	Net electrical power output (kW)
W_t	Net power of turbine (kW)
W_p	Net power of pump (kW)
W	Work inputs (kW)
X	Fraction of flow rate
Y	Power of pump or a turbine (kW)

Greek symbols

η_e	Exergy efficiency (%)
η_{th}	Thermal efficiency (%)
γ	Investment ratio

Subscripts

Brine	Geothermal fluid
Eva	Evaporator
In	Input
New	Time when the cost is desired
Old	Base time
Out	Output
p	Pump
T	Turbine

Chapter 5 – Design Methodology of the new ORC Binary Geothermal Power Plant

The aim of this thesis is to develop an approach for a feasibility study for flexible design (FSFFD) for the ORC development, which includes thermodynamic, component, resource, and cost considerations. This chapter proposes a design methodology for assessing design alternatives of a new binary geothermal plant. The plant will be installed in a potential geothermal resource with a low-to-moderate temperature based on thermodynamic and economic analyses. The methodology applies the economic and energy return on investment (EROI) analyses to predict the future benefits of the plant investments. The methodology has considered all of five main design variables in designing and optimizing the ORC plant. To illustrate the implementation of the proposed methodology, the pre-feasibility study of the existing geothermal resource in a location of Taupo Volcanic Zone (TVZ) was conducted. The previous chapters (Chapter 3 and 4) discussed the influence of the main design variables on the design performance and selection based on the thermodynamic and economic aspects.

5.1. Introduction

New Zealand has about 260 low temperature geothermal (LTG) energy sites. The surface fluid expressions are connected with wells, springs, faults and tectonic features. There are also about 170 other thermal sites such as disused coal mines, abandoned oil and gas wells and water wells [15]. These resources are widely spread across North and South islands, with some associated with areas of young volcanism and structural settings. Figure 5.1 shows the location of the resources across the country. These resources have not been yet exploited, because the development and

exploration of geothermal potential of New Zealand have been limited to high temperature resources due to the abundance of high temperature geothermal resources, the wide-spread availability of cheap hydro-generated electricity and natural gas [138]. The geothermal heat resources with temperatures above 150^0C are categorized as high-temperature heat sources, while moderate-temperature heat sources have temperatures between 90^0C and 150^0C. The low-temperature heat sources have temperature less than 90^0C.

The design stage is an important first step in the investigation of a design development. The important design decisions made in this stage can affect up to 80% of the total capital cost of a project [21]. It is important to determine if a particular design is feasible. The design and optimization of the relevant systems play an important role in the survival and growth of most industries due to growing competition in the world today [16]. Thus, this design stage is a design investigation that incorporates between the relevant inputs from analyses and experimentation and existing information on similar plant systems and processes to obtain an acceptable design.

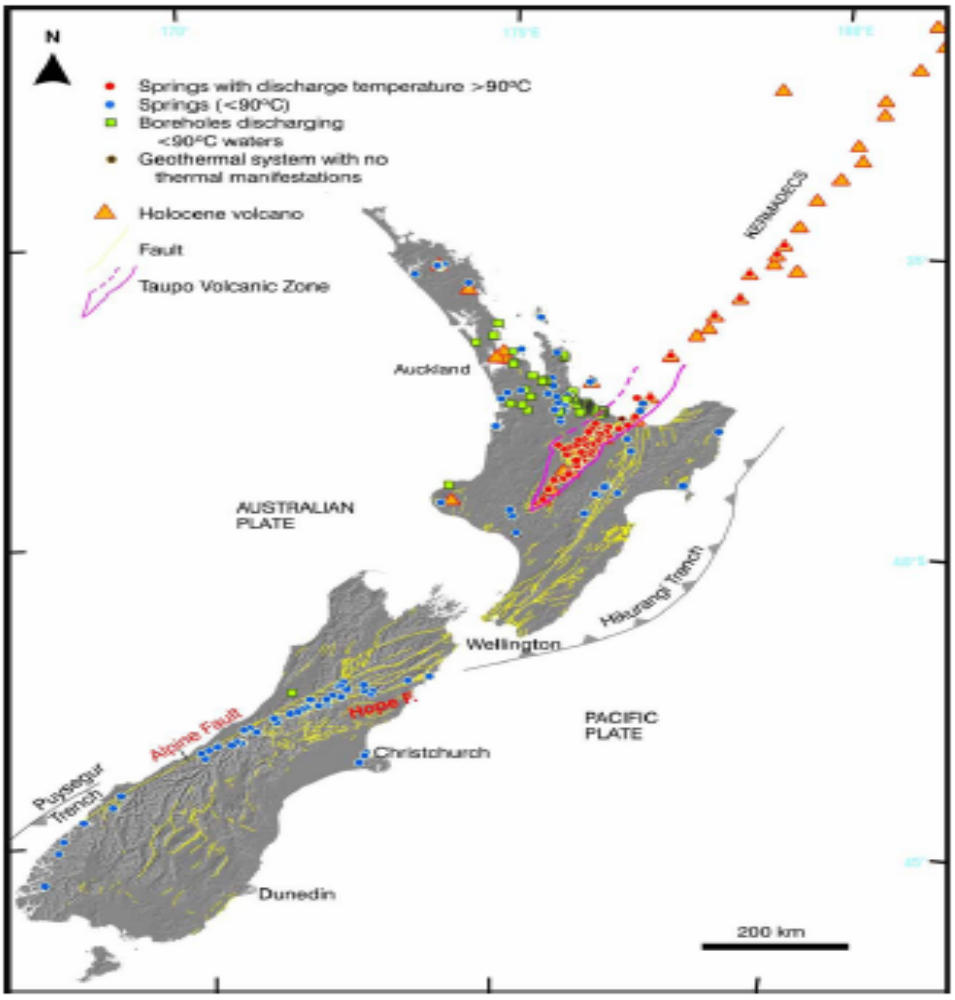

Figure 5.1: Location of hot springs, active volcanoes and the main active fault zones in New Zealand.

5.2. Methodology

A methodology is proposed to simplify an assessment of plant design alternatives because the assessment involves many design variables in a complicated design process. The methodology has considered all of five main design variables of the ORC design that have been explained in Chapter 2. Figure 5.2 shows a flowchart of the methodology. The methodology guides designers to select the most favourable design alternatives based on thermodynamic and economic analyses. In general, the methodology consists of four main steps of the FSFFD approach that have been

explained in Chapter 1. The main steps of the FSFFD approach are (1) initial step, (2) simulation step, (3) evaluation step and (4) result step. The breakdown steps of the proposed methodology is outlined in the following steps:

1. Problem specification:

   The main parameters that should be specified are geothermal fluid temperature (T_{geo}), geothermal rejection temperature (T_{rej}), geothermal fluid pressure (P_{geo}), mass flow of geothermal ($\dot{m}_{geo}$), ambient temperature (T_o) and ambient pressure (P_o).

2. Synthesis:

   Synthesis is concerned with combining separated elements into a thermodynamic cycle. The step consists of four system elements that should be conducted simultaneously.

   a. *Selection of working fluid*: the selection of the most appropriate working fluid has great implications for the performance of a binary plant [9]. The criteria used for the selection of the working fluid are good physical and thermodynamic characteristics providing high thermodynamic performance and high exploitation of the available heat source. The selected working fluid should be environmentally friendly indicated by low toxicity, minimised global warming potential and characteristics of low to zero in-flammability. In order to have good availability and low cost, several common working fluids in commercially available ORC plants are recommended. Table 2.5 shows the commercial working fluids that are commonly used in the ORC plants. The selection of working fluid is also closely related to the choice of

turbine type [41]. Thus, the choice of working fluid should be also synchronized to the limitations of the selected turbine.

b. *Selection of component types*: Type of four basic main components of the binary plant (turbine, evaporator, condenser and pump) should be selected for further analysis in the following steps. The technology selection depends on operating conditions and the size of the plant. The two turbine types used for a binary power plant are axial turbines and radial inflow turbine [9]. One-stage axial turbines are suitable for use in systems with high flow rates and low pressure ratios, while one-stage radial turbines are commonly used in a contrary condition. The shell-and-tube heat exchanger with brine on tube side and working fluid on shell side is the most commonly type used for the binary plants. DiPippo et al. [9] mentioned that the preheater can also use a horizontal cylinder and corrugated plate type. Moreover, they stated that the evaporator/superheater can use a horizontal cylinder or kettle-type boiler. The dry cooling system uses air-cooled condenser. The centrifugal pumps are widely used for industrial applications [21] and the type is also used in the geothermal areas. Due to limitation of the ORC system efficiency, an efficient pump must be selected with considering cost-effective ORC system. Afterward, the materials of the main components should be selected to calculate main component costs in the further analysis.

c. *Selection of cycle configurations*: another key aspect affecting the ORC system performance is the thermodynamic cycle configuration [74]. A basic binary geothermal power plant is designed by standard (Std) cycle [9]. A recuperative (Rec) cycle is used when T_{rej} has any temperature limitation.

The design is can able to increase T_{rej} and thermal efficiency, because the addition of a recuperator increases heat absorbed from geothermal fluid. The remaining vapour from turbine outlet can be utilised to preheat the high-pressure fluid before flowing to evaporator. However, the design is less economical than Std design because an additional exchanger is expensive and the regenerator will not increase the produced power [118]. The schematic diagram of both cycle configurations is shown in Figure 5.3.

d. *Determination of design parameters*: The some assumptions are required to create a thermodynamic cycle of the binary plant. These parameters have been discussed in Chapter 2. Table 5.1 summarises the common assumption values used by various ORC research groups. Note when the real models of pump and turbine are used, the pump and turbine efficiencies are calculated more precisely especially in their off-design conditions.

Table 5.1: Initial assumptions for creating a thermodynamic cycle

Assumptions of cycle parameter	Value
Superheat (sh) (^{0}C)	5
Sub-cooling (^{0}C)	5
Pinch Point (^{0}C)	5
Turbine isentropic efficiency (%)	85
Turbine mechanical efficiency (%)	98
Pump isentropic efficiency (%)	80

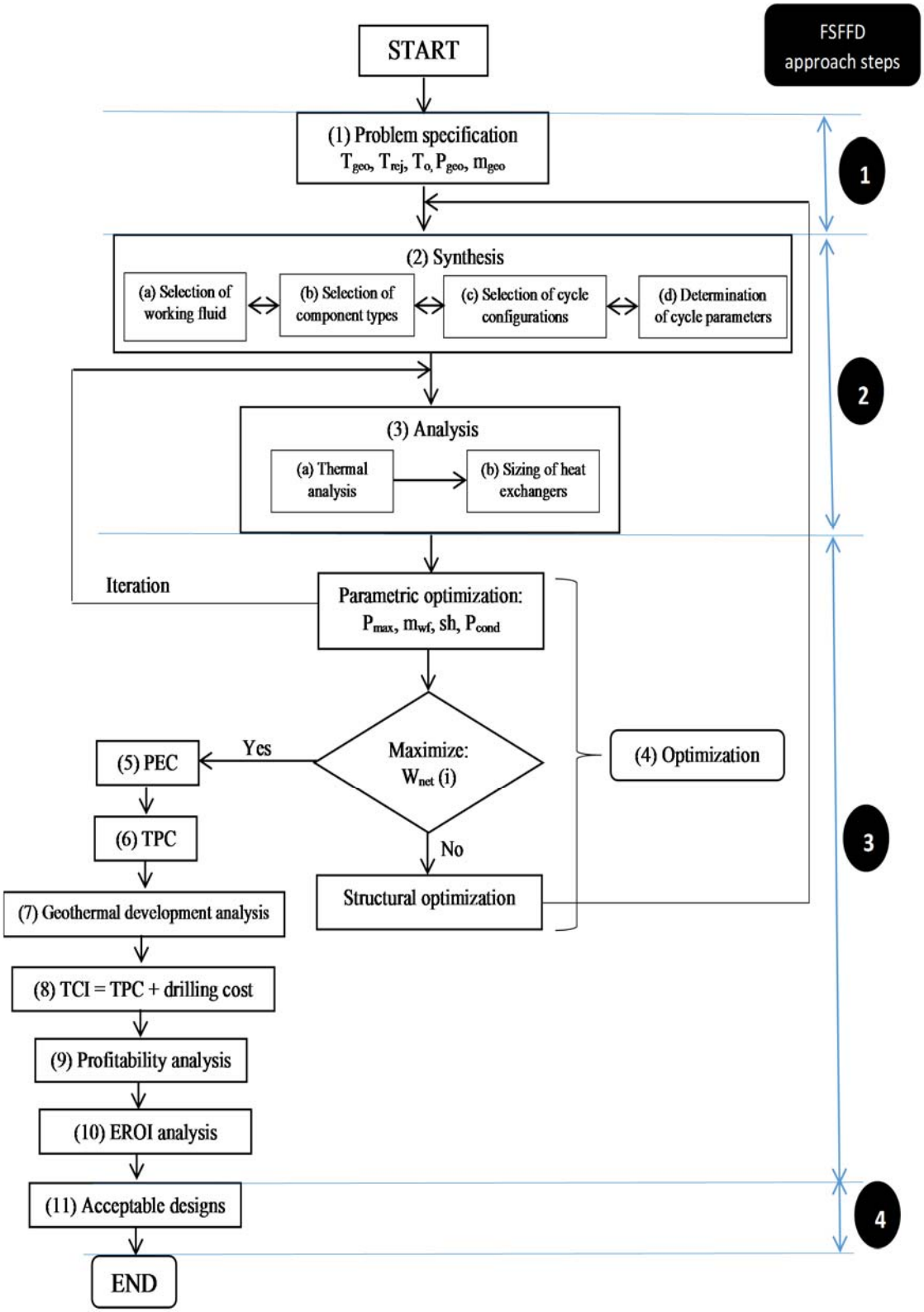

Figure 5.2: A flow chart for assessing a potential geothermal resource.

3. Analysis:

Analysis involves thermal analysis in system and component levels and sizing of heat exchangers.

a. Thermal analysis generally entails solving mass and energy balances in overall thermodynamic cycle and in each component of the cycle. The thermal analysis here is implemented based on the strategy proposed by Franco et al. [6]. The strategy divides the ORC cycle into three subsystems (thermodynamics cycle, evaporator and condenser) and two hierarchical levels which sequentially define system level (thermodynamic cycle) and component level (evaporator and condenser). Figure 5.3 shows hierarchical organization proposed by Franco et al. At the system level, the thermal problems (mass and energy balances) are solved by thermodynamic variables matching between the ORC cycle and heat resource. At the component level, the convergent results from the system optimization level produce the input data for the detail design of component level (evaporator and condenser). The results of the optimum component design (pressure losses (Δp), pumping power (W_p) and fan power (W_{fans}) are iterated in the system level. Thus, the results of the component level optimization can affect the results of the first level optimization particularly in the design of the dry cooling system.

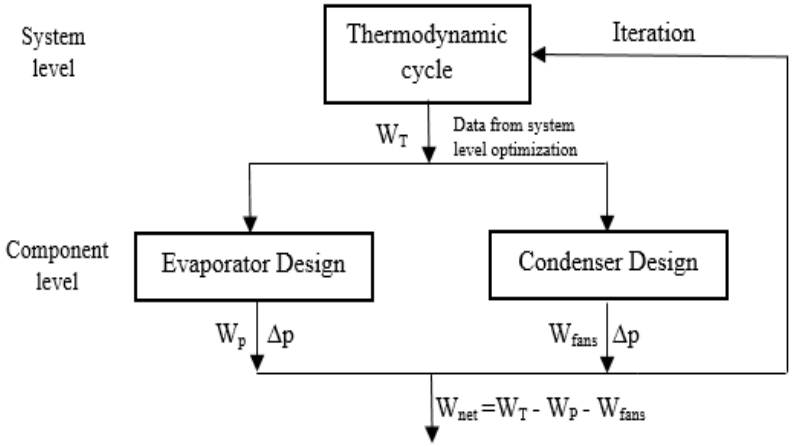

Figure 5.3: Hierarchical organization for the thermal analysis in the design of ORC plants

b. Sizing of heat exchangers. The dimensions of the various sections of the heat exchangers (pre-heater, evaporator, super-heater and condenser) are calculated by considering the required heat transfer, the allowed pressure drop and the minimum allowed temperature difference (pinch point).

4. Optimization:

Analysis and optimization are two consecutive steps that are connected each other. The objective of the analysis and optimization is to identify the preferred configuration among the configurations synthesized. The optimization involves two general optimization forms: parametric optimization and structural optimization. In parametric optimization, four decision variables are utilized to evaluate all remaining dependent quantities of the system: (1) cycle maximum pressure (P_{max}); (2) mass flow of the working fluid (m_{WF}); (3) degree of superheating (sh), measured from the specific entropy of the point on saturated vapour curve for subcritical cycles; (4) condensation pressure (P_{cond}) [87]. As mentioned in Chapter 2, the assumption of superheated value can be changed for the optimization purpose in the parametric optimization. The objective

function is to maximize net electrical power output (W_{net}). This factor is crucial due to economical aspect of geothermal power plants. The power output is even more crucial than exergy efficiency [37]. In structural optimization, the optimization occurs when the re-selection of system elements is required to achieve an acceptable objective function. Structural optimization is indicated in Figure 5.2 by returning the arrow linked to synthesis step. The structural optimization generally consists of the re-selection of the working fluid and the cycle configuration. Some alternatives are chosen for further analyses in profitability and EROI analyses. Note that "i" represents the number of the selected design alternatives before the economic analysis.

5. Purchased equipment costs (PEC):

   The first step for any detailed cost estimation is to evaluate the PEC. The type of equipment, its size, and construction materials have been determined from previous flow chart steps. The best source for estimating the cost can be obtained directly from vendors'quotations. In the preliminary stage, cost estimations can use some literatures providing various estimating cost charts and software packages.

6. Total plant costs (TPC):

   The TPC includes the plant capital cost and steam gathering system cost that is required for the geothermal plants. The plant capital cost accumulates four factors affecting capital costs of a plant: direct costs, indirect costs, contingency fees, and auxiliary facilities. According to Turton, Bailie [88] et al., the plant capital cost can be evaluated by grassroots cost (C_{GR}):

$$C_{GR} = 1.18 \sum_{i=1}^{n} C_{BM,i} + 0.50 \sum_{i=1}^{n} C_{BM,i}^{0} \quad (5.1)$$

where n represents the total number of pieces of main equipment, C_{BM} is the sum of the direct and indirect costs, and C_{BM}^{o} is the bare module cost evaluated at based conditions. The value of 15% and 3% of the bare module cost are assumed for contingency costs and fees, respectively. The over cost value of 50% is assumed for auxiliary facility costs because the binary power plant is assumed to be built on an underdeveloped land. The steam gathering system cost is the costs for the networking of pipes connecting the plant with all production and injection wells. For binary systems, only the hot brine line and the cooler brine injection lines are required. Entingh et al. [139] proposed the system cost of 95 USD per kW for binary power systems. CE Holt Company, California [140] suggested the lower cost of the steam gathering system cost at 30 USD per kW.

7. Geothermal development analysis:

a. Costs

The costs represent the drilling cost. The higher uncertainty is associated with the cost of drilling, because the cost is affected by resource characteristics which influences both the cost of individual wells and the total number of wells that must be drilled [141]. Stefansson et al. [132] suggested the drilling costs based on the analysis result of the drilling in 31 geothermal fields with capacities in the range 20-60 MW in the world. The drilling cost was calculated according to correlation between the total investment cost and surface equipment cost (the plant itself and the steam-gathering system). In order to bring this cost from 2002 to the end of 2014, the producer cost index for drilling of oil and gas wells was used (data from Bureau of Labour

Statistics, U.S. Department of Labour). The producer cost index is 115.6 and 450.7 in 2002 and December 2014, respectively. Table 5.2 summarises the drilling costs of geothermal power plants in 2014.

Table 5.2: The drilling cost of geothermal power plant in 2014 [132]

Drilling cost	Expectation value (USD/kW)	Range within a standard deviation (USD/kW)
In a known field	1170	1130-1949
In an unknown field	1805	1403-3119

b. Project duration

According to the geothermal energy association, a new geothermal power plant project takes a minimum of 3 to 5 years to start producing the electricity. Furthermore, Stefansson et al. [132] mentioned that a typical time schedule for a stepwise development of a geothermal field is about 6 years consisting of 3 years for reconnaissance, surface exploration and exploration drilling and 3 years for production drilling and power plant.

8. Total capital investment (TCI):

The TCI is the total investment amount that includes the TPC and drilling cost.

9. Profitability analysis:

The purpose of the assessment is to determine the positive economic benefits to the organization that the proposed energy system will provide. This assessment typically involves a method of profitability analyses such as discounted payback (DPB), net present value (NPV) and internal rate of return (IRR).

10. EROI analysis:

The analysis has a purpose to measure the future energy benefit from energy expenditure. The energy production systems such as binary plants are required to produce surplus energy beyond the energy expenditure to set the system in

place. The economic evaluations do not measure the energy provided to and from the system directly, since the evaluations can be influenced by temporal market distortions such as exchange rates, subsidies, interest rates, labour cost and electrical prices.

11. Acceptable designs:

    The last step is to summarize the acceptable designs among several alternatives.

5.3. Application of the methodology for a case study

5.3.1. Problem specification

A case study was used to illustrate the implementation of the methodology. Table 5.3 shows the actual data of a geothermal well and cooling air from a location in the Taupo Volcanic Zone (TVZ) in New Zealand.

Table 5.3: Data of a geothermal well and cooling air

Data	Value
T_{geo} (^{0}C)	131
T_{rej} (^{0}C)	92
P_{geo} (bar)	9
$\dot{m}_{geo}$ (kg/s)	520
T_o (^{0}C)	20
P_o (bar)	1.53

5.3.2. Synthesis

5.3.2.1. Selection of working fluid

The three common working fluids used in the commercial ORC power plants such as n-pentane, R245fa and R134a are used in the current chapter. The other common working fluids used in ORC industrial plants are listed in Table 2.5.

5.3.2.2. Selection of main component types

A single radial turbine is considered in this chapter and the shell-and-tube heat exchangers are used for evaporator and recuperator. An air-cooled condenser must be

selected because there is no water supply in the geothermal resource site. A centrifugal pump is selected for the feed pump. In addition, carbon steel (CS) is used as the material for cost calculation of the main plant components

Table 5.4: Properties of working fluids and list of ORC manufacturers [7].

Working fluid	T_c (^{0}C)	P_c (bar)	Manufacturer
n-pentane	196.5	33.6	ORMAT (US)
R245fa	154.0	35.7	Bosch KWK (Germany), Turboden pureCycle (US), GE CleanCycle (US), Cryostar (France), Electratherm (US)
R134a	101.1	40.6	Cryostar (France)

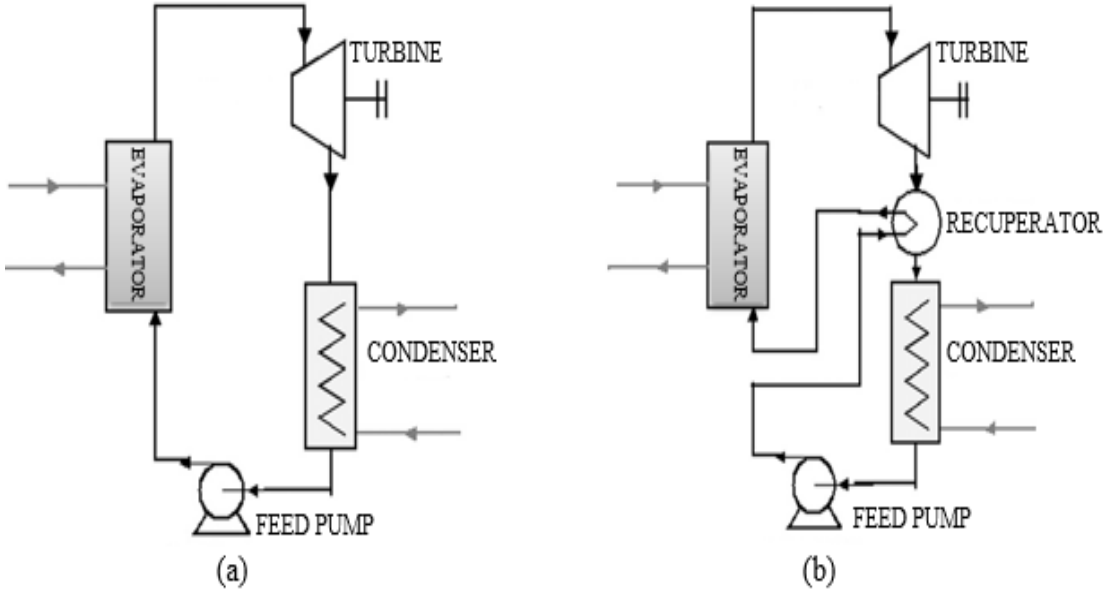

Figure 5.4: Schematic diagram of ORC: (a) Std cycle and (b) Rec cycle.

5.3.2.3. Selection of cycle configurations

The work in this chapter considers two types of the cycle configuration: Std and Rec cycles. The schematic diagram of both cycles is shown in Figure 5.4a and 5.4b. The Std design consists of a pump, an evaporator powered by geothermal fluid, a turbine and a condenser. The evaporator here represents preheater and evaporator. The generated high pressure vapour flows through the turbine and its heat energy is

converted to work. The turbine drives the generator and electrical energy is produced. The exhaust vapour exits the turbine and flows to the condenser where it is condensed into working fluid. The working fluid with low boiling point is pumped to the evaporator, where it is heated and vaporized into high pressure vapour. The high pressure vapour flows back to turbine and a new cycle starts again. The Rec design of ORC has a recuperator that can be installed as a liquid preheater between the pump outlet and the turbine outlet as illustrated in Figure 5.4b. This reduces the amount of heat needed to vaporize the fluid in the evaporator.

5.3.3. Analysis

The authors used Aspen plus version 8.6 environment [25] to carry out the thermal analyses and calculations for the case study. The thermodynamic properties of the working fluids were calculated using the cubic Peng-Robinson equation of state (EOS) [142] that has been adopted to calculated the thermodynamic and thermo-physical characteristics. The heat exchanger models are constructed by integration between Aspen plus and Aspen EDR (Exchanger Design & Rating) software from Aspen Technology, Inc [25].

5.3.4. Optimization

5.3.4.1. Objective function

The objective function is to maximize the Wnet. The Wnet is calculated using the Equation 2.3. The specific power consumed by the fans of the air cooled condenser is assumed to be 0.15 kW per kg/s of air flow [87].

5.3.4.2. Thermodynamic optimal design parameters

The optimal design parameters using three working fluid and two cycle configurations are summarised in Table 5.5. The recuperative cycle uses only n-

pentane, because the positive impact of a recuperator is higher for dry working fluids such as n-pentane than wet working fluids.

The Wnet of optimal designs with n-pentane and R245fa is comparable at around 11 MW, but the Wnet of design with R134a is lower than others at 9,364 kW. It occurs because the maximum pressure of the system is significantly higher than others at 40.5 bar and the R134a design has the highest mass flow rate of working fluid. Therefore, the comparable turbine power of R134a design is deducted with the highest pump power of 1,551 kW. The Std design with R134a has already been eliminated as not being feasible for this resource.

Table 5.5: Optimum design parameters of the design alternatives.

Fluid	n-pentane	n-pentane	R245fa	R134a
Cycle configuration	Std	rec	Std	Std
T_{rej} (^{0}C)	92	96.5	92	92
m_{wf} (kg/s)	184	184	366.2	410.3
P_{max} (bar)	7	7	16.1	40.5
$T_{T,in}$ (^{0}C)	113	113	116	121
P_{cond} (bar)	0.82	0.82	1.79	7.7
T_{cond} (^{0}C)	67.9	35.4	59.8	48.9
$m_{air, ACC}$ (kg/s)	7350	7700	7800	8400
W_T (kW)	12,600.4	12,600.4	12,858.9	12,175
W_P (kW)	253.9	253.9	543.3	1,551
W_{fans} (kW)	1,117.5	1,155	1,170	1,260
Wnet (kW)	11,229	11,191.5	11,145.6	9,364

5.3.5. Economic evaluation

5.3.5.1. PEC

The PEC of pumps and turbines are estimated using a correlation from Turton et al. [128]. The PEC evaluated in the base case (PEC^0) is calculated using Equation 4.2 where K values are given in Table 5.6 and Y is the output power in kW. The number of pumps is calculated, so that the maximum Y is less than or equal to 300 kW. The single radial turbine is considered in this work and the cost equation is used beyond its

maximum value at 1500 kW. The cost result is still considered valid, since the cost increase is the same pattern as results within a cost equation range. The cost increases algorithmically as a function of capacity increase.

Table 5.6: Parameters for the calculation of PEC in Equation (4.2).

Component	Y	K_1	K_2	K_3
Centrifugal Pumps	Power [kW]	3.3892	0.0536	0.1538
Radial turbines	Power [kW]	2.2476	1.4965	-0.1618

The cost deviations from the base conditions (base case of material: carbon steel and operation at near ambient pressure) are handled by pressure factor (F_p) and material factor (F_m) that depend on the equipment type, the system pressure and material construction. In this case, the F_p does not influence the cost deviations from the base conditions because the maximum pressure of the designs is 7 bar which is out of the F_p equation range (between 10 and 100 barg [gauge pressure]) proposed by Turton et al. [88]. Thus, the actual purchased equipment cost *(PEC)* is expressed by:

$$PEC = PEC^0 F_p F_m \tag{5.2}$$

where PEC^0 is calculated by Equation 4.2, F_p is assumed to be 1 and F_m is given in Table 5.7.

Table 5.7: Coefficients for the calculations of bare module cost factor in Equation (5.4).

Component	F_m	B_1	B_2
Centrifugal Pumps	1.5	1.89	1.35

The equation for updating PEC due to changing economic conditions and inflation [88] is calculated by Equation 4.4. The data of cost index is taken from info share of New Zealand statistics [129] in Table 5.8.

Table 5.8: Capital goods price index for the calculation of updated PEC prices.

Components	Year	
	2001	2014
Centrifugal Pump	1048	1381
Radial turbine	1064	1088

The costs of heat exchangers are calculated by Aspen EDR (Exchanger Design & Rating) version 8.4 software [25]. The cost is estimated by the Aspen software once all the geometry of each component part of the heat exchanger has been calculated. The calculations consider F_p and F_m. According to AspenTech support centre [25], the exchanger costs include three elements, which are the material cost, the labour cost, and the mark-ups on material and labour. It is assumed that the heat exchanger costs calculated by Aspen software have considered the direct and indirect costs, so that the results are equal to bare module equipment cost (C_{BM}).

Figure 5.5 shows the results of PEC calculation in three alternatives. The PEC of the Std designs with n-pentane and R245fa is comparable at 25,606 and 22,994 thousand USD. However, the PEC of Rec design with n-pentane is significantly higher PEC. This occurs because of an additional recuperator cost and because the smaller temperature difference in evaporator and condenser causes a higher size of heat exchangers and heat transfer requirement, particularly in the condenser. The PEC of the Rec design is 1.76 times the PEC of Std design with the same working fluid (n-pentane). Therefore, the Rec design with n-pentane has to be eliminated for the consideration as not being feasible for further investigation.

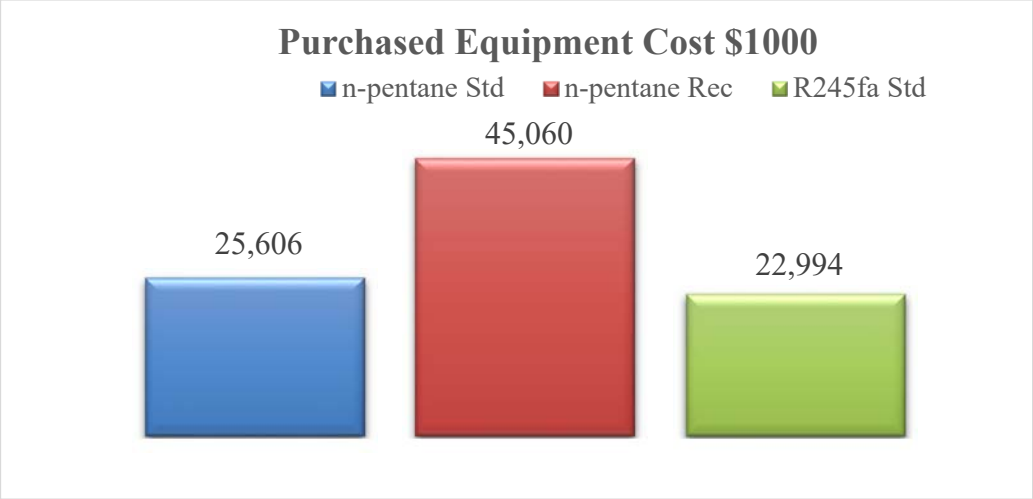

Figure 5.5: Total purchased equipment cost estimated in 2014 USD

5.3.5.2. TPC

The TPC consists of two main cost categories: plant capital costs and steam gathering system costs. The plant capital costs are total cost of the bare module cost for each piece of main equipment in the plant. Equation 5.1 is used to evaluate the grassroots cost that calculates the TPC.

The turbine and pump bare module costs are calculated based on the module costing technique (MCT) [88]. C_{BM} is the sum of the direct and indirect costs and it is defined as follow:

$$C_{BM} = PEC\ F_{BM} \tag{5.3}$$

where F_{BM} is bare module cost factor incorporating four factors: direct costs, indirect costs, contingency fees, and auxiliary facilities. F_{BM} for turbine with material of carbon steel is 3.5 [128] and the F_{BM} for pump is calculated by:

$$F_{BM} = B_1 + B_2 F_p F_m \tag{5.4}$$

where B_1, B_2 and F_m values are given in Table 5.7 and the pressure factor (F_p) is assumed to be 1. The C_{BM} of heat exchangers is calculated by Aspen EDR software [25].

The steam gathering system costs are assumed at 30 USD per kW according to NGGPP in 1996. The update of the cost used capital goods price index with asset type: other fabricated metal products from info share of New Zealand Statistics [129]. The price index raises 36.3% from 1996 to 2014, therefore the cost in 2014 is 41 USD per kW.

Table 5.9 displays the results of TPC and specific investment cost (SIC). The SIC is calculated by dividing TPC with the optimal W_{net}. The SIC of Std designs with n-pentane and R245fa is 4,069 USD/kW and 3,743 USD/kW, respectively. These values are fairly close to those shown by Quoilin et al. Quoilin, Van Den Broek [7] that the ORC module costs for the geothermal application with the size of few MWs is 3,000 EUR/kW (about 3,750 USD/kW). Roos et al. Roos, Northwest [131] reported that the ORC system cost has installed costs ranging from 2000 USD/kW to 4000 USD/kW. Jung et al. [97] reported that most of the systems (about 90%) assembled with the refrigerant system components have the specific capital cost ranging from 2,000 USD to 3500 USD/kW. The SIC of ORC system coupled by geothermal resources is a bit higher due to the additional costs for steam gathering system.

Table 5.9: Total plant costs (TPC) and specific investment costs (SIC) of the three optimal ORC designs.

Cycle Configuration		TPC (USD)	SIC (USD/kW)
n-pentane	Std	45,687,039	4,069
R245fa	Std	41,719,472	3,743

5.3.5.3. Geothermal development analysis

The geothermal field in this chapter is located in the Taupo Volcanic Zone (TVZ) in New Zealand where several geothermal power plants have been constructed.

Therefore, the drilling cost is assumed for a known field where the expected value is taken from Table 5.2 at 1170 USD per kW.

The construction time of the geothermal power plant in this chapter is assumed to take about 3 years. The plant can produce the electricity in the fourth year at the Wnet rate, multiplied by a plant availability factor. The plant available factor for commercial geothermal plants is around 90% [18].

5.3.5.4. Profitability analysis

5.3.5.4.1. Calculation methodology

Net present value (NPV) and discounted payback (DPB) are used to evaluate profitability of the projects. The NPV is calculated in Equation 2.5. The estimation of plant lifetime is about 30 years [143]. The electricity revenue price is about 0.083 USD/kW with 3% of electrical price increment per year over the plant lifetime [97]. According to geothermal energy association [141], the total operation and maintenance (O&M) costs is expected to average 0.024 USD/kWh where the cost includes operation cost of 7 USD/MWh, power plant maintenance of 9 USD/MWh and steam field maintenance & make-up drilling costs of 8 USD/MWh. The total O&M costs are based on the size of the power plant from 15 to 100 MW. However, the O&M costs are fairly variable and depend on the size of the power plant as well as various resource and site-specific characteristics. The value of inflation rate was taken from New Zealand Consumer Price Index (CPI) where the inflation rate has averaged around 2.7% since 2000 [135]. The financial model used the assumptions that 20% of TIC is expensed in the first two years for exploration and confirmation of resources and the remaining 80% is invested in the third year. Table 5.10 summarises the

assumption parameters used for calculating NPV and DPB in this study. The electrical price increases started from the first year of the plant investment.

Table 5.10: Assumptions for calculating NPV and DPB

Plant lifetime	30 years
Plant availability	90%
Electricity revenue unit price	USD $0.083/kWh
O&M cost	USD $0.024/kWh
Annual electricity price escalation	3.0%
Inflation rate	2.7%
Discount rate	10%

5.3.5.4.2. Calculation results

Table 5.11 shows the profitability factors for the two candidate designs. Both designs have almost the same values of TCI, NPV and DPB, where the design using R245fa has better economic performance than design with n-pentane. The NPV of the designs with n-pentane and R245fa is USD 34,296,419 and USD 37,059,060 respectively. The DPB of both designs is consistent between 15 years and 16 years. The total cost of investment ranges from USD 58,824,956 to USD 54,759,837.

Table 5.11: The results of NPV and DPB for two design alternatives.

Cycle Configuration	TCI (USD)	NPV (USD)	DPB (Years)
n-pentane Std	58,824,956	34,296,419	15.96
R245fa Std	54,759,837	37,059,060	15,00

5.3.6. EROI analysis

5.3.6.1. Calculation methodology

The energy return on investment is given by general form [144]:

$$EROI = \frac{E_{out}}{E_{in}} \tag{5.5}$$

where E_{out} is the summation all energy produced for a given timeframe and E_{in} is the sum of direct and indirect energy costs. Figure 5.6 shows how the energy flows vary

and cumulate over the energy facility's lifetime [145]. The energy facility requires a total energy input for construction ($\dot{E}_c$) over the construction time (t_c). Once the energy facility starts producing energy, a constant gross flow of energy at rate $\dot{E}_g$ over the whole lifetime t_L. During the production time, an energy flow ($\dot{E}_{op}$) is required to operate and maintain the energy facility. Finally, an energy flow ($\dot{E}_d$) is required for decommission at the end of the project lifetime. Assuming that investments and returns from those investments occur in the same time period, the EROI can be calculated as follows:

$$EROI = \frac{E_g}{E_c + E_{op} + E_d} \tag{5.6}$$

Because the availability of energy data is limited for high level energy analysis and pricing data is more readily available than energy data, a conversion approach using energy intensity value is often used to convert dollars to energy units for most of the energy assessment calculations. The average energy intensity for the U.S. economy in 2005 was 8.3 MJ/USD [145]. They recommended to use consumer price index to deliver that value for another nearby year. The consumer price index from Bureau of Labour Statistics, U.S. Department of Labour was used. The conversion result of the average energy intensity in 2014 was 6.85 MJ/USD. In the calculation of this work, the decommissioning energy (E_d) is neglected from the calculations because the pricing data for decommission of the four plant alternatives at the end of the plant lifetime is practically equal and does not impact the optimal selection.

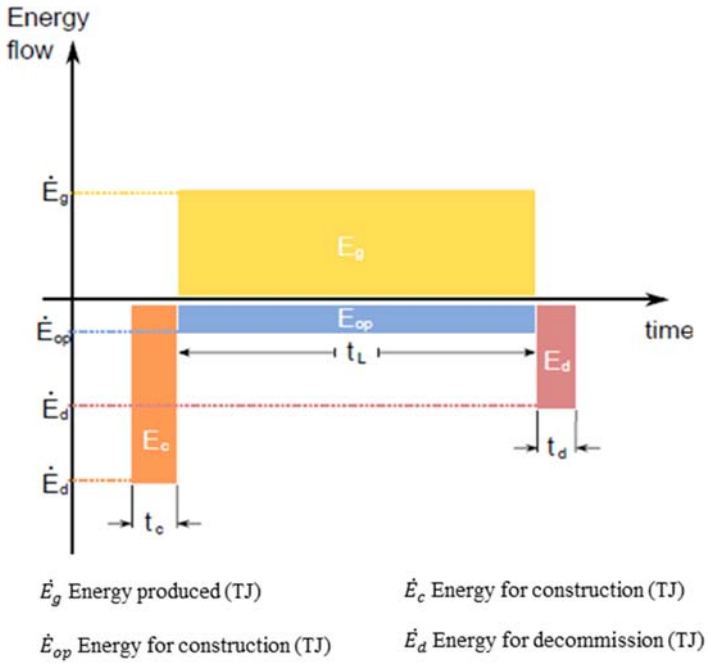

Figure 5.6: Energy inputs and outputs for an energy facility [145]

5.3.6.2. Calculation results

The EROI for Std n-pentane and Std R245fa is 5.35 and 4.83, respectively. Table 5.12 details the calculated results of E_g. E_c, and E_{op} for each design alternative. The EROI of Std n-pentane is higher than EROI of R245fa, because the design has a higher system pressure and mass flow rate influencing to a higher pump power, resulting a higher value of E_{op}.

The study of EROI calculation results with EROI literature reveals that the results of some researchers are fairly close to the EROI calculated in this paper. Frick, Kaltschmitt [146] used current data from European geothermal plants to calculate an average EROI of 4.5 for low temperature binary geothermal plants. Southon and Krumdieck [147] calculated that EROI of small geothermal power plants had an EROI of 3.2 and 2.4 for the Waikite system and the Chena power plant, respectively. Icerman et al. Icerman [148] calculated that the EROI of a flashed steam

geothermal plant between 7.0 and 11.3. The flash steam geothermal plants have a higher EROI than binary geothermal power plants.

Table 5.12: The results of EROI calculation for two design alternatives.

Item	Values		Units
	Std n-pentane	Std R245fa	
E_g	10,729	10,949	TJ
E_C	403	375	TJ
E_{op}	1,604	1,892	TJ
EROI	5.35	4.83	-

5.3.7. Acceptable designs

The designs with n-pentane and R245fa are acceptable designs for this potential geothermal resource. However, considering the superior availability of n-pentane over R245fa in the market, the Std design with n-pentane is preferable.

5.4. Conclusion

The main objective of this chapter was to propose a design methodology for a new binary geothermal power plant with considering technical, thermodynamic, EROI and economic analyses. The methodology guides designers to select the best designs among alternatives. The work in this chapter still deals with uncertainty cost analyses, as the scope of cost breakdown included in the capital cost is quite variable and unclear in the preliminary study. Furthermore, the drilling cost has higher uncertainty due to resource-specific characteristics. Analysing geothermal investment costs is a long and difficult process. The change of assumptions in further analyses will impact the change of profitability and EROI results. However, this methodology includes a breakdown of typical costs of geothermal power plant projects.

The design methodology is applied to the existing geothermal well located in the Taupo Volcanic Zone (TVZ) in New Zealand. Three common working fluids n-pentane, R245fa and R134a and two cycle configurations Std and Rec cycles are analysed. The results of analyses indicate that the design using R134a has the lowest net electrical power output (Wnet) at 6,980 kW. The PEC of the Rec design is significantly expensive. The total PEC of Rec design is about 1.76 times PEC of Std design with the same working fluid. Therefore, both designs are not considered for further analyses. Furthermore, the Std designs with n-pentane and R245fa are feasible to be implemented in the geothermal resource. The profitability analysis reveals that the Std design with R245fa is more economical than the Std design with n-pentane. The different NPV and DPB of both designs are very small at 8 % and 6.4 %, respectively. The EROI comparison of both designs shows that the EROI of n-

pentane Std design is higher than the EROI of R245fa Std design at 5.35 and 4.83, respectively. The Std design with n-pentane is preferable design considering the superior availability of n-pentane over R245fa in the market,.

5.5. Nomenclature

C	Cost (USD)
DPB	Discounted payback (Year)
E_c	Energy for construction (TJ)
E_d	Energy for decommission (TJ)
E_g	Energy produced (TJ)
E_{op}	Energy required for operation and maintenance (TJ)
EDR	Exchanger Design & Rating
EROI	Energy return on investment
F	Factor
I	Cost index
In	Input
IRR	Internal rate of return
Old	Base time
Out	Output
ORC	Organic Rankine cycle
$\dot{m}$	Mass flow rate (kg/s)
New	Time when the cost is desired
N	Equipment lifespan
NPV	Net present value (USD)
P	Pressure (bar)
Δp	Pressure drop (bar)
PEC	Purchase Equipment Cost (USD)
q	Interest rate (%)
R	Annual income (USD)
Rec	Recuperative
Std	Standard
sh	Superheating (^{0}C)
T	Temperature (^{0}C)
TCI	Total capital investment (USD)
TPC	Total plant cost ($)
TVZ	Taupo Volcanic Zone
W_{fans}	Net power of fans (kW)
Wnet	Net electrical power output (kW)
W_p	Net power of pump (kW)
W_t	Net power of turbine (kW)
Y	The power of pump or radial turbine (kW)

Subcripts:

ACC	Air cooled condenser
BM	Bare module
C	*Critical*
cond	Condenser
ex	Exit
geo	Geothermal
GR	Grassroots
in	Inlet
m	Material
max	Maximum
n	number of main components
o	Ambient condition
p	Pressure
P	Pump
rej	Rejection
T	Turbine
wf	Working fluid

Chapter 6 - Design Methodology for Designing ORC Plants using Design to Resource (DTR) Method

The aim of this thesis is to develop an approach for a feasibility study for flexible design (FSFFD) for the ORC development, which includes thermodynamic, component, resource, and cost considerations. This chapter explains a design methodology for designing and optimising the ORC systems using the "design to resource" (DTR) method. To illustrate the implementation of design methodology, a lab-scale ORC is evaluated as a case study. The experiments were conducted to obtain the data for identifying the heat transfer coefficients of the real processes and validating the simulation model results. Chapter 5 explored the design methodology for assessing a potential geothermal resource with low-to-moderate temperatures that will be installed by the binary geothermal power plant. The methodology discussed in this chapter is a deeper design methodology which considers the selection of main components and heat resource as constraints of the design optimization. The methodology uses the selection of main components as a starting point for designing and optimising the ORC systems. Chapter 3 and 4 discussed the effect of main design variables on the design performance based on the thermodynamic and economic analyses.

6.1. Introduction to DTR method

The DTR method considers selection and design as two terms that are interchangeable during the design process. According to Jaluria et al. [16], the selection and design must be employed simultaneously in the development of a

system. Design involves basic concepts, modelling and evaluating different designs. A final design is obtained by fulfilling given requirements and constraints. Based on design results, the requirements and specifications of the desired component or equipment are matched with whatever is available in the markets in the selection process. If an item possessing the desired characteristics is not available, the design is used to redesign one that is acceptable for the specific purpose. The novel aspects of the DTR method in the ORC design are the setting of technical constraints on an available heat resource and turbine selections, which are a reflection of realistic engineering development projects, and focusing the cost optimization on the most cost-affected components - the heat exchanges. The objective of the DTR method is to obtain the best design, which is the closest match to the resource and the most cost-effective.

Our lab-scale ORC plant, which uses the exhaust gas from a 30 kW Capstone gas turbine, is used as a case-study for the DTR method implementation. The plant was built up over the course of a Mechanical Engineering Undergraduate Final Year Project. The main design process was selecting available main components in the market, and trying to meet a goal of generating 1 kW due to the limiting factor of turbine availability. The DTR method is used to design a waste heat ORC from the Capstone gas turbine and investigate the degree of under or over-designed components when the selection of components is limited. Thermo-economic investigations are required to optimize the plant performance. The investigation has been conducted by conducting experiments and developing numerical models. The main components are modelled in detail according to real products. The models are validated by experimental data to have more reliable prediction of the system performance.

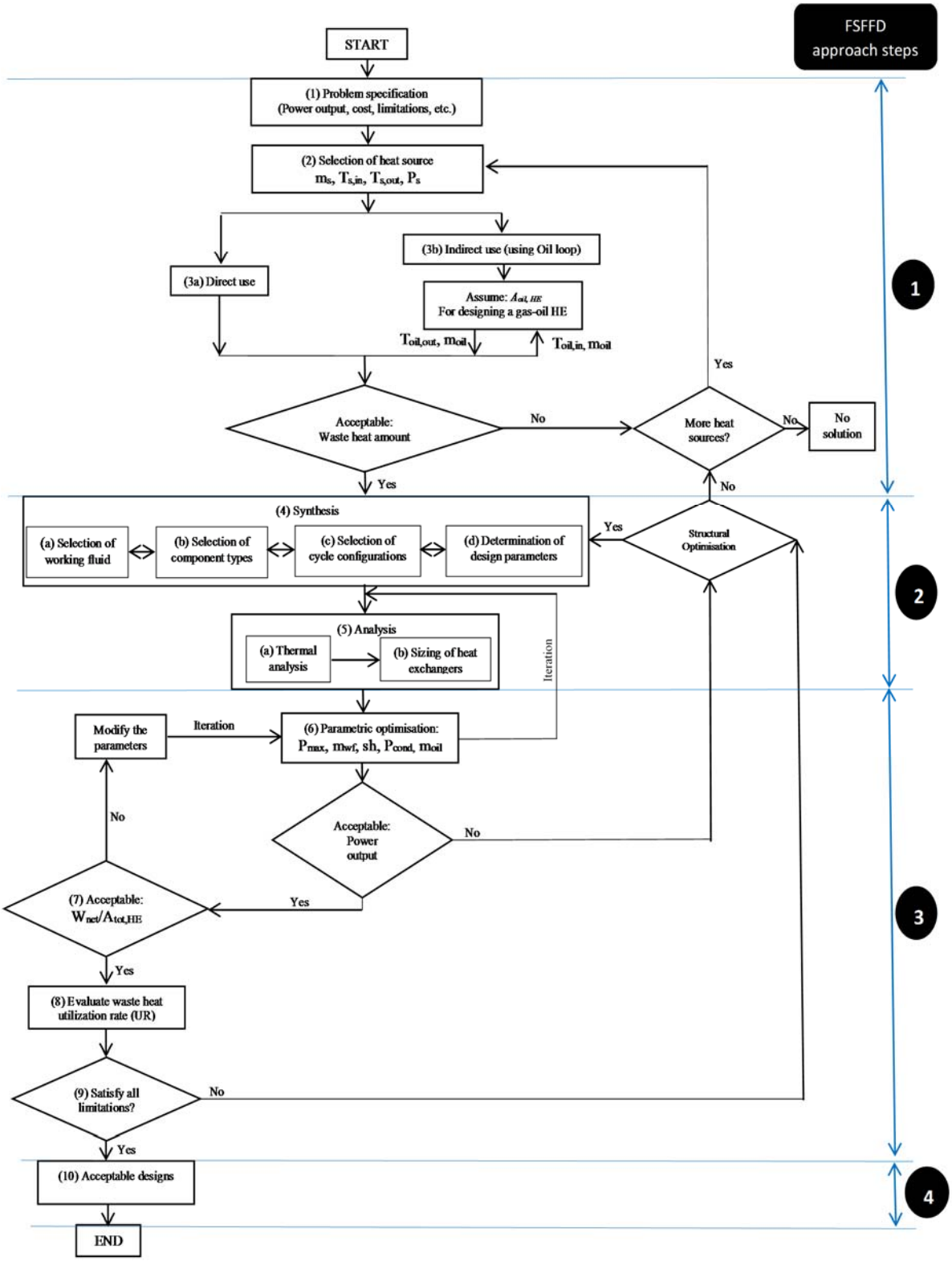

Figure 6.1: Flow chart for developing the ORC designs based on DTR method

6.2. DTR Methodology

Figure 6.1 shows a flow chart of the proposed design methodology based on the DTR method for WHR applications. The design methodology considers all of five main design variables of the ORC design. In general, the methodology consists of four main steps of the FSFFD approach that have been explained in Chapter 1. The main steps of the FSFFD approach are (1) initial step, (2) simulation step, (3) evaluation step and (4) result step. The breakdown steps of the proposed methodology is outlined in the following steps:

1. Problem specification:

   The goals and some limitations of the cycle and each component are fixed. Two important goals are power output and optimal cost. These goals have to be satisfied with all the steps in the methodology. The limitations must be fulfilled in the cycle in order to achieve the target of power output.

2. Selection of heat source:

   The possible heat sources need to be evaluated to identify sources with higher heat power level using energetic and/or exergetic studies. The maximum heat available in the exhaust gas is that heat rejected under the hypothesis that the exhaust gas is cooled to the ambient temperature at 25^0C [149]. However, in some cases the exhaust gas temperature ($T_{s,out}$) of waste heat resources requires to be above the dew temperature level to prevent corrosive effects [76]. The selected heat sources must have the available heat power higher than power output objective. If the amount of available waste heat is less than the requirement, the design problem has no solution.

3. Selection of heat recovery setup:

   Two different setups can be used in waste heat recovery (WHR) system [19]:

(3a) *Direct use*: direct heat exchange between the waste heat source and the working fluid

(3b) *Indirect use*: a heat transfer fluid loop is integrated to transfer the heat from the waste heat site to the evaporator.

Most commercial ORC installations for WHR use an intermediate heat transfer loop because direct use faces a number of problems [7]:

- The working fluid can deteriorate when its maximum chemical stability temperature is reached at high temperatures of operation (e.g. during start-up and transients)
- The controllability and the stability of the systems are difficult to achieve.

The heat transfer area of a gas-oil heat exchanger ($A_{oil,HE}$) is assumed based on the objective of power output and an oil pump flow rate (m_{oil}) used in the oil loop. Therefore, the oil-loop can deliver the heat power according to the ORC system requirement.

4. Synthesis:

Synthesis is concerned with combining separated cycle elements into a thermodynamic cycle. This step is similar to step 2 of the methodology steps explained in Section 5.2. The step consists of four-cycle elements that should be conducted simultaneously.

a. *Selection of working fluid*: The selection of the most appropriate working fluid is a very important step in designing ORC systems because the used working fluid type influences a produced power output, sizes of the components, system stability, cost, safety and environmental issues. A large number of working fluids have been investigated in the literature, but only a few of them are used in the ORC units for waste heat recovery.

To obtain a good working fluid candidate with good availability and low cost, the common commercial working fluids are recommended. The commercial working fluids and detail working fluid selection were explained in Chapter 2. The commercial working fluids are listed in Table 2.5.

b. *Selection of component types*: Figure 6.2 displays optimum operating map for three turbine technologies for WHR application [150]. The turbine can be categorised into two main types: turbomachines (the axial turbine and the radial inflow turbine) and positive displacement types (piston, scroll, screw and vane expanders). The turbomachines are not suitable for very small-scale units because their rotating speed increases significantly with decreasing turbine output power [7]. The positive displacement types are good for small scale ORC units, while technically mature turbomachines are available on the market for large ORC units. A small scale ORC plant requires a much lower flow rate with the same pressure, positive displacement pumps are more suitable to be used for this purpose.

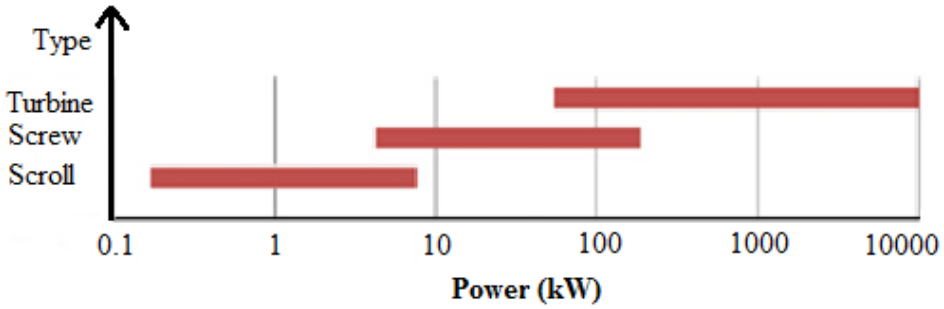

Figure 6.2: Selection of turbine technologies according to the power output in WHR.

c. *Selection of cycle configurations*: Four types of cycle layouts are available for ORC cycle: 1) subcritical cycle without a recuperator, 2) subcritical

cycle with a recuperator, 3) supercritical cycle without a recuperator, and 4) supercritical cycle with a recuperator. The common ORC cycle for low-temperature heat resource is the subcritical cycle. The supercritical cycle is only justified for lower critical temperature working fluids with a high heat source temperature if it can improve the match between temperature profiles in the evaporator and if there is no limitation on the high pressure [92]. A recuperator is only used when $T_{s,out}$ has any temperature limitation. This has been explained in Chapter 5.

d. *Determination of design parameters*: the initial values for creating a thermodynamic cycle may use the assumption values in Table 5.1.

5. Analysis

This step is similar to step 3 of the methodology steps in Chapter 5 consisting of thermal analysis and sizing of heat exchangers. The Wnet is calculated using the Equation 2.3. The specific power consumed by fans (W_{fans}) is neglected if the system uses water-cooled condensers because the water-cooled condensers use a significantly lower power than the air-cooled condensers. The sizing of heat exchangers is skipped in the analysis step when the design requires no design modifications of the heat exchangers.

6. Parametric optimization

The parametric optimization in this methodology involves five decision parameters. An additional decision parameters is mass flow of oil loop (m_{oil}) if the indirect use is selected for recovering the waste heat. Other four decision parameters have been explained in Chapter 2 and 5. The iteration is generally necessary to obtain an acceptable power output. If the power output obtained from the parametric optimization does not satisfy the target of power output

[151], structural optimization and/or heat sources selected will have to be reconsidered. If not, the design problem has no solution. This optimization is similar to step 4 of the methodology in Chapter 5.

7. Acceptable: $W_{net}/A_{tot,\ HE}$

   The ratio of total net power output (W_{net}) to total heat transfer area ($A_{tot,\ HE}$) is suggested as an objective function to obtain the best cost-effective design [23]. This is based on the assumption that the total cost of the heat exchanger area dominates largely to the total cost of ORC especially for the system utilizing a low temperature of waste heat.

8. Evaluate waste heat utilization rate

   In order to further analysis of heat recovery capability of each ORC design, the concept of waste heat utilization rate (UR) is applied. This concept is able to indicate how match between the design and the heat resource. The waste heat UR is the ratio of heat absorbed by the ORC system to maximum available heat power in a heat source [149].

9. Any limitations have been fulfilled by the designs:

   Other pre-imposed limits and targets must be evaluated before determining the best final design. In this last step, other feasibility criteria such as limitations of component operating conditions and/or maximum installation cost could be evaluated and the best final design must fulfil all the limits that have been fixed in the first step.

10. Acceptable designs

    The last step is to conclude the acceptable designs among several design alternatives.

The methodology is implemented in the small-scale ORC plant in our laboratory to illustrate the methodology implementation in redesigning the heat exchangers of the plant.

6.3. The ORC plant in the thermodynamic laboratory

The small-scale ORC plant in our laboratory was built as a preliminary design to develop a better design of an ORC plant. The main components of the plant are chosen from available items in the market. An ORC system consists of individual constituents that interact with each other. The design performance sometimes cannot be achieved in a real operation due to some reasons: inappropriate size of components, inappropriate piping system and unpredicted working fluid behaviour inside components. Thus, study of the overall ORC system behaviour is required to evaluate the entire system performance.

6.3.1. Description of the ORC plant for WHR application

Figure 6.3 shows the principle schematic diagram of the bottoming ORC for WHR of the Capstone gas turbine. The ORC system consists of four separate fluid circuits: exhaust gas flow (in red line), thermal oil circuit (in blue line), ORC circuit (in black line) and cooling water (in green line). All circuits are connected through heat exchangers. The whole system operates as follows: the exhaust gas from the Capstone gas turbine rejects heat to thermal-oil circuit through a gas-oil HE and then is discharged to atmosphere; working fluid in vapour state (point 1) flows into the scroll expanders, and its enthalpy is converted into expansion power; low pressure vapour (point 2) exits from scroll expander and flows into condenser where it uses cooling water to condense working fluid into saturated liquid (point 3), the buffer tank after the condenser is used to maintain sufficient liquid therefore pump does not run

dry; working fluid is pumped into high pressure state (point 4), and then is boiled through evaporator and leaves as a superheated vapour (point 1). Thus a whole cycle completes. The cycle is repeated in a closed loop to generate continuative power.

The current ORC system consists of a scroll expander, a feed pump, an oil pump, oil-working fluid heat exchanger (evaporator), a water-working fluid heat exchanger (condenser) and a gas-oil heat exchanger. The main characteristic parameters of these components are shown as follows:

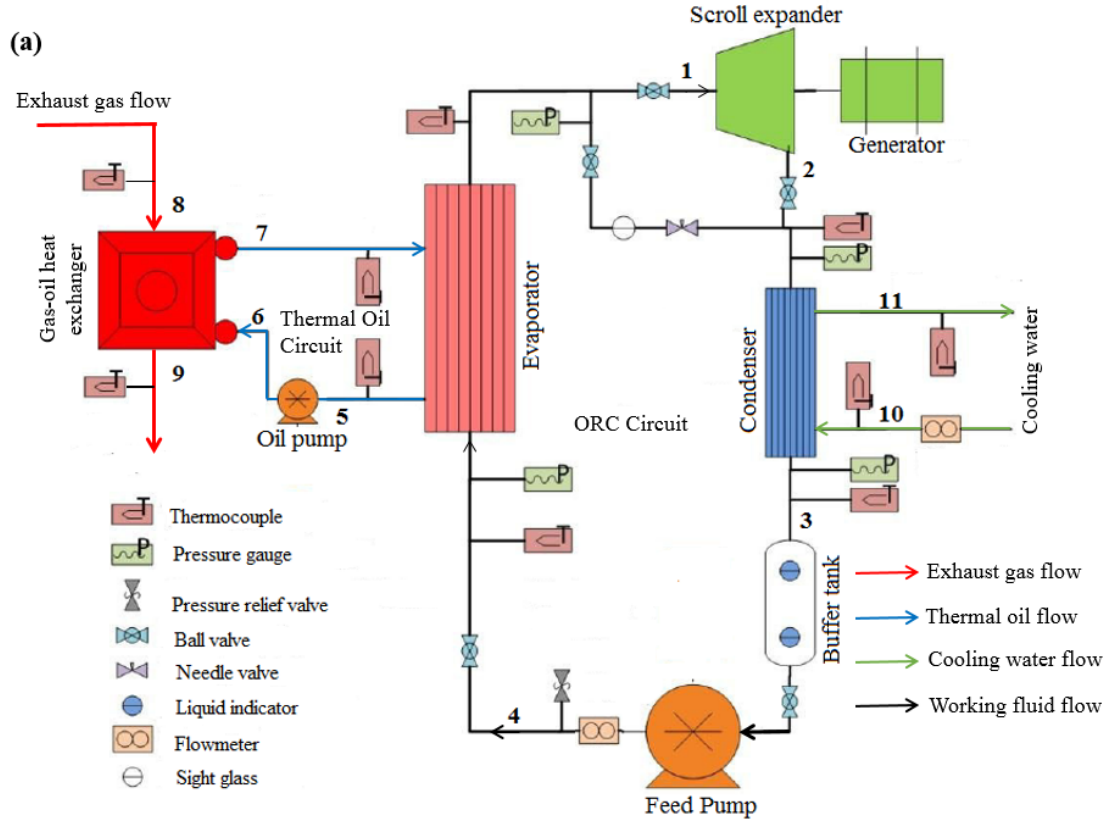

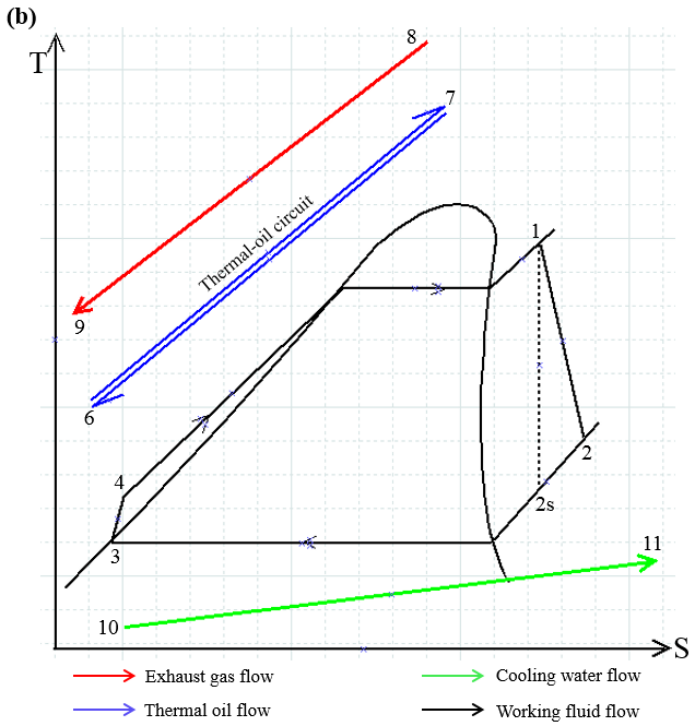

Figure 6.3: Schematic diagram (a) and T-S diagram of the ORC system for WHR (b)

Scroll expander

The selected scroll expander is designed to produce power up to 1 kW for the expansion generators in the WHR systems. It is characterized by an expansion ratio of 3.5:1 and displacement of 12 cc/rev. a high expansion ratio is an advantage in ORC cycles, where pressure ratios are generally higher than in a refrigeration cycle. The patented scroll expander is rated up to 1 kW, based on a maximum inlet pressure of 13.5 bar. A speed of 3600 RPM and inlet temperature of 175 ^{0}C are a maximum limit of the scroll expander operation. Air Squared from USA manufactures the scroll expander.

Figure 6.4: Scroll expander

Feed Pump

The pump is a positive displacement plunger pump. The pump characteristics are provided in Table 6.1.

Table 6.1: Feed pump characteristics

	Model	2SF22ELS
	Manufacturer	Cat Pumps
	Flow	8.3 l/min
	Max. Discharge pressure	140 bar
	Max. RPM	1725

Oil Pump

The pump is a positive displacement gear pump. Its characteristics is provided in Table 6.2.

Table 6.2: Oil pump characteristics

	Model	AZPF - 12/011 RH030KB
	Manufacturer	Bosch Rexroth
	Displacement	11 cm^3/rev
	Max. Operating pressure	280 bar
	Max. RPM	3500
	Direction of Rotation	Clockwise
	Hydraulic fluid temperature range	Max. $+110^0$ C with FKM seal

Heat exchangers

a. Evaporator and condenser

Table 6.3: Evaporator and condenser characteristics

	Specification	Evaporator	Condenser
	Manufacturer	Kaori	Kaori
	Type	K205 / single pass plate heat exchanger	K095 / single pass plate heat exchanger
	Number of plate	60	40
	Total surface area	6.4 m^2	1.805 m^2

b. A gas-oil heat exchanger (a gas-oil HE)

Table 6.4: Evaporator and condenser characteristics

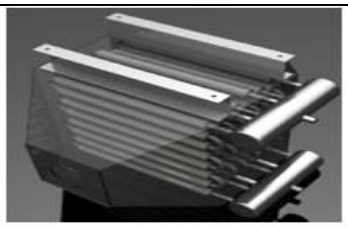 	Manufacturer	Advance boiler service
	Type	Finned tube heat exchanger
	Flow direction	Cross flow
	Shell dimension [mm]	360 x 662 x 545
	Length of straight tube part	500 mm
	Total oil-side surface area	1.025 m^2
	Total gas-side surface area	23.19 m^2

Table 6.5 shows the accuracy of the instrumentation and measurement used in the current ORC plant in our laboratory.

Table 6.5: Accuracy of instrument devices as specified by the manufacturers [152]

Component	Accuracy
Thermocouples	K-type $\pm$ 1.5^{0}C, T-type $\pm$ 0.5^{0}C
Pressure transducers	LP side $\pm$ 14 kPa, HP side $\pm$ 28 kPa
Electrical clamp meter	$\pm$ 2.5% of measured value

6.3.2. Modelling the ORC system

This section explains the models of the different components of the ORC system under investigation. The modelling approach consists of developing a semi-empirical model for a scroll expander and LMTD method for heat exchangers. The model uses R245fa as a working fluid to represent a zeotropic mixture (M1) used in the ORC system. The M1 consists of R245fa and R365mfc with a mole fraction of 50% and 50%, respectively. Both fluids have almost similar properties. Table 6.6 shows the properties of both fluids. The simulation model is particularly complex. Each component of the system is developed in subprogram using EES software [24]. Each

subprogram consists of input and output variables and a certain number of equations. The main program of the system is built by interconnecting the subprograms of the different components. This represents the real physic connections that occur between components as shown in Figure 6.3.

Table 6.6: Properties of fluids used in the experiments and modelling [153]

Fluid	Molecular weight (g/mol)	Normal Boiling point (^{0}C)	Critical pressure (MPa)	Critical temperature (^{0}C)
R245fa	134.05	15.14	3.65	154.01
M1	139	24	3.46	167.30

6.3.2.1 The scroll expander model

The semi-empirical model of a scroll expander used here-under is adopted from one proposed and validated by Lemort et al. [154]. In this model, the evolution of the fluid through the expander is decomposed into the following steps (as shown in Figure 6.5):

(a) Adiabatic supply pressure drop (su →su,1)

(b) Isobaric supply colling-down (su,1→su,2)

(c) Adiabatic and reversible expansion to the "adapted" pressure imposed by the built-in volume ratio of the machine (su,2→ad)

(d) Adiabatic expansion at a constant machine volume (ad→ex,2)

(e) Adiabatic mixing between supply and leakage flows (ex,2→ex,1)

(f) Isobaric exhaust cooling-down or heating up (ex,1→ex)

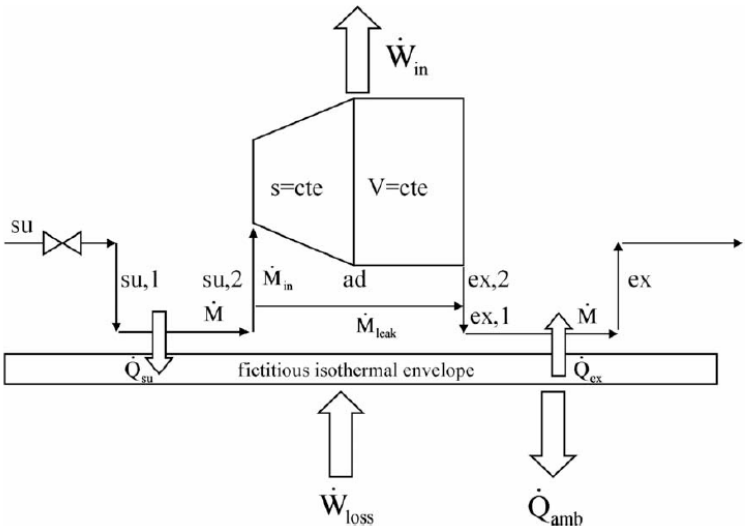

Figure 6.5: Conceptual scheme of the expander model

One working cycle of the scroll expander consists of three processes such as suction, expansion and discharge. The internal power ($\dot{W}_{in}$) produced by the machine is the summation of the suction, the expansion, and discharge powers. The internal power ($\dot{W}_{in}$) is expressed as:

$$\dot{W}_{in} = \dot{M}_{in}\left[(h_{su,2} - h_{ad}) + v_{ad}(P_{ad} - P_{ex,2})\right] \quad (6.1)$$

where h_{ad}, v_{ad}, and P_{ad} are the specific enthalpy, the specific volume and the pressure of the fluid at the end of isentropic part of the expansion, respectively. $h_{su,2}$, $P_{ex,2}$ and $\dot{M}_{in}$ are the specific enthalpy at beginning of adiabatic processes and the pressure of fluid at the end of adiabatic processes and the internal mass flow rate, respectively. The internal mass flow rate ($\dot{M}_{in}$) is the difference between the mass flow rate entering the expander ($\dot{M}$) and the leakage mass flow rate ($\dot{M}_{leak}$).

The internal mass flow rate is obtained from a ratio between volume flow rate ($\dot{V}_{s,T}$) and the specific volume of the fluid ($v_{su,2}$) after pressure drop and cooling down. The volume flow rate ($\dot{V}_{s,T}$) is the swept volume ($V_{s,T}$) multiplied by the expander rotational speed (N). These correlations are shown as follows:

$$\dot{M}_{in} = \dot{M} - \dot{M}_{leak} = \frac{\dot{V}_{s,T}}{v_{su,2}} = \frac{N.V_{s,T}}{v_{su,2}} \quad (6.2)$$

The leakage mass flow rate is calculated by applying the mass and energy conservation equations through a simply convergent nozzle, whose throat diameter is the equivalent supply port diameter (d_{su}).

The expander mechanical power ($\dot{W}_T$) can be divided into the internal expansion power and the mechanical losses ($\dot{W}_{loss}$). These losses are lumped into one unique mechanical loss torque T_{loss}, that is a parameter to identify. The expander mechanical power is expressed by

$$\dot{W}_T = \dot{W}_{in} - \dot{W}_{loss} = \dot{W}_{in} - 2\,\pi\,N\,T_{loss} \quad (6.3)$$

where N is rotating speed of the expander shaft.

The ambient losses are calculated by introducing a global heat transfer coefficient AU_{amb} between the envelope and the ambient:

$$\dot{Q}_{amb} = AU_{amb}(T_w - T_{amb}) \quad (6.4)$$

The uniform temperature of a fictitious envelope (T_w) is computed by establishing a steady-state heat balance on this envelope, as proposed by Winandy, Saavedra [155]:

$$\dot{W}_T - \dot{Q}_{ex} + \dot{Q}_{su} - \dot{Q}_{amb} = 0 \quad (6.5)$$

where $\dot{Q}_{su}$ and $\dot{Q}_{ex}$ are supply and exhaust heat transfers that are calculated by introducing a fictitious metal envelope of the uniform temperature (T_w). The Figure 6.6 shows inputs, outputs and parameters of the semi-empirical model.

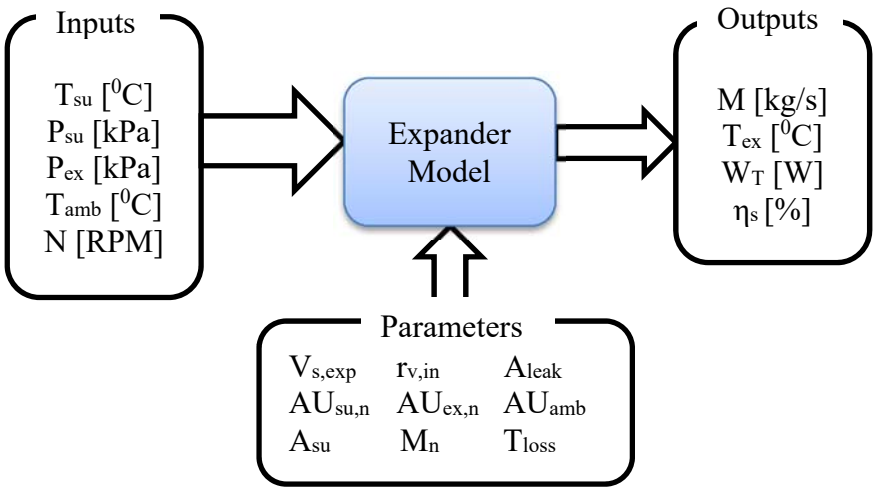

Figure 6.6: Semi-empirical model

6.3.2.2. Evaporator and condenser models

The evaporator and condenser use the plate heat exchangers and they are modelled by means of the LMTD method for counter-flow heat exchangers. The heat exchanger is subdivided into three zones. Every zone is characterized by a heat transfer area (A) and a heat transfer coefficient (U). The modelling paradigm in the case of the evaporator is shown in Figure 6.7 [48].

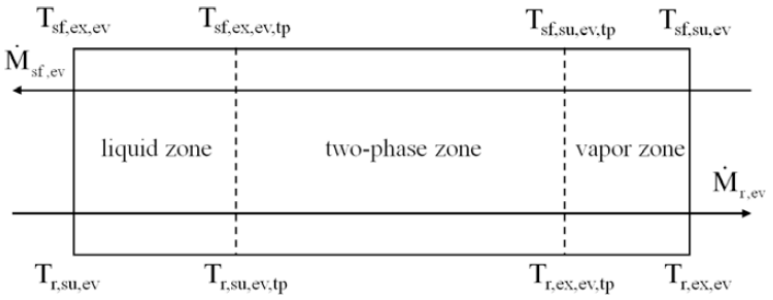

Figure 6.7: Three-zone modelling of the evaporator

The heat transfer coefficient U in each zone is calculated by considering two convective heat transfer resistances in series (refrigerant and secondary fluid sides).

$$\frac{1}{U} = \frac{1}{h_r} + \frac{1}{h_{sf}} \tag{6.6}$$

The total heat transfer area of the heat exchanger is summed the respective heat transfer area of each zone:

$$A_{tot} = A_l + A_{tp} + A_v \quad (6.7)$$

In the present work, the pressure drops are neglected in both evaporator and condenser models, because no accurate differential pressure sensors were installed on the heat exchangers in the experimental setup and the value is relatively very low.

6.3.2.2.1. Single-phase

Forced convection heat transfer coefficients of a plate heat exchanger are typically expressed by calculating the Nusselt number [156]:

$$Nu = 0.2536\ (Re)^{0.65} Pr^{0.4} \quad (6.8)$$

6.3.2.2.2 Two-phase

In open access literature, there are only limited available data on boiling and condensation heat transfer coefficients in a vertical plate heat exchanger using fluid M1. Therefore, the experiment results using R-410A flowing in a vertical plate heat exchanger were used in the models. Quoilin et al. [48] used the same correlations in the modelling of their test rig using R245fa.

The boiling heat transfer coefficient is estimated by the Hsieh correlation [157], created for the boiling of refrigerant R410a in a vertical plate heat exchanger. The boiling coefficient is considered as constant during the whole evaporation process and is calculated by:

$$h_{tp} = C\ h_l\ Bo^{0.5} \quad (6.9)$$

where *Bo* is the boiling number and h_l is the all-liquid non boiling heat transfer coefficient. C is identified from experimental results.

The condensation heat transfer coefficient is estimated with an expression derived from Kuo correlation [158], created for the condensation of refrigerant R410a in a vertical plate heat exchanger.

$$h_{tp} = C\ h_l \left(0.25\ Co^{-0.45}\ Fr_l^{0.25} + 75\ Bo^{0.75}\right) \quad (6.10)$$

where h_l is the all-liquid non condensation heat transfer coefficient, Fr_l is Froude number in saturated liquid state, *Bo* is the boiling number and *Co* is the convection number. C is identified from experimental results.

6.3.2.3. The gas-oil heat exchanger model

The gas-oil heat exchanger is modelled by means of the LMTD method for a cross-flow heat exchanger. The heat transfer process is in single phase between heat transfer oil and the exhaust gas of waste heat. The heat transfer coefficient from the inside tube surface is calculated by [159]:

$$Nu = \left\{Nu_{m,T,1}^3 + 0.7^3 + \left[Nu_{m,T,2} - 0.7\right]^3\right\}^{1/3} \quad (6.11)$$

where:

$$Nu_{m,T,1} = 3.66 \quad (6.12)$$

$$Nu_{m,T,2} = 1.615\sqrt[3]{RePrd_i/l} \quad (6.13)$$

The correlation can be represented in the entire $0 < RePr\ {}^{d_i}/_{l} < \infty$, with deviations of less than 1%.

The heat transfer coefficient for the flow over finned tube banks is recommended by Zukauskas et al. [160] by mean Nusselt number for staggered tube bundles:

$$Nu = 0.192\left(\frac{X_t^*}{X_l^*}\right)^{0.2}\left(\frac{S}{d_o}\right)^{0.18}\left(\frac{e_f}{d_o}\right)^{-0.14} Re^{0.65}Pr^{0.36}\left(\frac{Pr}{Pr_w}\right)^{0.25} \quad (6.14)$$

where X_t^* and X_l^* are nondimensionalized transverse and longitudinal tube pitch (shown in Figure 6.8). *S,* e_f and d_o are measurement of fin spacing, fin height and outside diameter of a circular tube, respectively. This correlation is valid for small Reynolds number ($10^2 < \mathrm{Re} < 10^4$).

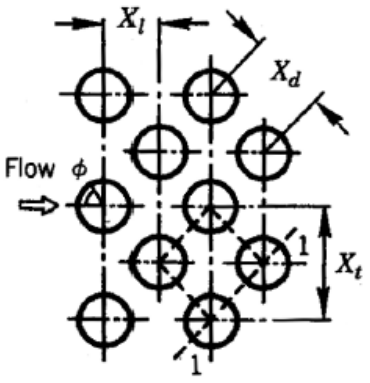

Figure 6.8: Geometrical properties of staggered tube bundle arrangements

The overall surface efficiency is related to the fin efficiency, η_{fin}, and the ratio between total fin area, $A_{fin,tot}$, and total surface area, A_{tot}:

$$\eta_o = 1 - \frac{A_{fin,tot}}{A_{tot}}\left(1 - \eta_{fin}\right) \tag{6.15}$$

where total fin area, $A_{fin,tot}$, is the total suface area of the plates (both sides) less the area that is occupied by the tubes and total surface area is the sum of total fin area, $A_{fin,tot}$, and the total un-finned tube wall surface. The fin efficiency, η_{fin}, is calculated by using internal function programmed in EES [24] which the fin type is annular rectangular fin.

6.3.2.4. Pump model

A non-isentropic compression process models the pump. The isentropic efficiency is assumed constant and can be expressed as

$$\eta_{p=\frac{H_{4,S}-H_3}{H_4-H_3}} \tag{6.16}$$

where $H_{4,S}$ is the enthapy of working fluid at the outlet of the pump under the isentropic compression condition

On the basis of the enthalpy raise, the pump power input is

$$W_p = \dot{M}(H_4 - H_3) \tag{6.17}$$

6.3.2.5. Cycle performance

Based on classical thermodynamics, the thermal efficiency (η_{th}) and the exergy efficiency (η_e) are calculated based on Equation 2.1 and 2.2, respectively. This is the exergy rate entering the ORC system ($\dot{E}_{in}$) is $\dot{E}_7$ based on Figure 6.3.

6.3.3. Comparison between experimental and model results

To ensure that the experimental data are collected in steady state conditions, a steady state standard proposed by Woodland et al. [161] was used. Based on the steady state standard and our current condition of the test rig, Table 6.7 summarises the comparison criteria for each measurement of steady state condition. Steady state is achieved when the criteria in Table 6.7 are fulfilled by exhaust gas, working fluid and cold water. The mass flow is not used as a criterion, because analog flowmeter used currently is inaccurate. The most recent 10 minutes of data are averaged to obtain the measurement values of the steady state. These values are used to validate the models and develop the performance curve of the feed pump.

Table 6.7: The criteria for each measurement for steady state conditions.

Measurement	Steady state criteria
Temperature	Difference <0.5 K
Pressure	Change < 2%
Rotating equipment speed	Change < 2%

6.3.3.1. Expander model validation

The input variables of the model are the supply pressure, the supply temperature, the exhaust pressure, the ambient temperature and the rotational speed of the expander. The parameters of the expander model are tuned to best fit the three model outputs (the mass flow rate displaced by the expander, the delivered mechanical power and the exhaust temperature) to experimental data.

The parameters of the model are identified by minimizing an error-objective function accounting for the errors on the prediction of the mass flow rate ($\dot{M}$), shaft power ($\dot{W}_T$), and exhaust temperature (T_{ex}) (using a direct algorithm available in the EES software):

$$error = \frac{1}{3}\left(\sqrt{\sum_1^{N_{tests}}\left(\frac{\dot{M}_{calc}-\dot{M}_{meas}}{\dot{M}_{calc}}\right)^2}\right) + \frac{1}{3}\left(\sqrt{\sum_1^{N_{tests}}\left(\frac{\dot{W}_{T,calc}-\dot{W}_{T,meas}}{\dot{W}_{T,calc}}\right)^2}\right) + \frac{1}{3}\left(\sqrt{\sum_1^{N_{tests}}\left(\frac{T_{ex,calc}-T_{ex,meas}}{\dot{T}_{ex,calc}}\right)^2}\right) \quad (6.18)$$

The model requires nine parameters that is identified to best match the values of the outputs to the experimental results. They are listed in Table 6.8:

Table 6.8: Parameters of semi-empirical model.

Swept volume	$V_{s,T}$	12 cm^3
Built-in volume ratio	$r_{v,in}$	3.5
Leakage area	A_{leak}	11.53 mm^2
Supply heat transfer coefficient	$AU_{su,n}$	26.02 W/K
Exhaust heat transfer coefficient	$AU_{ex,n}$	144.7 W/K
Heat transfer coefficient with the ambient	AU_{amb}	144.5 W/K
Supply port cross-section area	A_{su}	44.17 mm^2
Nominal mass flow rate	$\dot{M}_n$	1.207 kg/s
Mechanical loss torque	T_{loss}	0.6024 Nm

A relative error between model results and the measurements is about 9.6% for the exhaust temperature, 8.3% for mass flow rate and 8.5% for electrical power output.

6.3.3.2. Heat exchanger model validation

The experimental data of the ORC-B plant in our laboratory is used to validate the heat exchanger models described above. The *C* values for two-phase of the evaporator and condenser are identified by imposing some measurements as input

variables and by minimising the deviation between the measured and model output variables. The values of C are listed in Table 6.9.

Table 6.9: Heat exchanger model parameters.

Evaporator	Condenser
$h_{tp} = 19.18 h_l Bo^{0.5}$	$h_{tp} = 4.253\, h_l \left(0.25\, Co^{-0.45}\, Fr_l^{0.25} + 75\, Bo^{0.75}\right)$

For given inlet temperatures of hot and cold fluids and saturation pressure, the evaporator and condenser models calculate the heat flow rate and the exhaust temperature. Figure 6.9 shows that the exhaust temperature of evaporator and condenser models is predicted with a relative error of about 4.3% and 1%, respectively.

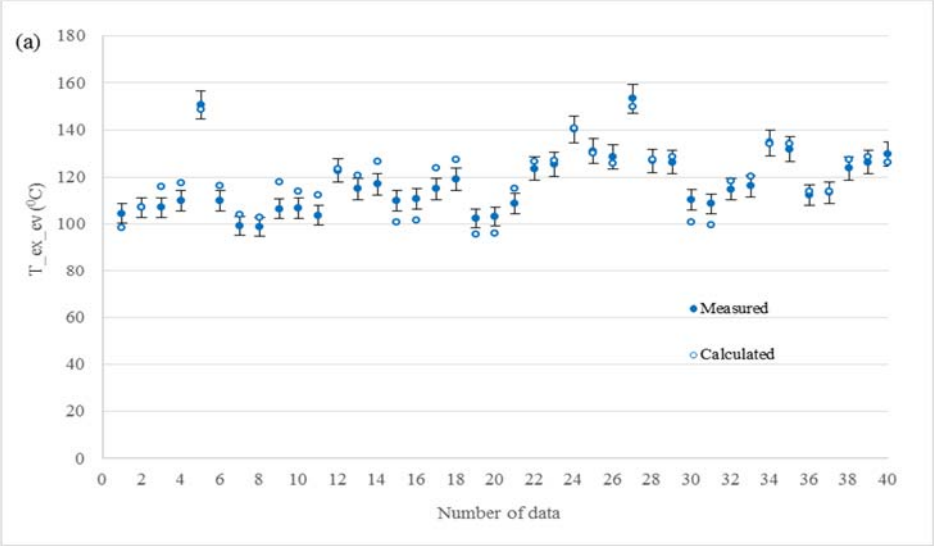

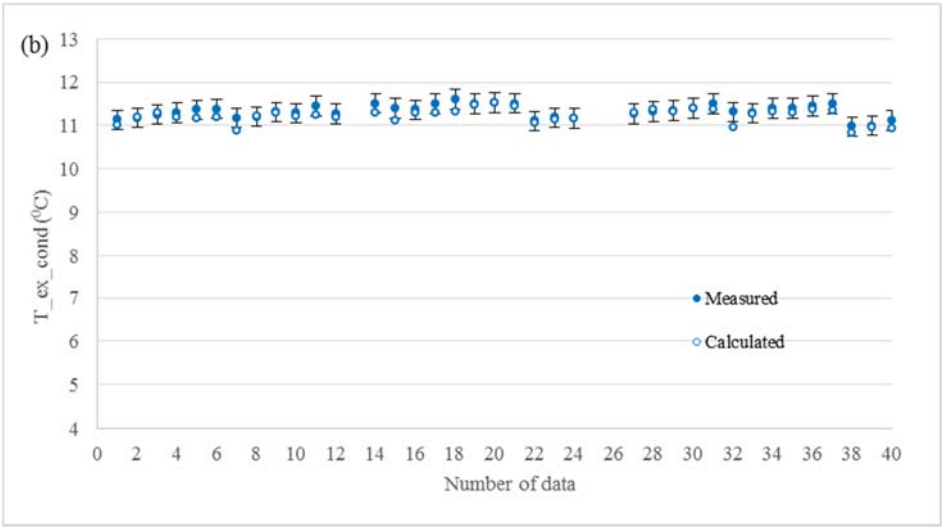

Figure 6.9: Comparison between measured and calculated data (a) evaporator model (b) condenser model.

The gas-oil heat exchanger in the oil loop calculates the outlet temperatures and heat flow rate for given inlet exhaust gas and oil temperature and the pressure level of both fluids. Figure 6.10 shows the comparison between measured and predicted exhaust oil temperatures of the gas-oil HE with a relative error of about 2.25%.

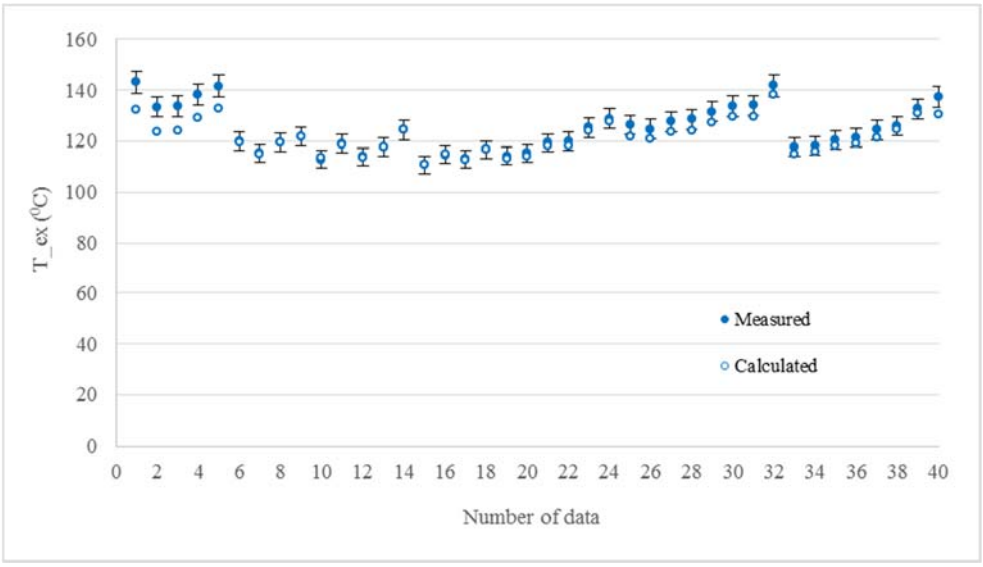

Figure 6.10: Comparison exhaust oil temperature between measured and calculated data.

6.3.4. Feed pump performance curve

Figure 6.11 presents the performance curve of the feed pump based on the experimental results. The performance of the pump is only dependent on the revolution per minute (RPM). The positive displacement pumps attempt to deliver the same mass flow of fluid regardless of the pressure (resistance) that must be overcome in the discharge line [162]. The pump was tested from 600 RPM to 1650 RPM and the maximum RPM is 1725 RPM based on the manufacturing data. The results shows that the pump has a good performance in maintaining the mass flow regardless of the differential pressure. However, the mass flow rate has a small decrease in high differential pressure in some cases.

6.3.5. Base case design performance

The possible maximum performance of the ORC plant using the selected main components described above are calculated as a base case. The base case is calculated as a basic reference for comparison to new design alternatives provided by applying the proposed methodology. Table 6.10 shows the existing ORC plant performance with three Capstone gas turbine load conditions. The main parameters of Capstone gas turbine in each condition are shown in Table 6.12. The optimization of the plant performance is constrained by the maximum outlet temperature of the evaporator in oil side at 100^0C (point 5 in Figure 6.3) to avoid the damage of the seals in the oil pump [163] and maximum characteristic parameters of the main components such as pinch points of the heat exchangers and a revolution speed (RPM) of the expander.

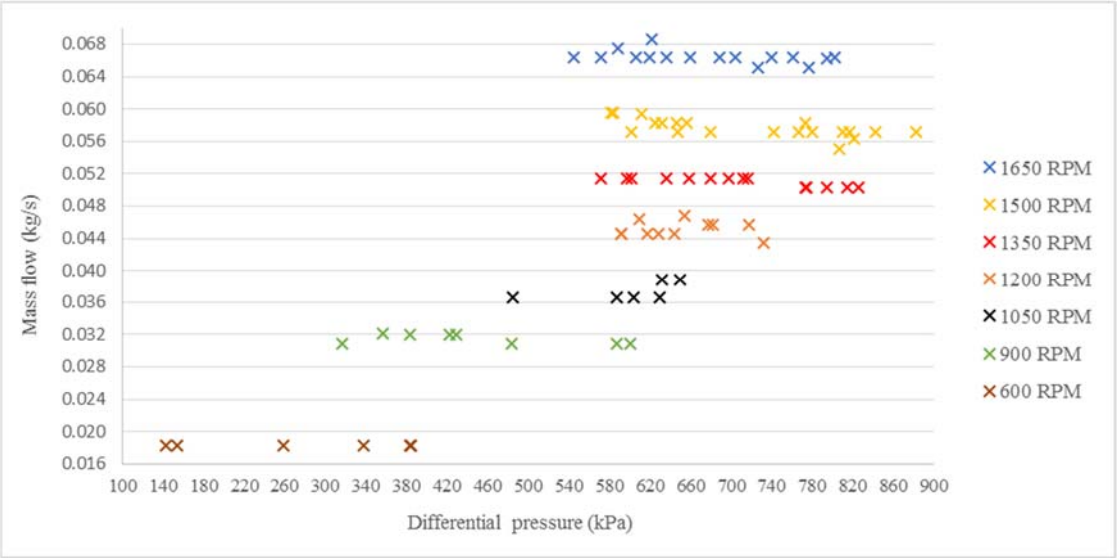

Figure 6.11: The performance curve of the feed pump.

Table 6.10: The possible maximum performance of the current ORC plant.

Parameters	Condition 1	Condition 2	Condition 3
N (RPM)	1950	3134	3189
$\dot{M}$ (kg/s)	0.0312	0.0498	0.0525
P_{max} (kPa)	499	675	717
$T_{T,in}$ (^{0}C)	126.7	121.5	129.2
P_{cond} (kPa)	107	124	124
m_{oil} (kg/s)	0.12	0.31	0.24
$T_{out,oil}$ (kg/s)	89.33	100	100
Pinch point$_{gas\text{-}oil\ HE}$ (^{0}C)	70.2	65.3	88
Pinch Point$_{ev}$ (^{0}C)	1.24	1.75	3.14
Pinch Point$_{cond}$ (^{0}C)	0.24	0.38	0.47
W_T (W)	154	449	515
W_P (W)	11.1	25	28
W_{net} (W)	143.4	424	487

6.4. Application of the methodology

The proposed methodology is implemented to a small scale of ORC plant described above for modifying the size of the heat exchangers in the system to obtain the more economical designs. The preliminary design (base case) is used as a reference for comparisons. Three heat exchangers in the system are a gas-oil HE, evaporator and condenser. The four design alternatives that are investigated in the

application of the methodology are shown in Table 6.11. Note that "ν" means that the heat exchanger is redesigned and "-" means that the heat exchanger is not redesigned.

Table 6.11: Design alternatives investigated by the methodology application.

Heat exchanger	Design 1	Design 2	Design 3	Design 4
Gas-oil HE	ν	ν	-	-
Evaporator	ν	ν	ν	ν
Condenser	ν	-	ν	-

6.4.1. Problem specification

It has been shown in previous works of the WHR system that the power output should be maximized instead of the cycle efficiency [36, 71]. However, the most economical design is considered as the most important goal of the design.

Considering these aspects into account, the methodology is applied by two objectives:

- Maximum ratio of $W_{net}/A_{tot,HE}$
- New designs must have a higher power output than a base case in the same Capstone gas turbine condition.

The limitations of the problems are fixed as follows:

- The same expander and working fluid for all design alternatives. The expander is a scroll expander and the working fluid is a zeotropic mixture (M1). The specification of the scroll expander and the zeotropic mixture (M1) have been explained in detail in Section 6.3.1 and Table 6.6, respectively.
- Available heat resource with three different conditions.
- The maximum outlet oil temperature of the evaporator at 100^0 C to avoid melted seals in the oil pump.

6.4.2. Selection of heat source

The selection process depends on the objectives and limitations established in the specification problem (first step). The used expander has a design capacity of 1

kW. The heat source candidates must have an available power higher than 1 kW considering target of the power output and heat losses during energy conversion process. The heat source in this study used a waste heat of the Capstone gas turbine. Three important conditions of the engine operation are shown in Table 6.12.

The available power between the inlet and outlet condition (8 and 9) of each heat source is calculated considering the gases as ideal and perfect gases using an energetic analysis:

$$Q = \dot{M}(H_8 - H_9) = \dot{M}\, c_p(T_8 - T_9) \quad (6.19)$$

where C_p is 1 kJ/kgK and 1.15 kJ/kgK for fresh air and combustion gases, respectively. The values of C_p are delivered from the mean value of the specific heat in the range between the highest and lowest temperature. The ambient conditions are considered as the reference state. Assuming that the exhaust gas is cooled into 100^0C, then the available power of the waste heat in three different Capstone gas turbine load conditions is shown in the Table 6.12.

Table 6.12: Three typical conditions of the Capstone gas turbine.

Parameters	Condition 1	Condition 2	Condition 3
Engine Power output [kW]	5	10	15
Temperature of exhaust gas [C]	230	251	268
Mass flow of exhaust gas [kg/s]	0.14	0.18	0.21
Available power [kW]	20.9	31.3	40.6

6.4.3. Selection of heat recovery setup

The indirect use (using oil loop) system is selected in this chapter to recover the heat source due to more stable and controllable systems than choosing a direct use setup. The existing heat transfer area of gas-oil heat exchanger ($A_{oil,HE}$) at 1.025 m^2 (oil-side area) is used as an initial assumption. The mass flow rate of oil (m_{oil}) ranging from 0.028 kg/s to 0.354 kg/s is used in the optimization purpose for achieving

acceptable waste heat source amount. In the case of design 1 and design 2, both $A_{oil,HE}$ and m_{oil} are used in optimization because these cases redesign the gas-oil exchanger design.

6.4.4. Synthesis

6.4.4.1. Selection of working fluid

For this study, a zeotropic mixture (M1) has been considered as a working fluid. The fluid is selected because the fluid is available in New Zealand with a small quantity at approximately 15 kg [163]. Moreover, the zeotropic mixture is expected to perform better than pure fluids in an ORC system. Heat can be supplied or rejected at variable temperature but still at constant pressure, because the boiling temperature varies during the phase change and the binary mixture evaporates over a wide range of temperature, resulting in a temperature glide. The gliding temperature alleviates the temperature mismatch between hot and cold streams in the heat exchangers, which reduces the exergy destruction in the power cycles [52, 164].

6.4.4.2. Selection of main components

The scroll expander and positive displacement pump are selected, since the design is for a small-scale ORC plant. The plate heat exchanger is selected as a heat exchanger construction type for evaporator and condenser. The water-cooled condenser is used in the system. The detail specifications of each component are explained in section 6.3.1.

6.4.4.3. Selection of cycle configurations

In WHR applications, the output power should be maximized instead of the cycle efficiency [71]. The subcritical cycle without a recuperator is therefore selected in the present work. The basic configuration integrates four main components: an evaporator, a turbine, a condenser and a working fluid pump.

6.4.4.4. Determination of cycle parameters

Initial assumptions use the values given by Table 5.1. The assumptions of superheat, sub-cooling and pinch point are required by the design alternatives for redesigning heat exchangers. The constant isentropic efficiency of the pump is set at 80% and the semi-empirical model calculates the turbine efficiency. The semi-empirical model represents more precisely the real turbine performance.

6.4.5. Analysis

Analysis and optimization (step 5 and 6) are two consecutive steps that are connected each other. The main objective function of optimization is to maximize the ratio of W_{net}/A_{HE} considering a higher power output than the base case at the same condition of Capstone gas turbine. The optimization is constrained by using the same expander and working fluid in all design alternatives and the maximum allowable outlet oil temperature of the evaporator is 100^0C. These constraints have been set in the problem specification (in the first step). The optimization of models is carried out by means of a direct algorithm available in the EES software [24]. An iterative process is conducted between step 5 and step 7 in Figure 6.1. The optimization parameters are progressively optimized to achieve the highest ratio of W_{net}/A_{HE}.

Two heat exchanger models (one modelling the evaporator and one for the condenser) are used to calculate the heat transfer areas required by every heat exchanger in the ORC system. The inputs of the component models are the optimal results of the system level (described in Figure 5.3). In this calculation, the pressure drops are neglected, since no accurate differential pressure sensors were installed on the exchangers in the experimental rig. The sizing results of heat exchangers are shown in Table 6.13. The sizes of the existing evaporator and condenser (the base case) are significantly larger than the required heat transfer areas especially under the

low Capstone gas turbine load condition (condition 1). In comparison to design 3, which has the same size of the gas-oil HE as the existing ORC plant, the oversize of the existing evaporator and condenser under condition 1 is 153% and 137%, respectively. These oversized figures decrease by increasing Capstone gas turbine load (from condition 1 to condition 3). The oversize of the evaporator and condenser under condition 2 are 67% and 88%, respectively, while condition 3 reduces the oversize of evaporator and condenser at 42% and 58%, respectively. Moreover, the size of the existing gas-oil HE is significantly small for condition 1 and 2. The existing size is more suitable for condition 3, in which the different size of base case from design 1 and design 2 under condition 3 is only 5% and 13.9%, respectively.

The pinch point limits the heat transfer rate in the heat exchanger that involves a phase change for one or both fluids [116]. As a result, discontinuity in the specific heat that occurs during a phase change can lead to the limitation of heat transfer rate to a much greater extent than would be expected based only the inlet fluid temperatures to a heat exchanger. As shown in Table 6.14, the condenser has the lowest pinch point in the system for all calculations, because the profile of water source inlet temperature is located closely to the condenser pressure. As a results, the pinch point of condenser constrains the heat transfer rate of all heat exchangers in the system. Moreover, the pinch point of both evaporator and condenser under the base case constrain heat transfer rate of the system because both pinch point figures are very small. Therefore, the power output produced by the base case is lower than new designs. Note that pinch point of the new heat exchanger design is set at 5^0C (see Table 5.1).

Table 6.13: Heat exchanger sizes.

HE areas		Base case	Design 1	Design 2	Design 3	Design 4
Condition 1	$A_{gas\text{-}oil\ HE}$ (m^2)	1.025	1.877	2.314	1.025	1.025
	A_{ev} (m^2)	6.400	3.662	3.457	2.531	2.52
	A_{cond} (m^2)	1.805	0.944	1.805	0.759	1.805
	A_{tot} (m^2)	9.23	6.483	7.576	5.814	5.350
Condition 2	$A_{gas\text{-}oil\ HE}$ (m^2)	1.025	1.236	1.215	1.025	1.025
	A_{ev} (m^2)	6.400	4.209	4.021	3.828	3.507
	A_{cond} (m^2)	1.805	1.049	1.805	0.961	1.805
	A_{tot} (m^2)	9.23	6.494	7.041	5.814	6.337
Condition 3	$A_{gas\text{-}oil\ HE}$ (m^2)	1.025	0.973	0.883	1.025	1.025
	A_{ev} (m^2)	6.400	4.257	3.880	4.517	3.981
	A_{cond} (m^2)	1.805	1.104	1.805	1.141	1.805
	A_{tot} (m^2)	9.230	6.334	6.568	6.683	6.811

Table 6.14: The pinch point of a gas-oil HE, evaporator and condenser.

Pinch Point		Base case	Design 1	Design 2	Design 3	Design 4
Condition 1	Gas-oil HE (^{0}C)	70.16	25.07	17.48	47.56	47.33
	Evaporator (^{0}C)	1.24	31.65	34.26	38.98	39.17
	Condenser (^{0}C)	0.24	5.07	2.50	5.07	0.88
Condition 2	Gas-oil HE (^{0}C)	65.32	58.71	57.12	69.01	67.10
	Evaporator (^{0}C)	1.75	28.35	29.24	29.80	32.11
	Condenser (^{0}C)	0.37	5.07	2.48	5.07	2.37
Condition 3	Gas-oil HE (^{0}C)	88.80	81.92	87.83	78.83	88.27
	Evaporator (^{0}C)	3.14	27.84	29.76	29.80	30.84
	Condenser (^{0}C)	0.47	5.07	2.54	5.07	2.53

6.4.6. Acceptable power output

Figure 6.12 shows the results of optimum power outputs produced by four design alternatives with three Capstone gas turbine conditions. They are compared to the power outputs produced by the base case. The optimal design parameters obtained at different designs are summarised in Table 6.15. The new four designs produce

higher power outputs than the base case under different Capstone gas turbine load conditions. The power outputs produced by four design alternatives under condition 1 increase significantly in comparison to the base case under the same condition 1, because the power output of base case is very low. This occurs because the existing gas-oil HE size is smaller and the existing evaporator is significantly larger than the requirement size of the heat exchangers for the load condition (condition 1). As a result, they cause a crossover of both temperature profiles with only a low mass flow rate of oil loop in the base case results. Thus, re-sizing of the gas-oil HE and evaporator under condition 1 and 2 influences on significantly higher increment of power output than the base case. The power outputs increase with an increasing of the Capstone gas turbine load conditions (from condition 1 to condition 3), because higher grade of the exhaust gas is easier to be recovered by the ORC system.

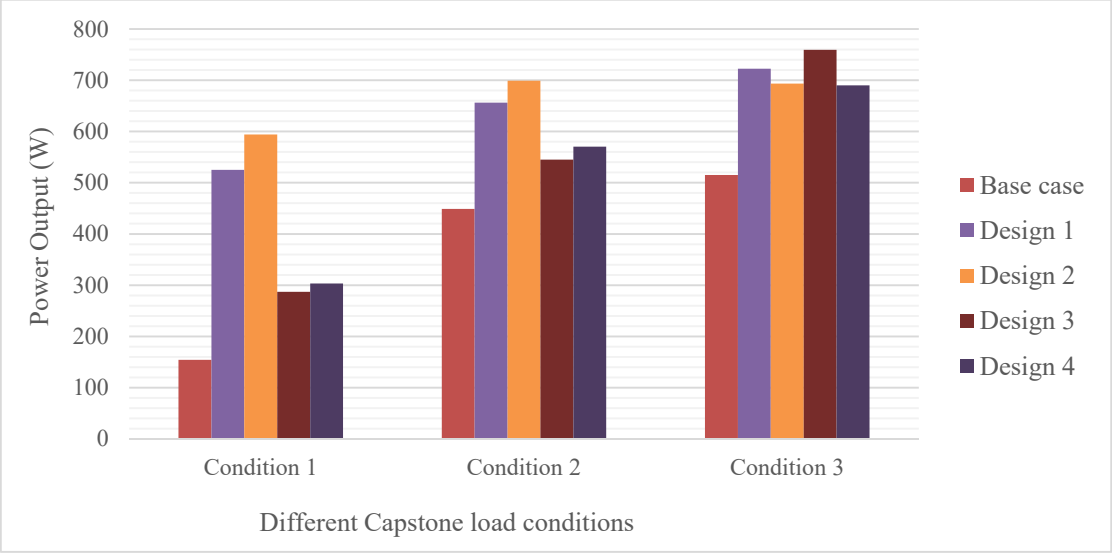

Figure 6.12: The optimum power output of four designs compared to the base case.

Table 6.15: Optimum design parameters of new four designs.

Parameters		Condition 1	Condition 2	Condition 3
Design 1	N (RPM)	3590	3590	3570
	$\dot{M}$ (kg/s)	0.0597	0.0667	0.0704
	P_{max} (kPa)	685.2	766.7	810
	$T_{T,in}$ (^{0}C)	79.41	83.77	85.96
	P_{cond} (kPa)	128	128	128
	m_{oil} (kg/s)	0.25	0.29	0.35
Design 2	N (RPM)	3541	3491	3591
	$\dot{M}$ (kg/s)	0.0609	0.0666	0.0660
	P_{max} (kPa)	703	773.3	758.4
	$T_{T,in}$ (^{0}C)	80.4	84.11	83.35
	P_{cond} (kPa)	108.8	107.8	108
	m_{oil} (kg/s)	0.26	0.31	0.34
Design 3	N (RPM)	3096	3564	3478
	$\dot{M}$ (kg/s)	0.0465	0.0608	0.0726
	P_{max} (kPa)	562.8	700	844.4
	$T_{T,in}$ (^{0}C)	72.04	80.23	87.63
	P_{cond} (kPa)	128	128	128
	m_{oil} (kg/s)	0.26	0.28	0.35
Design 4	N (RPM)	2651	3298	3397
	$\dot{M}$ (kg/s)	0.0449	0.0597	0.0664
	P_{max} (kPa)	575	708.7	779.4
	$T_{T,in}$ (^{0}C)	73	80.7	84.4
	P_{cond} (kPa)	106	106	108
	m_{oil} (kg/s)	0.26	0.29	0.25

In addition, design 1 and design 2 can increase the power output significantly in comparison to the base case especially under condition 1 and 2. This occurs because design 1 and design 2 resize both gas-oil HE and evaporator in the system. It means that the size of both current heat exchangers (the gas-oil HE and the evaporator) is not appropriate for condition 1 and 2. The appropriate size of heat exchanger is discussed in more detail in the section 6.4.6. Moreover, four new designs under condition 3 increase the power output at comparable level around 700 W, which the highest power output is produced by design 3. This occurs because design 3 has a bigger size of the gas-oil HE and evaporator than other alternatives in condition 3.

6.4.7. Acceptable W_{net}/A_{HE}

Figure 6.13 shows the results of objective function with three different conditions of Capstone gas turbine load for base case and four new design alternatives. The figures are generally increased by increasing Capstone gas turbine load (from condition 1 to condition 3). This pattern is the same trend as the power output because the figure is influenced by the power output level. The objective function achieves the highest level for the design 1 and the lowest level for the design 4 in three Capstone gas turbine load conditions. Moreover, the objective function of design 3 increases significantly and reaches almost the same level as design 1 under condition 3, but the figure of design 3 is lower than the design 1 and 2 under condition 1 and 2. This occurs because the heat transfer area of the current gas-oil HE is more suitable for condition 3, but it needs to be larger for load condition 1 and 2 (see section 6.4.5).

6.4.8. Waste heat utilisation rate (UR)

The UR analysis is investigated to measure the capability of the ORC design to recovery the waste heat. In other words, this figure measures how match the design to heat resource. The higher the UR level which is achieved, the better the match is between the design and the heat resource. As shown in Figure 6.14 that the ORC designs are more suitable for low Capstone gas turbine load conditions such as condition 1 and condition 2, because all designs under condition 3 have the lowest UR level (less than 50%) among other load conditions. The highest UR level is achieved by design 2 and design 1 under condition 1 at 76.90% and 73.83%, respectively.

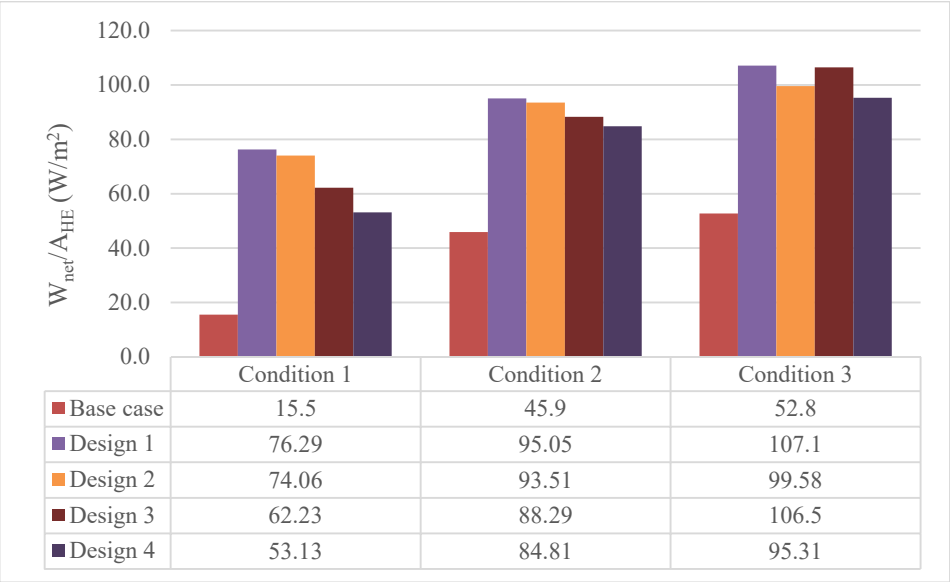

	Condition 1	Condition 2	Condition 3
Base case	15.5	45.9	52.8
Design 1	76.29	95.05	107.1
Design 2	74.06	93.51	99.58
Design 3	62.23	88.29	106.5
Design 4	53.13	84.81	95.31

Figure 6.13: The ratio of Wnet/A_{HE} of four designs in comparison to the base case.

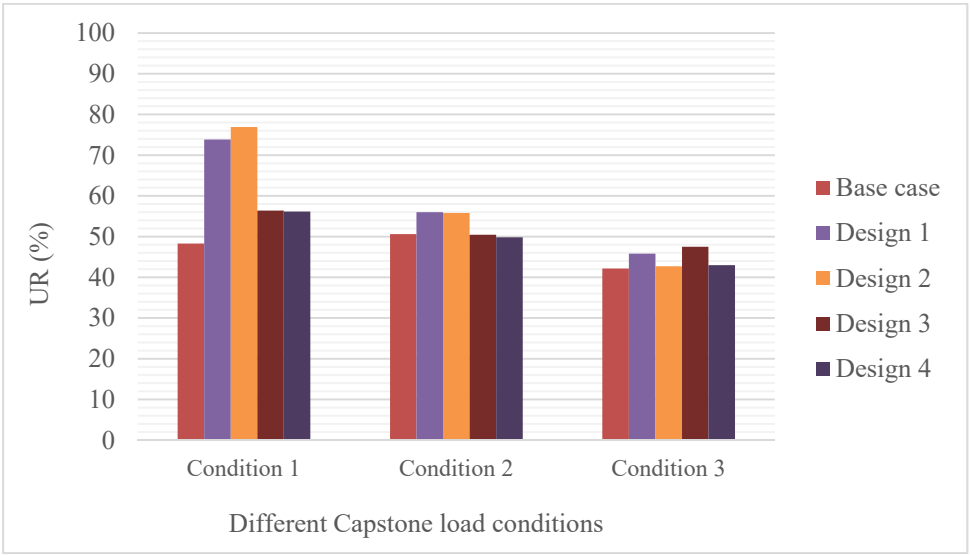

Figure 6.14: The UR of four designs in comparison to the base case.

6.4.9. Cycle performance

The cycle performance is closely related to net power output of the cycle. As shown in Table 6.16, the results indicate design 1 and 2 under condition 1 and 2 have higher efficiencies than design 3 and design 4. However, the four designs under condition 3 have comparable efficiency results because the power output of all designs under condition 3 are almost at the same level.

Table 6.16: Thermal and exergy efficiencies of different designs with three Capstone gas turbine load conditions.

Cycle performance		Design 1	Design 2	Design 3	Design 4
Condition 1	η_{th} (%)	3.42	3.74	2.44	2.60
	η_e (%)	1.41	1.50	0.77	0.82
Condition 2	η_{th} (%)	3.77	4.04	3.47	3.69
	η_e (%)	1.51	1.51	1.34	1.33
Condition 3	η_{th} (%)	3.91	4.03	3.95	3.98
	η_e (%)	1.39	1.47	1.43	1.72

6.4.10. Acceptable designs

The best modification of the existing ORC plant depends on the Capstone gas turbine load condition (the heat resource) and the number of modified exchangers in the system.

- Design 1 achieves the highest objective function in all design alternatives. This increases the objective function from 100% to 391% of the base case depending on the Capstone gas turbine load conditions. This design has a new design in all heat exchangers in the system.
- Design 2 is the best choice when the number of modified heat exchanger is limited to two units. The gas-oil HE and the evaporator need to be modified especially under condition 1 and 2.
- Design 3 is the best choice when the Capstone gas turbine runs in condition 3 because the design is able to produce the highest power output with comparable objective function to design 1 (Note that design 1 has the highest level of objective function in all design alternatives).
- Design 4 is the best choice when the Capstone gas turbine runs in condition 1 because the design is able to increase the power output and objective function

from the base case at 96% and 242%, respectively. This design only modifies one unit of the heat exchanger, which is the evaporator.

6.5. Conclusions

This chapter proposes a comprehensive methodology to design and optimize an ORC system based on DTR method for WHR applications. The design based on DTR method aims to develop a cost-effective design that is the best match to a heat resource. The methodology has been tested in a lab-scale ORC system. The design methodology is also valid for a larger-scale ORC system and other applications because all ORC systems have the same principle. This methodology shows that the selection of main components needed for an ORC system is involved in designing process. Thus, the methodology employs the selection and design together in the development of the ORC system.

Four design alternatives have been investigated for redesigning the heat exchangers in the ORC system. All designs are constrained by an available heat resource and available main components in the market (especially turbine and working fluid) that usually occur during the real process of the ORC design. Design 1 describes a new design of the ORC plant because this design redesigns all the heat exchangers in the system, while other alternatives (design 2, design 3 and design 4) describe design modifications. The UR analysis measuring the match between design and heat resource shows that the current ORC plant is more suitable to Capstone load at condition 1 with the highest UR of 76.9%.

The four new designs can still use the existing feed pump in our lab-scale ORC system. However, design 1 and design 3 under condition 3 require a mass flow more than the maximum level of the tested pump mass flow at 0.0686 kg/s to achieve the

best performance. Therefore, these designs under condition 3 might not achieve the best performance.

6.6. Nomenclature

A	Heat transfer area (m^2)
AU	Heat transfer conductance (W/K)
Bo	Boiling number (-)
C	Coefficient
C_p	Specific heat (J/kgK)
Co	Convection number (-)
d_i	Inner diameter of the tube (m)
d_o	Outer diameter of the tube (m)
$\dot{E}$	Exergy flow (W)
e_f	Fin height (m)
Fr	Froude number (-)
H	Specific enthalpy (J/kg)
h	Heat transfer coefficient (W/m^2K)
HE	Heat exchanger
l	Length of the tube (m)
$\dot{M}$	Mass flow rate (kg/s)
$\dot{m}_{oil}$	Mass flow rate of oil (kg/s)
N	Rotating speed (RPM)
Nu	Nusselt number (-)
Out	Output
P	Pressure (kPa)
Pr	Prandtl number (-)
Q	Total energy transfer by heat (J)
Re	Reynold number (-)
$r_{,v,in}$	Build-in volume ratio (-)
S	Fin spacing (m)
s	Specific entropy (J/kgK)
T	Temperature (^{0}C),
T_{loss}	Torque (Nm)
U	Overall heat transfer coefficient (W/m^2K)
v	Specific volume (m^3/kg)
$\dot{V}$	Volume flow rate (m^3/s)
W_{net}	Net electrical power output (W)
W_p	Power of pump (W)
W_T	Power of turbine (W)

Subcripts:

1,2,3,..	State point in the system
ad	Adiabatic
amb	Ambient condition
calc	Calculated data
cond	Condenser
e	Exergy
ev	Evaporator
ex	Exhaust
In	Inlet
l	Liquid
max	Maximum
meas	Measured data
n	Number of main components
p	Pressure
P	Pump
T	Turbine/ Expander
th	Thermal
tp	Two-phase
r	Refrigerant
s	Isentropic, swept
sf	Secondary fluid
su	Supply
sh	Superheating (^{0}C)
tot	Total
v	Vapour
w	Wall

Greek Symbols:

η	Efficiency (%)
Δ	Delta
Δp	Pressure drop (kPa)

Acronyms:

LMTD	Log-Mean Temperature Difference Method
ORC	Organic Rankine Cycle
WHR	Waste heat recovery

Chapter 7 - Designing a Binary Geothermal Plant considering degradation of geothermal resource productivity

The aim of this thesis is to develop an approach for a feasibility study for flexible design (FSFFD) for the ORC development, which includes thermodynamic, component, resource, and cost considerations. This chapter proposes a novel design strategy for designing the optimum binary geothermal plant, which takes into consideration thermal resource degradation. The behaviour and performance of four plant designs are analysed and compared over their whole plant life to obtain the best design, based on thermodynamic and economic analyses. The four alternatives are sized and designed based on four points that are selected from the thermodynamic properties of a geothermal resource between the highest and lowest values over the whole plant life. Chapter 5 discussed the methodology for assessing a potential geothermal resource over which the new binary geothermal power plant will be installed. The initial well exploitation data is used without considering the off-design operations. Chapter 6 explored a design methodology based on the DTR method that considers a selection of available main components in the market and an available heat resource as a constraint of design optimization. The current chapter enhances the design investigation by proposing a novel lifetime strategy that includes consideration of the thermal resource degradation. This chapter also discusses how to overcome the resource degradation in two ways through operational parameters adjustments and adaptive designs.

7.1. Introduction

Based on the historical data of big geothermal production wells in the world such as the Geysers geothermal field, California, Larderello-Valle Secolo area and Wairakei geothermal reservoir, most geothermal wells experience a decline in the temperature, pressure, enthalpy and/or flow as exploitation proceeds [90, 165, 166]. The reinjection of the cooled brine has been suggested as contributing to temperature reduction of the resource, particularly over a long operational life and for the low temperature geothermal resources. This occurs if production and injection reservoirs are connected. Lovekin [167] has analysed a conceptual model of the life cycle of a geothermal field. Figure 7.1 illustrates the life cycle of a geothermal field. The life cycle of a geothermal field is divided into four periods: (1) developing, (2) sustaining, (3) declining, and (4) renewable. In phase (1), increments of plant capacity come on line in steps. In phase (2), a reasonable steady state is achieved over an extended period of time. In phase (3), make-up wells are drilled to compensate the decline in well outputs with lower thermodynamic properties of the resource. Finally, a sustainable level can be achieved in phase (4), but at the sacrifice of some capital equipment that will no longer be useful. The remaining power plants can still be useful and profitable for a very long time, but at a significantly lower capacity than an initial plant capacity. The prudent management of the resource is required in this last phase.

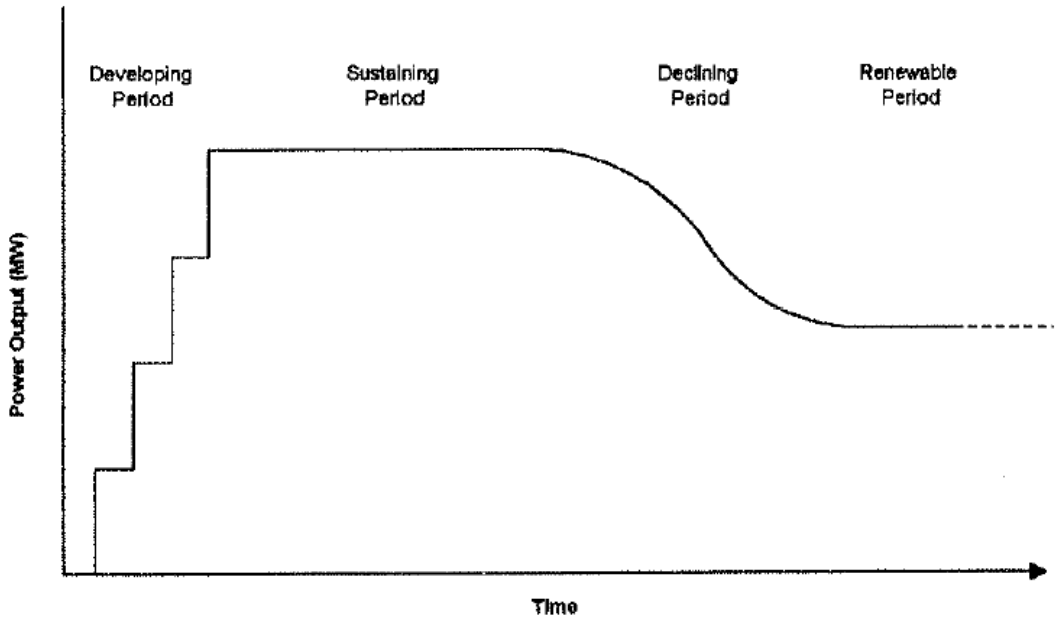

Figure 7.1: Life cycle of a geothermal field.

Most geothermal developers install a power plant capacity based on initial thermodynamic properties of the geothermal resources without considering the resource degradation that impacts to a lower plant outputs over the whole plant life. The larger geothermal plants may not be more economical. In choosing the optimal size of a geothermal plant, a trade-off occurs between obtaining maximum power output from a large plant size and obtaining a lower capital cost of the plant. Thermodynamic and economic performances of the power plant designs must be investigated over the whole plant life to find the best point that can be used as a base to size and design the most profitable binary plant for developers.

7.2. Methodology of lifetime design strategy

A thermodynamic cycle of the binary geothermal power plant is designed based on the given heat resource and heat sink conditions. The heat resource decreases over the whole plant life. The degradation is estimated based on historical data from the geothermal exploitations. Four design points are selected from the thermodynamic properties of a heat resource at the start of the plant life, 25% of the plant life, 50% of

the plant life and the end of the plant life. Four different size plants are designed from four different points. Then the best design performance over the reservoir life among the four points is identified based on thermodynamics and economic analyses. The heat sink corresponds to the median or mean ambient temperature at the plant location [107]. The constant mean ambient temperature is used in all design alternatives. The objective function for design optimization is maximizing the net electrical power output (Wnet) [125]. This is the standard approach for economic aspects of an available resource for the geothermal plant design. The modelling strategy is to build a model of the ORC that can analyse the performance of the binary geothermal power plant in off-design conditions. The net present value (NPV) and energy return on investment (EROI) are used as the measure of success for comparing economic benefit and energy utilization among the design alternatives.

7.3. The binary geothermal power plant

The standard cycle binary ORC geothermal power plant [9] uses subcritical pressure, which is best suited to the low temperature geothermal resource. Figures 7.2 and Figure 7.3 show a simple schematic and T-s diagram of the binary ORC geothermal power plant using n-pentane working fluid. The standard ORC cycle has four state points: working fluid at point 1 is pumped into high pressure state (point 2) and exits the heat exchangers (preheater and vaporizer) as a superheated vapour at (point 3). The high pressure working fluid vapour is subsequently expanded in a turbine that drives an electrical generator. The low pressure working fluid vapour exiting the turbine (point 4) is condensed in an air-cooled condenser (ACC) and pumped back to the geothermal fluid heat exchangers. The energy from brine (geothermal fluid) (point 5) is used to heat the pressurized n-pentane working fluid in a

shell and tube heat exchanger and the geothermal fluid is pumped at pressure into re-injection wells (point 6).

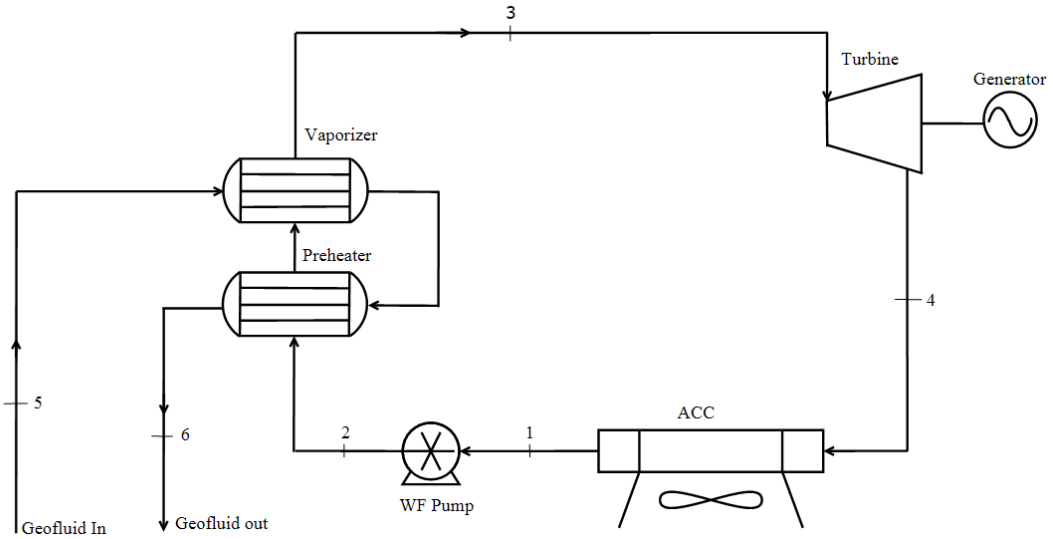

Figure 7.2: Simple binary ORC geothermal power plant schematic.

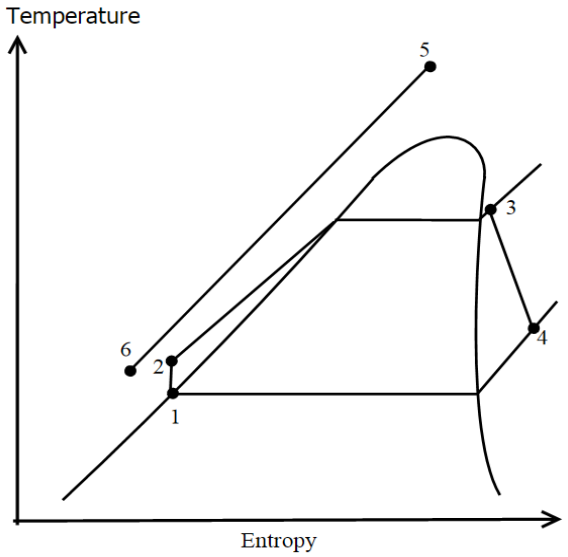

Figure 7.3: T-s diagram of binary ORC geothermal power plant.

7.4. A case study of geothermal resource characteristic

The Wairakei geothermal resource located in the Taupo Volcanic Zone (TVZ) in New Zealand is used to illustrate the lifetime design strategy. The geothermal resource has the starting temperature of the brine at 131^{0}C and the maximum allowable mass

flow rate that can be utilized is 200 kg/s. The rejected temperature of cold brine is maintained with minimum value of 92^0C to avoid scaling problem during the operation. The brine pressure is set at 9 bar for all conditions. The subcooling and superheating are set at 4^0C to avoid malfunction of the pump and turbine operations. The pinch point of heat exchangers is 5^0C. The temperature and mass flow rate decrease during its exploitation. The degradation of both parameters are assumed based on historical data of Wairakei field exploitation over 40 years of production [90]. The temperature decrease is 0.5^0C per year for the first twenties years, after which the decline rate slows to about 0.2^0C per year until end of the plant life time. The decline of brine flow rate is predicted by average annual production mass flows of Wairakei field from 1962 to 2000. The percentage of flow rate decline (D) is defined as a function of time (year):

$$D = 7.167 - 0.778\,Tm + 0.027\,Tm^2 - 0.00029\,Tm^3 \quad (7.1)$$

Figure 7.4 shows the temperature and mass flow degradation over the whole plant life used in the lifetime design strategy case study.

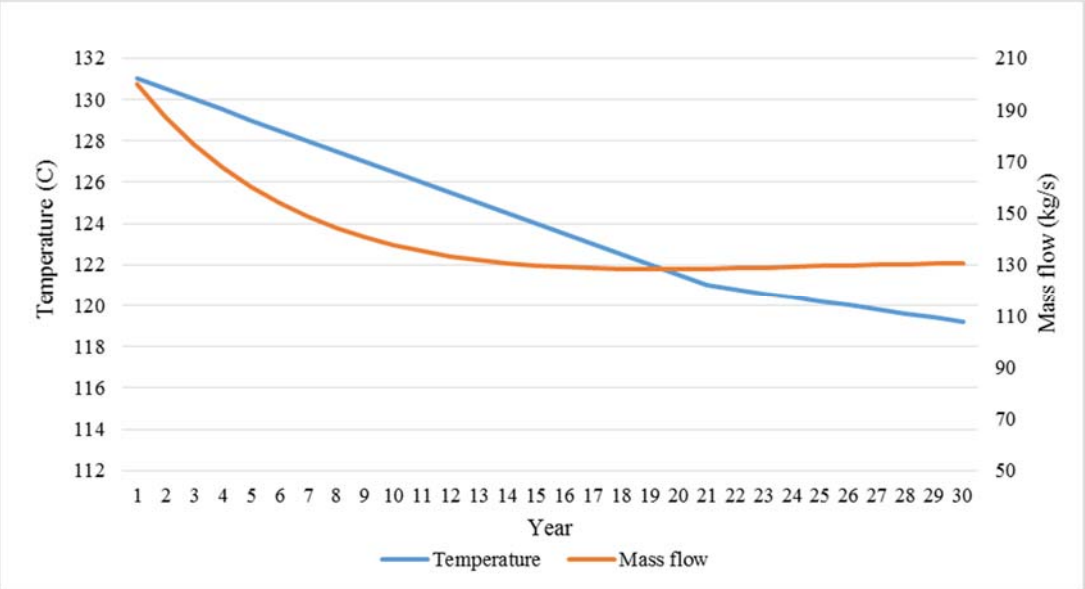

Figure 7.4: The temperature and mass flow rate of the brine over the whole plant life.

A separate size and design selection are carried out for the four resource conditions. The thermodynamic properties of geothermal resources that are used to design the plants are temperature and mass flow rate of the brine. Design point 1, design point 2, design point 3 and design point 4 correspond to the 1st year, 7th year, 16th year and 30th year of the plant operation with temperature and mass flow rate as shown in Figure 3. Design 1, design 2, design 3 and design 4 are sized, designed and optimized based on the points shown in Figure 7.5.

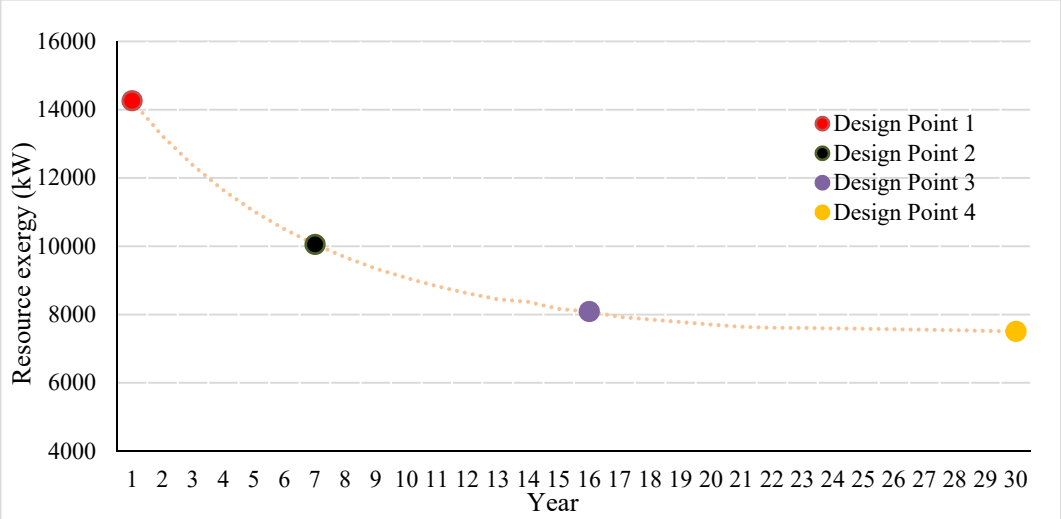

Figure 7.5: The position of design points over the whole plant life.

The median or mean temperature across the year 2015 in Taupo area (latitude at -38.68^0, longitude at 176.07^0, and height at 385m) is set at 12.8^{0}C. The four alternatives use the same value of mean temperature. The data was extracted from Met service climate database [168]. The ambient temperature in year 2015 includes mean monthly, mean daily maximum, and mean daily minimum temperature plotted in Figure 7.6.

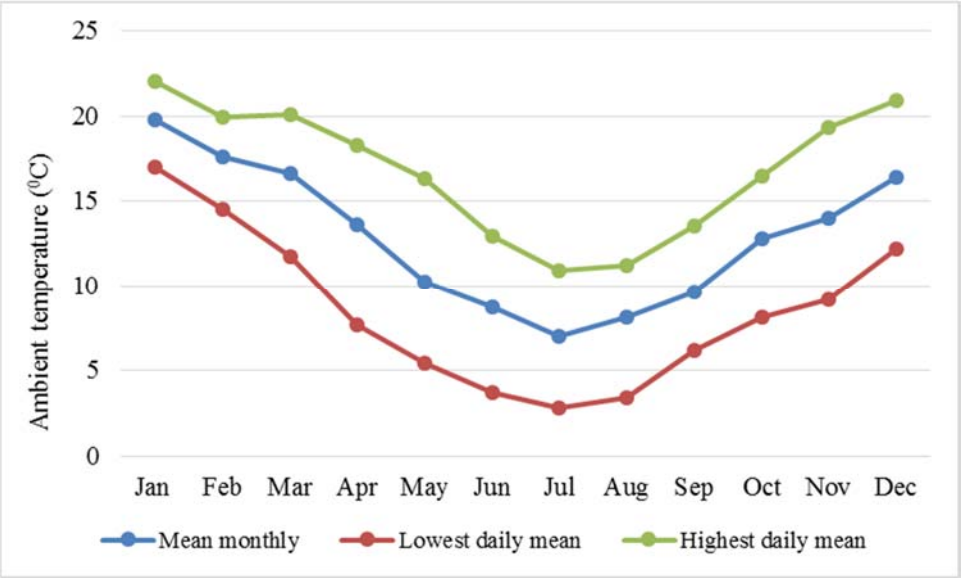

Figure 7.6: Mean air temperature in Taupo in year 2015

7.5. Mathematical Models

The aim of model development is to analyse the off-design behaviours and performance of the binary geothermal power plants. The simulation models have been developed using Aspen plus and Aspen Exchanger Design and Rating (EDR) software [25]. The flowchart of the models are shown in Figure 5.2. The objective function is to maximize Wnet within constraints required by the system. The manipulated variables are mass flow rates of n-pentane and air cooling. The default optimization algorithm, Sequential Quadratic Programming (SQP) method, is used for the convergence optimization problem. This algorithm is a state-of-the-art, quasi-Newton nonlinear programming algorithm. The method is suitable to this optimization case because it requires fewer iterations than other optimization method in Aspen plus. As a result, it reduces the overall number of iterations and time required every evaluation. The constraints are the minimum value of subcooling and superheating, the pinch point of heat exchangers and the minimum temperature of rejected cold brine. Two user-defined Fortran calculator blocks were needed for off-design simulations of the

thermodynamic systems to ensure reliable results because Aspen software does not provide any build-in facilities for off-design modelling. Two user-defined Fortran calculator blocks are used calculating inlet pressure in off-design based on Stodola's ellipse approach (Equation 7.2) and the turbine isentropic efficiency in off-design (Equation 7.6). The system model is built by interconnecting the subprograms of the different components such as turbine, pump and heat exchangers.

7.5.1. Thermodynamic modelling

The Peng-Robinson property method was used to calculate the thermodynamic and thermophysical characteristic of working fluid and air properties, while the STEAM-TA property method (1967 ASME steam table correlations for thermodynamic properties, International Association for Properties of Steam (IAPS) correlations for transport properties) was used to calculate geothermal fluid properties. A user-defined simulation sequence of the standard cycle was created to solve a recycle loop of the plant. The simulation sequence of the standard cycle is pump block, preheater and vaporizer block, turbine block and ACC block. A user-defined simulation sequence of the recuperative cycle was also created as follows: pump block, recuperator block, preheater and vaporizer block, turbine block, recuperator block and ACC block. These simulations iteratively calculate the inlet turbine pressure.

7.5.1.1. Turbine

The turbine operation is assumed to be modelled using the sliding pressure mode with fixed nozzle area [84, 169]. Therefore, inlet pressure in off design operation can be evaluated by Stodola's ellipse approach in Equation 7.2 [20]. This formula has been recommended by Brown Boveri Corporation and Siemens - Allis, Inc [169]. It is derived from the proportionality between mass flow coefficient in off design and mass

flow coefficient at the point given in Equation 7.5. The "Stodola constant", Y_d, is fixed for all turbine loads.

$$P_{in-off} = \sqrt{\dot{m}_{in-off}^2 \, T_{in-off} \, Y_d + P_{ex-off}^2} \tag{7.2}$$

where:

$$Y_d = \frac{P_{in-d}^2 - P_{ex-d}^2}{P_{in-d}^2 . \Phi_d^2} \tag{7.3}$$

$$\Phi_d = \frac{\dot{m}_d \sqrt{T_d}}{P_{in-d}} \tag{7.4}$$

$$\frac{\Phi_{off}}{\Phi_d} = \frac{\sqrt{1-\left(\frac{P_{ex-off}}{P_{in-off}}\right)^2}}{\sqrt{1-\left(\frac{P_{ex-d}}{P_{in-d}}\right)^2}} \tag{7.5}$$

where P is pressure, $\dot{m}$ is mass flow rate of working fluid, T is temperature, Y_d is Stodola constant of the turbine and ϕ is mass flow coefficient in temperature form. Subcripts *in*, *ex*, *off* and *d* refer to inlet, exit, off-design and design point, respectively.

The turbine isentropic efficiency in off-design conditions is evaluated using the correlation [170]:

$$\eta_{off} = \eta_d \sin\left[0.5\pi \left(\frac{\dot{m}_{in-off}}{\dot{m}_{in-d}} \frac{\rho_{in-d}}{\rho_{in-off}}\right)^{0.1}\right] \tag{7.6}$$

where ρ is mass density of working fluid.

The turbine is assumed to be adiabatic and the power generated is evaluated from the energy balance:

$$\dot{W}_t = \dot{m} \, (h_3 - h_4) = \dot{m} \left(h_3 - h_{4,is}\right) \eta_{off} \tag{7.7}$$

where h is the specific enthalpy. Subscript *4,is* refers to isentropic state point 4. Subscripts *3* and *4* refer to state points in Figure 7.3.

7.5.1.2. Pump

The working fluid pump was modelled only from a thermodynamic point of views. The pump is assumed to be adiabatic with constant isentropic efficiency of η_p = 0.80. The mechanical power required by the pump is found from the energy balance:

$$\dot{W}_P = \dot{m}(h_2 - h_1) = \frac{\dot{m}(h_{2,is} - h_1)}{\eta_P} \quad (7.8)$$

where subscript 2,is refers to isentropic state point 2. Subscripts 1 and 2 refer to state points in Figure 7.3.

7.5.1.3. Heat exchangers

A shell and tube heat exchanger with the geothermal brine on the tube side is the standard preheater and vaporizer for ORC power plants. A finned tube air cooled condenser (ACC) with fans to push ambient air across the tube-bank is the standard design for ORC's. The shell and tube heat exchanger is designed with 3 exchangers (shell) in series to anticipate an oversized heat exchanger due to the resource degradation. The calculation procedures for the geometry characteristics and cost of heat exchangers are as follows. Firstly, an initial size of heat exchangers for each point is selected by Aspen Exchanger Design and Rating (EDR) V8.4 under "design mode". Then the heat exchanger models with a given size are embedded in the ORC power plant in Aspen plus V8.6 under "simulation mode". Finally, the overall heat transfer coefficient, the pressure drops and the thermodynamic characteristic of the outlet streams are calculated as a function of the inlet streams for every operative condition. Heat transfer coefficients provided by Aspen EDR software are employed to design all heat exchangers [25]. The recommended method Heat transfer and fluid-flow service (HTFS) is selected to calculate heat transfer coefficients. The correlation method has

been developed over 40 years of research is continually updated and compares well to known correlations for heat transfer coefficients in the literature [171].

7.5.1.4. Cycle performance

The cycle performance is evaluated using an exergy efficiency, because this approach accounts for all exergy destructions within the ORC system [172]. As a result, the exergy analysis gives a better understanding of the irreversibility of the whole system. The overall exergy efficiency of a geothermal plant is calculated using formula in Equation 2.2. The exergy of the brine is calculated using the enthalpy and entropy of the brine inlet (subscript 5) and of the dead state (subscript 0). The notation is referred to Figure 7.3. The dead state temperature and pressure for the cycles are 20^0C and 1 bar, respectively.

7.5.2. Economic modelling

The economic modelling is conducted by using the same sequence as the economic calculation flowchart in section 5.3.5 and 5.3.6 in Chapter 5. The sequence calculation is purchase equipment cost (PEC), total plant cost (TPC), geothermal development analysis and total capital investment (TCI). Finally, two measures of success (net present value (NPV) and the lifetime energy return on energy investment (EROI)) are calculated for comparison among alternatives.

The PEC of pumps and turbines are calculated by the correlations from Turton et al. [88] that has been explained in detail in Section 5.3.5.1. In this case, the F_p does not also influence the cost deviations from the base conditions because the maximum pressure of the designs is 6.7 bar which is out of the F_p equation range (between 10 and 100 barg [gauge pressure]) proposed by Turton et al. [88]. The type of pump and

turbine that is used in the power plant is centrifugal pump and radial turbine. Aspen EDR software [25] is used to calculate the costs of heat exchangers.

The TPC is calculated by summing the plant capital cost and steam gathering system cost required by the power plant. This calculation method has been explained in Section 5.3.5.2. The steam gathering system cost is assumed at 30 USD per kW based on suggestion from the Electric Power Research Institute (EPRI) in 1996 [140]. It is updated using capital goods price index with asset type: other fabricated metal products from info share of New Zealand Statistics [173]. The updated cost of the steam gathering system in 2015 is 41 USD per kW. The binary plant systems require only the hot brine and the cool brine injection lines [141].

The geothermal development analysis is conducted by using two assumptions. The first assumption is that the drilling cost is assumed in a known field. The cost is expected at 1170 USD per kW [125]. The second assumption is that the construction time of the geothermal power plant is to be 3 years. The plant starts to produce an electricity in the fourth year with plant availability at 90% [18].

The NPV is a standard economic analysis which accounts for the time value of money. The NPV is calculated using Equation 2.5. Table 7.4 summarises the assumption for calculating the NPV. The escalation of electrical price and the total operation and maintenance (O&M) cost is started in the fourth year when the plant has started to generate the electricity.

Table 7.1: Assumptions for calculating NPV

Plant lifetime	30 years
Plant availability	90%
Electricity revenue unit price	USD $0.083/kWh
O&M cost	USD $0.024/kWh
Annual electricity price and Q&M cost escalation	3.0%
Inflation rate	2.7%
Discount rate	10%

The EROI is calculated by using calculation methodology in Section 5.3.6.1. The energy assessment calculations in this chapter used the average energy intensity for the U.S economy in 2015 at 8.3 MJ/USD.

7.6. Discussion and results

The main parameter results for the four solutions at their design points are shown in Table 7.2. The highest gross power output is produced by design 1 because it is based on the highest point of the geothermal resource (the initial point), and this design has the highest size of the main components. The lowest gross power output is produced by design 4 because the design has the lowest size of the main components. The plant capacity level is influenced by geothermal resource condition. Design 1 has the lowest Stodola's constant of the turbine. The figure is followed by design 2, design 3 and design 4. The Wnet calculation is calculated with a step of 3 years. The Wnet value that is not calculated is assumed to have the same value as the closest year because the annual thermal decrease of the heat resource is very small. The operating conditions of the binary geothermal power plants for each of the four points were calculated over the whole life time of the plants from 1st year to 30th year with a step of 3 years.

Table 7.2: Main design parameters of the four binary plant designs at their design points.

Parameters	Design 1	Design 2	Design 3	Design 4
Temperature of the resource (^{0}C)	131	128	123.5	119.2
Mass flow of the resource (kg/s)	200	148.6	129.1	130.7
Mass flow of n-pentane (kg/s)	66.7	46	34.8	30.5
Inlet turbine pressure (bar)	6.71	6.38	6.09	5.76
Stodola constant of the turbine (m^{-2} s^{-2} C^{-1})	860,311	1,649,459	2,645,817	3,166,509
Heat transfer area of preheater and vaporizer (m^2)	5819	3967	3923	3459
Heat transfer area ACC (m^2)	181,765	104,704	86,622	76,997
Net power output (kW)	4,356	2,939	2,015	1,713
Gross power output (kW)	5,111.8	3,462	2,566.9	2,182

7.6.1. Off design simulation results

The mass flow rate of n-pentane and the turbine inlet pressure decrease over the life of the plants (Figures 7.7 and Figure 7.8). The correlation between n-pentane mass flow rate and inlet turbine pressure is based on the basis of Stodola's ellipse. The mass flow rate of n-pentane decreases because of degradation of the resource and maintaining the rejected cold brine temperature with a minimum value at 92^0C. A sharp decrease of n-pentane mass flow rate occurs for the designs (design 1 and design 2) based on the initial thermal resource characteristics because their operative conditions are further away from their design values over their plant life. The n-pentane mass flow rate of the designs (design 3 and design 4) with design points near the end thermal resource exploitation decreases gradually because higher thermal resource properties at the initial resource exploitation cannot be utilized maximally due to the limited capacity of the heat exchangers (a smaller size of heat transfer area). After 20 years of the operation, the decrease of n-pentane mass flow rate is steady because the decline of the thermal resource is slower than the decline in the beginning of resource exploitation. The increase of mass flow of n-pentane is limited by a few degrees of superheat that is required to avoid liquid droplets at the inlet of the turbine [87]. The superheating is set with a minimum superheat at 4^0C in every operating condition. The moist condition inside the turbine has been considered non-feasible because it can cause severe mechanical damage to the rotor and stator that have been designed for dry steam [174]. Four plants are designed with different Stodola's constant of the turbine which influences the level of inlet turbine pressure. Because design 1 is designed by the lowest Stodola's constant of the turbine, its inlet turbine pressure level is the lowest. It is followed by design 2, design 3 and design 4.

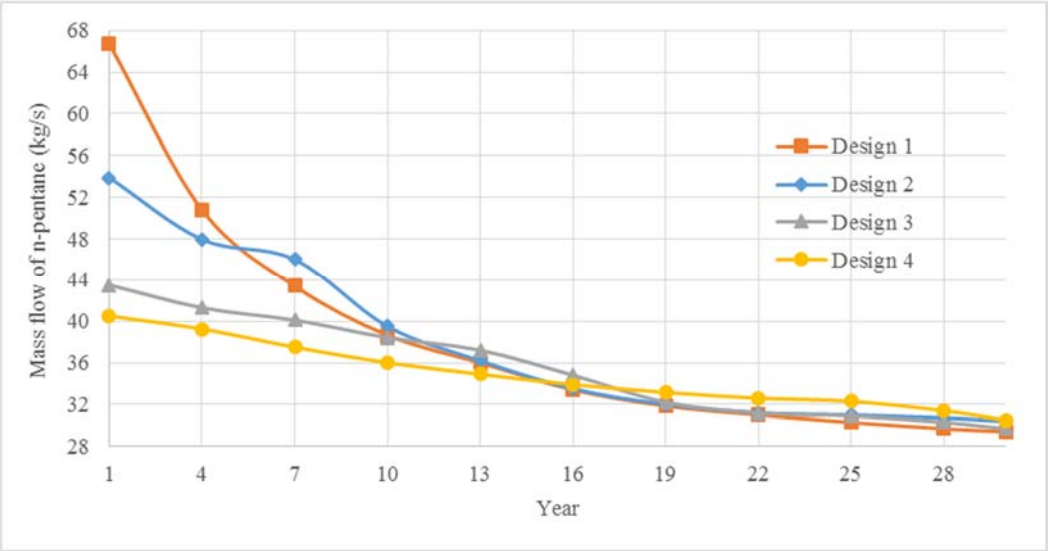

Figure 7.7: Variation of the n-pentane mass flow rate over the lifetime of the plants.

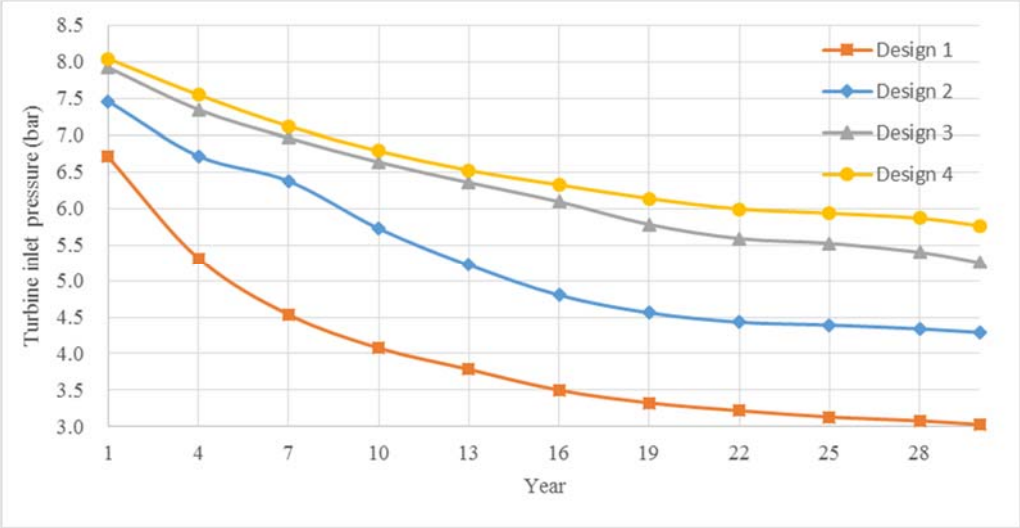

Figure 7.8: Variation of the turbine inlet pressure over the lifetime of the plants

Figure 7.9 and Figure 7.10 show the variation of net electrical power output (Wnet) and exergy efficiency of the plants designed by four conditions over the whole plant life. The degradation of heat resource induces obviously a reduction of Wnet and exergy efficiency of the plants. Design 1 and design 2 produce a higher Wnet in the initial plant life, resulting in a higher exergy efficiency, but their Wnet decreases more significantly over the plant lifetime than design 3 and design 4. The higher Wnet during the initial plant life time of design 1 and design 2 is due to the bigger heat

exchanger sizes of these designs that have capacity to utilize more thermal input of the heat resource. A reason for a significant reduction of the Wnet of design 1 and design 2 is because mass flow of n-pentane decreases significantly due to the limitation of geothermal rejected temperature and degradation of thermal heat resource. The Wnet decrease of design 3 and design 4 is slight over the whole life of the plants because the increase of n-pentane mass flow rate from design 3 and design 4 is slight. This means that these plants cannot utilize more thermal input of the resource in the initial plant life due to the smaller heat exchanger sizes of these plants. The higher total exergy flow rate of the brine and the lower Wnet in the initial plant life influence the lower exergy efficiency of design 3 and 4. The highest exergy efficiency occurs at the design point of every design except design 4. The exergy efficiency of design 4 is stabilized starting after 13 years plant operation, because the decrease of Wnet and total exergy flow rate of the brine is closely equivalent.

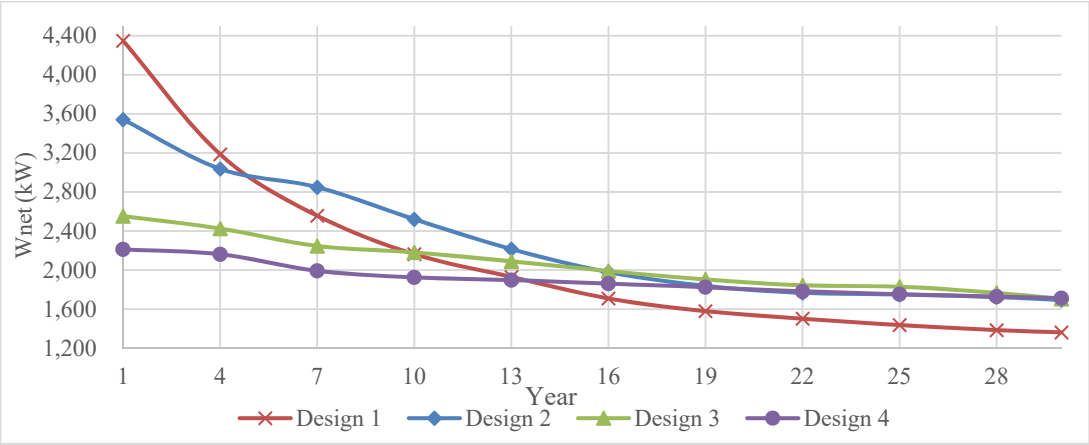

Figure 7.9: Variation of the net power output (Wnet) over the lifetime of the plants.

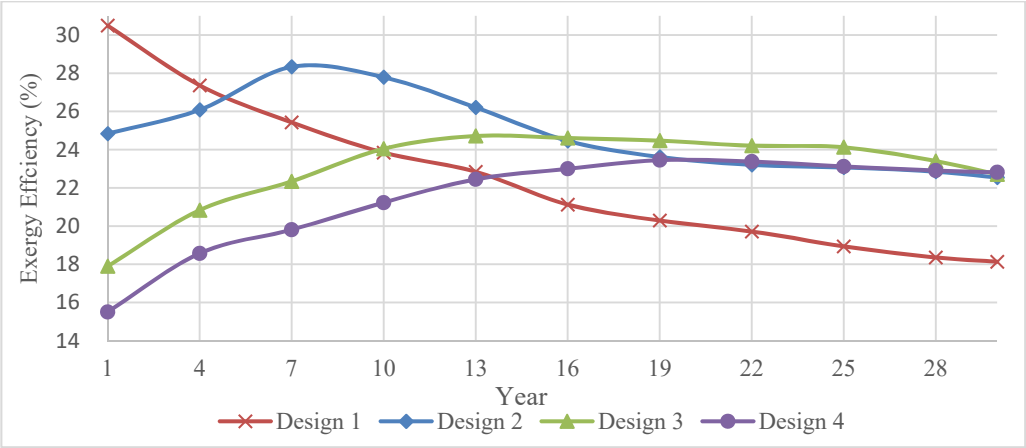

Figure 7.10: Variation of the exergy efficiency over the lifetime of the plants.

7.6.2. Selection of the best lifetime design

The selection of the best geothermal power plant has been conducted by comparing the NPV and EROI of every geothermal plant through the whole plant life, representing both the thermodynamic and economic point of views. The NPV is a useful tool for using the time value of money to determine whether a long-term project investment will result in a net profit or a loss. The EROI is a useful tool to measure the total net energy gains from an energy resource. These analyses are considered in the selection of the best design because renewable technologies have high initial costs, but have relatively low ongoing costs.

Table 7.3 shows the calculation results of TPC and specific investment cost (SIC). The TPC divided by the design Wnet gives SIC. These results are fairly close to the values that have been reported by Jung, Krumdieck [97]. They reported that most of the systems (about 90%) assembled by the refrigerant system components have the SIC from 2,000 USD/kW to 3,500 USD/kW.

Table 7.3: Total plant cost (TPC) for the four designs and specific investment cost (SIC) results at the design point capacity

Plant	TPC (USD)	SIC (USD/kW)
Design 1	8,519,295	1,956
Design 2	6,299,918	2,144
Design 3	5,217,490	2,589
Design 4	4,613,246	2,694

Table 7.4 shows the results of TCI and NPV for the four plant designs. Design 1 has the most expensive TCI of all designs because the plant with design 1 is the biggest plant. The TCI level of design 1 is followed by design 2, design 3 and design 4. Design 1 has the lowest NPV over 30 years of the operation at USD 3,024,543 and design 2 has the highest NPV at USD 6,894,615. Design 3 and design 4 have the NPV in the middle level at USD 6,677,361 and USD 6,270,212, respectively. NPV is largely influenced by the production revenues over the lifetime.

Table 7.4: The results of TCI and NPV calculation for four designs over the 30 years lifetime

Plant	TCI (USD)	NPV (USD)
Design 1	13,616,308	3,024,543
Design 2	9,738,432	6,894,615
Design 3	7,575,460	6,677,361
Design 4	6,617,014	6,270,212

Table 7.5: The results of lifetime EROI calculation for four designs

Item	Design 1	Design 2	Design 3	Design 4
E_g (TJ)	2,066	2,280	2,270	2,213
E_C (TJ)	93	66.5	51.74	45.2
E_{op} (TJ)	415.3	484.2	642.6	712.8
EROI	4.07	4.15	3.27	2.92

The lifetime EROI calculations of four designs are summarised in Table 7.5. Design 2 has the highest lifetime energy production, E_g. Lifetime energy production is largely a factor of plant capacity. Design 1 has the highest construction energy, E_c

since it has the largest capacity and the highest TCI, but this design has the lowest operation energy input. Design 1 has the lowest turbine inlet pressure and the largest heat transfer area of ACC. As a result, design 1 consumes the lowest operation energy input, E_{op}. However, design 4 has the highest operation energy input because this design has the highest turbine inlet pressure and the smallest heat transfer area of ACC. The operation energy input is mostly influenced by energy consumptions by pumps and fans and O&M costs. From Table 7.5, it can be summarised that the design with the lowest TCI requires the highest energy for operation. The highest EROI is positioned by Design 2, followed by design 1, design 3 and design 4. Thus, design 2 has the highest NPV and EROI among the other designs in this case. It is interesting to note that if the value of the generation capacity for design 1 was used, and resource degradation was not counted, the lifetime energy generation would be much higher, E_g = 4,353 TJ and the EROI would be doubled. This delivers an inaccuracy data during design selection in the plant investment.

7.6.3. Performance improvement

This section discusses two possible ways to improve the plant: adjusting plant operational parameters and adaptive plant designs. These improvements are required to mitigate the worst effects of the geothermal resource degradation over the whole plant life.

7.6.3.1. Plant operation parameters

The influence of the inlet turbine pressure on the off-design performance of the ORC binary plant is investigated by using constant mass flow of n-pentane. The operational parameters need to be adjusted to optimize the plant performance due to the thermal resource degradation over the whole plant life. Figure 7.11 shows off-design performance of the ORC binary plant with variation of inlet turbine pressure for

design 1 and design 2 (estimated at the first year of the operation). W_p and W_{fans} decrease, but the decrease of W_t is significantly higher than the decrease of W_p and W_{fans}. As a result, the Wnet decreases with increasing turbine pressures. This mainly occurs because the pressure ratio of the turbine decreases with increasing turbine pressures. The Stodola's ellipse is used to correlate between inlet and outlet turbine pressures. The design ambient temperature is set a constant value at 12.8^0C in this analysis. The lowest possible outlet turbine pressure is 0.63 bar. The outlet turbine pressure lower than 0.63 bar impacts the cross-over temperature in the ACC. This characteristic occurs in the four designs over the plant life time. The highest Wnet occurs when the turbine can expand to the lowest possible outlet turbine pressure. The increment of the inlet turbine pressure affects a reduction of the Wnet. Figure 7.7 and Figure 7.8 above have shown the optimal mass flow of n-pentane and the optimal turbine inlet pressure in each year over the plant life time because the calculations already used the lowest possible outlet turbine pressure as the input data of the models.

Both optimal mass flow rate of n-pentane and optimal turbine inlet pressure decrease over the plant life time. The parameters decrease significantly in the first 15 years of the operation. Therefore, these optimal parameters after 15 years of the operation (year 16) are significantly less than the optimal parameters of the initial operation (year 1). The optimal n-pentane mass flow rate of design 1, design 2, design 3 and design 4 at 16^{th} year of the operation compared to the initial value (at 1^{st} year of the operation) decreases at 50%, 38%, 20% and 16%, respectively. The optimal turbine inlet pressure of design 1, design 2, design 3 and design 4 at 16^{th} year of the operation compared to the initial value (at 1^{rt} year of the operation) decreases by 48%, 36%, 23% and 21%, respectively. The n-pentane mass flow is provided by centrifugal pumps. The typical characteristic curve of the centrifugal pump shows that the pump

head increases by the decrease of the flow as shown in Figure 7.12 [162]. The pump speed is used to control the working fluid mass flow rate in most binary systems [7]. Because the optimal mass flow rate of n-pentane and the optimal inlet turbine pressure are significantly less than the initial operational values especially for design 1 and design 2, the original working fluid pumps would be significantly oversized by the plant half-life (year 16). The solution is to replace the working fluid pumps in order to maintain the plant performance after the plant half-life.

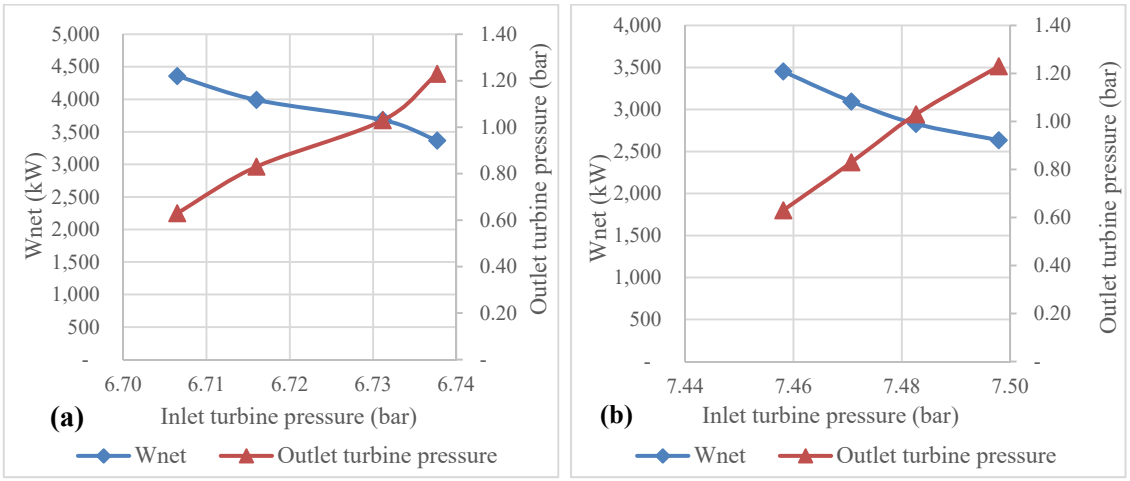

Figure 7.11: Off-design models of the ORC plant for design 1 (a) and design 2 (b) (calculated at initial operational conditions – year 1).

The main thermal resource degradation impact is the reduction of heat input to the plant. As the heat input decreases, some of the condenser fans can be switched off to reduce the parasitic load of the plant. Figure 7.13 shows the annual optimal air mass flow over the plant life time. A few degrees of subcooling at a minimum value of 4^0C has been set to avoid vapour condition at the inlet of the working fluid pump. The design with a bigger size of ACC (a larger heat transfer area) requires a lower mass flow rate of air cooling. Thus, the ACC of design 1 consumes the lowest mass flow rate of air and it is followed by design 2, design 3 and design 4.

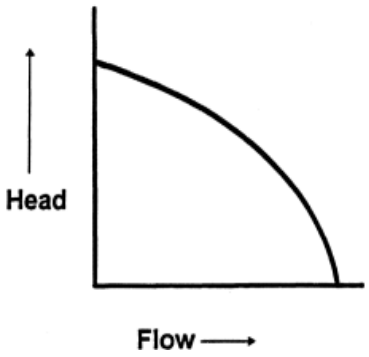

Figure 7.12: The typical characteristic curve of centrifugal pump

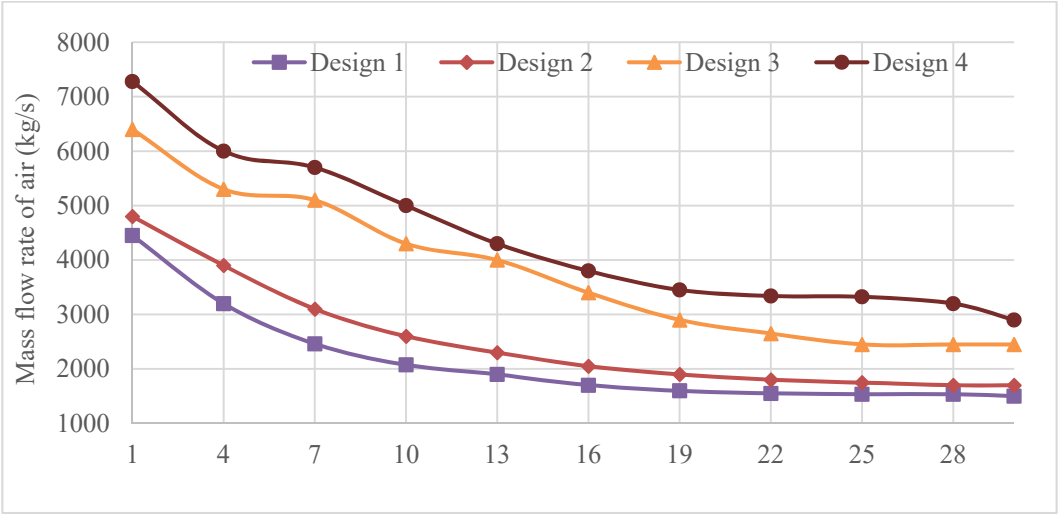

Figure 7.13: Mass flow rate of air through the air-cooled condenser over the plant lifetime for the four designs.

7.6.3.2. Adaptive plant designs

In the previous results, the Wnet in each year was optimized by adjusting key plant operational parameters of working fluid pump speed and ACC condenser fan load. Further increases in plant performance can be achieved by removing any imposed operating constraints or by modifying plant components. The geothermal plant could reasonably be re-configured during the plant lifetime by two adaptive design changes: adding a recuperator or replacing the preheater and vaporizer with smaller heat exchangers. These possible adaptive designs would improve plant performance at the plant half-life. Design 1 and design 2 are used in these analyses as representative cases.

Adding a recuperator improves the cycle performance of the ORC because it can maintain the heat duty of the vaporizer (the most expensive component) while preventing the geothermal rejection temperature from dropping below the scaling limit [92, 118]. As a result, the mass flow rate of working fluid can be increased to improve the cycle performance. The recuperator reduces the temperature difference between the heat resource and the working fluid, thus reducing the irreversibility of the heat exchangers.

Figure 7.14 shows the results of Wnet calculation before and after installing the recuperator in the plants using design 1 and design 2. The maximum working fluid mass flow rate is limited by the cross over temperature in the recuperator. The average increase in Wnet from 16th year to the 30th year of the operation is about 17% and 16.2% for design 1 and design 2, respectively.

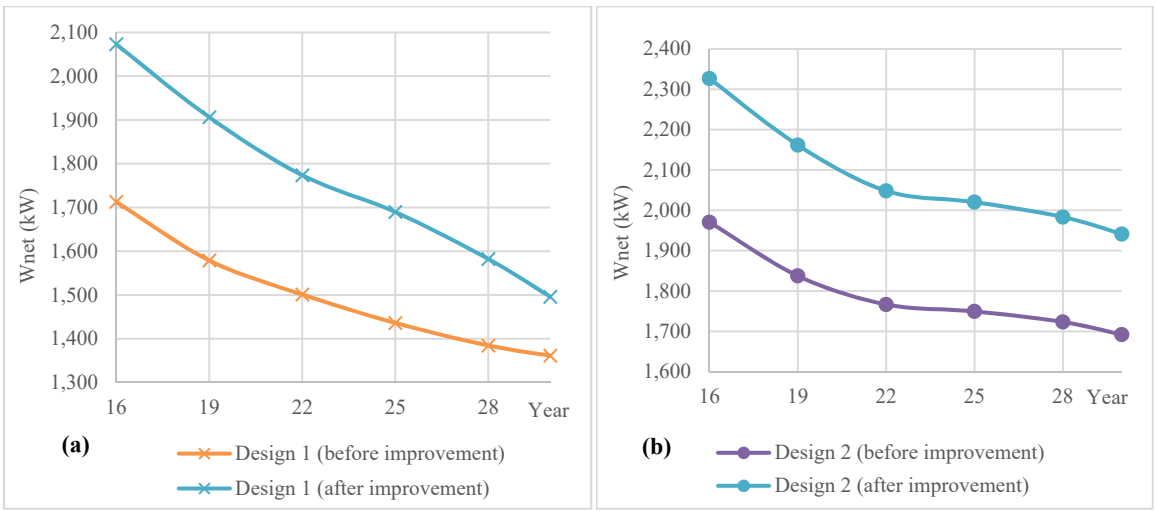

Figure 7.14: The Wnet of design 1 (a) and design 2 (b) before and after installing a recuperator from 16th to 30th year of the plant operations.

Another adaptive design is to downsize the heat exchangers to reduce the heat transfer areas of the preheater and vaporizer. The degradation of heat resource

influences the reduction of the required heat transfer areas of the plant heat exchangers especially for the preheater and vaporizer over the plant life. Figure 7.15 shows the ratio between the available and required heat transfer areas of the preheater and vaporizer for design 1 and design 2. The ratio at the half-life for design 1 and design 2 is 9.51 and 4.15, respectively. One approach for reducing irreversibility of the oversized exchangers is to reduce the heat transfer area. This could be done by un-installing 2 units of 3 units of the exchangers. This reduces the pressure drop causing a reduction of the required pump power. The mass flow rate of n-pentane can be increased to maintain the geothermal rejection temperature. The increase of the n-pentane mass flow rate occurs because the heat exchangers can work more effectively and need less heat input from the geothermal resource to achieve the same performance as with the oversize heat exchangers. Figure 7.16 shows the comparison of Wnet before and after the heat exchanger downsize for design 1 and design 2. The cumulative Wnet improvement for the final 15 years of the operation is 6.1% and 11.8% for design 1 and design 2, respectively.

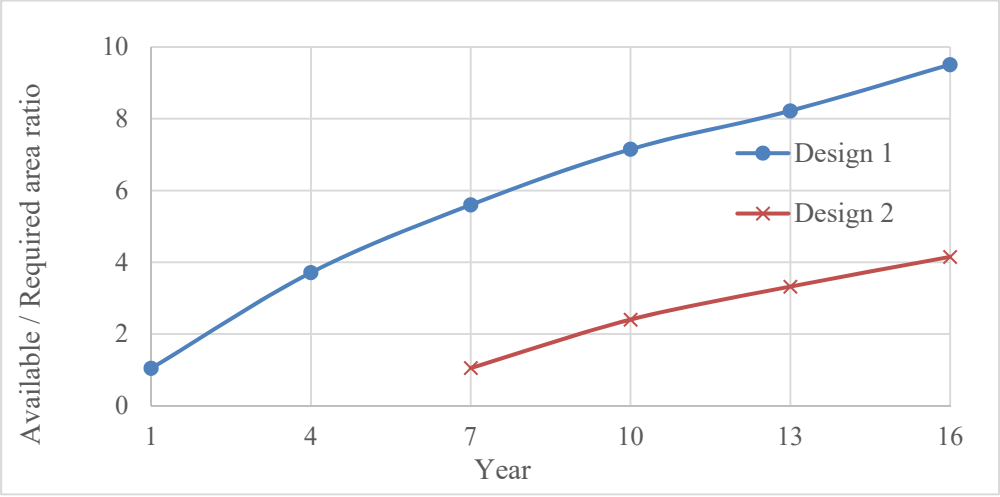

Figure 7.15: The ratio between available and required heat transfer area of preheater and vaporizer for design 1 and design 2 from 1rt to 16th year of the operation.

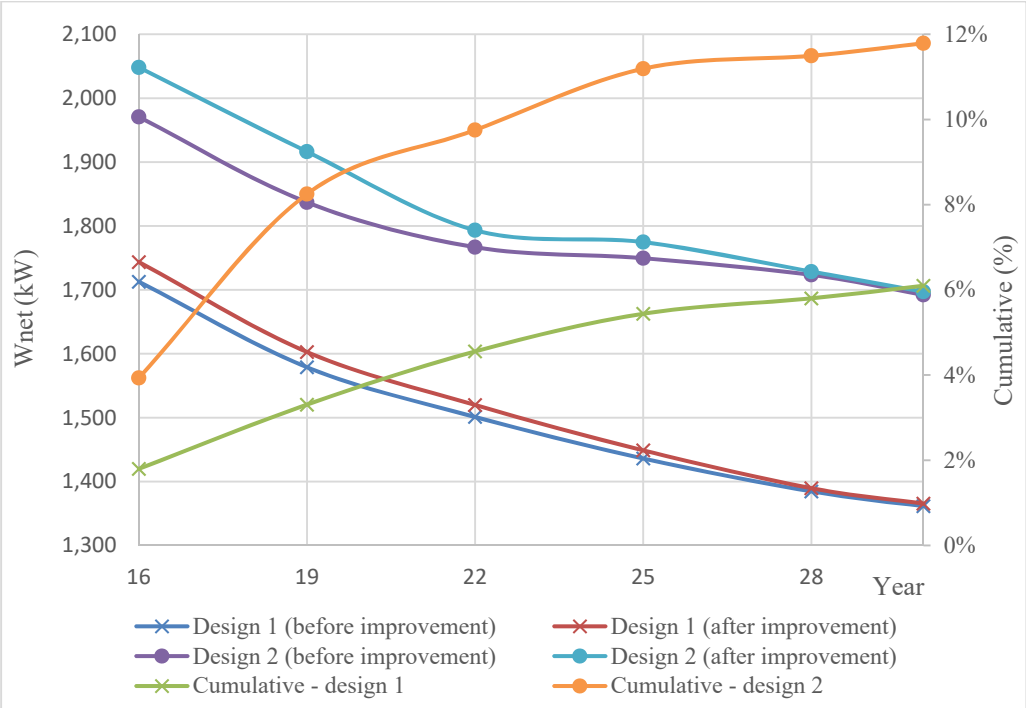

Figure 7.16: The Wnet of design 1 and design 2 before and after reduction of heat transfer areas from 16th to 30th year of the plant operation.

7.7. Conclusion

A strategy was presented for geothermal ORC design considering the degradation of the geothermal resource over the lifetime. A model for expected resource degradation was proposed for a 30 year plant lifetime. The four design points were taken from different values of the brine thermodynamic properties during well exploitation.

The real geothermal resource in Taupo Volcanic Zone (TVZ), New Zealand was used for the case study analyses. Two different analyses were performed:

1. Lifetime design point: evaluate the behaviour and performance of the binary power plant in off-design operation and afterward the best lifetime design point was selected;
2. Technical plant improvements: adjust the operational parameters of working fluid flow rate and air flow rate or adapt the standard design by adding a recuperator or down-sizing the preheater and vaporizer at the plant half-life.

The results of lifetime design point analysis show that there is a large and not necessarily obvious trade-off between an oversized lifetime design that allows nearly double the power production for the first few years, but diminished efficiency over the second half life. Is it better to build a more modest plant that runs near its design point over the lifetime, but is not capable of fully utilizing the available resource in the first ten years? To answer this question, both economic and energy analyses were calculated for the four plant alternatives. The best lifetime point is achieved by design 2 (year 6). This design has the highest economic return with NPV = 6,894,615 USD, and the highest energy return at EROI = 4.15. However, designers in this sector commonly use the initial thermal resource properties (point 1) to design and size the plant, resulting in sub-optimum lifetime performance.

The results of the second analysis reveal that mass flow rate of n-pentane and mass flow rate of air cooling need to be adjusted gradually over the whole plant life to maintain the plant performance. Because the optimal mass flow rate of n-pentane and the optimal turbine inlet pressure at the half-life operation (at 16^{th} year) are significantly less than the initial conditions, the working fluid pumps need to be replaced to maintain the plant performance. Two half-life adaptive designs to mitigate the impact of off-design operation on the plant performance were evaluated. The power gain from installing a recuperator is higher than from down-sizing the vaporizer. An additional investment at plant mid-life would be required to install a recuperator, but an over-investment would be required to build an adaptable vaporizer that could be down-sized, such as using three in-series shell and tube heat exchangers initially and removing two of them at mid-life.

A great deal of future work is needed to explore these ideas further. In particular, it will be vital to ensure the future role of geothermal in the mix of sustainable energy generation that the past plant life, performance and adaptive operation be studied. We have found the lack of data and experience gained from the numerous long-running geothermal power plants around the world to be a huge missed opportunity for advancement of the technology and growth in development.

7.8. Nomenclature

ACC	Air-cooled condenser
D	Percentage of flow decline rate (%)
EDR	Exchanger Design & Rating
EROI	Energy return on investment
In	Input
Out	Output
ORC	Organic Rankine cycle
$\dot{m}$	Mass flow rate (kg/s)
NPV	Net present value (USD)
P	Pressure (bar)
PEC	Purchase Equipment Cost (USD)
T	Temperature (^{0}C)
TCI	Total capital investment (USD)
Tm	Time (year)
TPC	Total plant cost (USD)
TVZ	Taupo Volcanic Zone
W_{fans}	Net power of fans (kW)
Wnet	Net electrical power output (kW)
W_p	Pump power (kW)
W_t	Turbine power (kW)
Y	The power of pump or radial turbine (kW)
Y_d	Stodola constant of the turbine (m^{-2} s^{-2} C^{-1})

Subcripts:

1,2,3,..	State point in the system
C	*Critical*
cond	Condenser
d	Design point
ex	Exit
geo	Geothermal
GR	Grassroots
in	Inlet
m	Material
max	Maximum
n	number of main components
o	Ambient condition
off	off-design
p	Pressure
P	Pump
T	Turbine

Greek symbols

η	Efficiency (%)
ρ	Mass density (kg/m^3)
ϕ	Mass flow coefficient, temperature form (m s$\sqrt{C}$

Chapter 8 - Summary and Future Work

This thesis has presented the guidelines for designing and optimizing an ORC system for low temperature resources by using an FSFFD approach. These guidelines are of primary importance in initial feasibility investigations for a geothermal development prospect and could provide a solid foundation for investment decisions without having the knowledge-based engineering (KBE) in ORC technology. The motivation of this thesis arose from the limited available KBE in open literature for the ORC development. For this reason, the thesis addressed the research question of how to design and optimize the ORC designs to obtain the most profitable design based on thermodynamic and economic analyses. It also answered the research question of how to design the optimum binary geothermal power plant, which take into account of resource degradation over the whole plant life.

8.1. Feasibility Study

This section presented an assessment of a particular aspect of the design variables that were deemed feasible to improve the plant performance using thermoydnamic and economic analyses. The design variables that have been assessed were type and size of the heat exchanger designs and the type of thermodynamic cycle configurations.

Conclusions:

The heat exchanger design influences greatly on the plant ROI. The analysis results show that the plate HE is the most cost-effective type. Although the plate HE is the cheapest HE in different types of heat exchangers with the same heat duty, the applications in the geothermal plants have to consider brine characteristics. The brine characteristics are known to have fouling and unique characteristics. The superheat

influences the size of the heat exchanger design. The superheat of 5^0C is required to be set in the evaluation of the heat exchanger design to obtain the optimal size. The optimal size of heat exchanger design delivers the optimal plant ROI. The ORC design with a recuperator is not preferable design because the ROI of plant is significantly lower than the ROI of the standard design.

The main factors influencing the plant performance and total plant investment cost are the working fluid type and type of cycle configurations. Three working fluids (R245fa, n-pentane and R134a) that are most commonly used in the commercial ORC units are used in this thesis. The comparison results between 2-stage design and 1-stage design show that the 2-stage design produces higher net electrical power output, and higher thermal and exergy efficiencies than the 1-stage design. However, the added technical complexity and larger heat exchangers can make the 2-stage designs less feasible than 1-stage designs. Similarly, designs using recuperator heat exchanger and regenerator mixing tank can reduce the heat exchanger size required by the ORC system. However, the investment ratio of Wnet to purchased equipment costs (PEC) must be investigated and compared to the standard designs and other possible designs to obtain the best optimum design. Thus, the design investigation using technical, thermodynamic and economic analyses must be conducted in every case of the design objective and requirements.

Implications:

The assessment results are intended to be used as an useful reference during the ORC design especially during selection of design variables such as type of heat exchangers and type of thermodynamic cycle configurations.

The feasibility studies that have been conducted in this thesis can be used as an example of feasibility studies for investing the ORC power plant using technical, thermodynamic and economic aspects for another case study.

8.2. Methodology

This section developed the guideline techniques for assessing design alternatives of a new binary geothermal plant and for designing a cost-effective design of the ORC system using the DTR method.

Conclusions:

The first design methodology uses thermodynamic and economic evaluation. The thermodynamic evaluation is used to evaluate the ORC plant performance by varying design variables. The economical evaluation is used to evaluate the component costs of the plants. Finally, the most-optimum designs of several alternatives are selected. The economic and energy analyses are implemented to select the best designs. This is important because renewable technologies have high initial costs, but have relatively low ongoing costs.

A new design methodology based on the DTR method is proposed in the second methodology. This methodology provides more accurate heat exchanger designs because the design evaluation is constrained by an available heat resource and available main components in the market. These are common constraints during the design of a real ORC system. The design methodology can be used to design a new plant and to redesign an existing plant.

More accurate heat exchanger sizes have been calculated using heat transfer coefficients validated by experiments. The evaluation results reveal that the sizes of the evaporator and the condenser installed in the small scale of our ORC plant in the

thermodynamic laboratory are significantly larger than the required heat transfer areas. The oversize of the heat exchangers is decreased by increasing the operational load of the Capstone gas turbine, which is used as a heat resource of the ORC system. The gas-oil HE installed in the ORC test rig is more suitable for the operational load of the Capstone gas turbine with condition 3. The size of the gas-oil HE is significantly small for condition 1 and 2 of the Capstone gas turbine operation.

Implications:

The two design methodologies provide the guidelines and analytical tools to select the optimum design of the ORC system for two different purposes. These methodologies are expected to become a very useful tool for designers and investors in this field because the methodologies can be used to conduct feasibility studies for investments of the ORC plants and expedite design evaluation processes. For example, the methodology is applicable for conducting a feasibility study of a potential geothermal resource over which the ORC binary geothermal power plant will be installed. The methodologies employ both selection and design together in the development of the ORC system. The design uses main ORC components that are easily available in the market over the ranges of interest. The time required to conduct the design evaluation using these methodologies depends on the complexity of the ORC modelling and software types. The simplest evaluation of a potential geothermal resource using Aspen software is about 2-3 hours.

8.3. Design Strategy

This section proposed a design strategy for designing binary power plant designs considering the power plant lifetime and performance improvements after half-life of the plant operation.

Conclusions:

The historical data of the geothermal resource exploitations indicate that thermodynamic properties of the resource decline under continuing exploitation. This must be considered in designing the binary plant to obtain the most profitable design. T*rade-off* between maximising power output influenced by a plant size and minimizing an investment cost occurs during a design evaluation. Therefore, the lifetime design strategy is needed to select the best design point over the whole plant life that can be used as a base to size the most profitable design.

The operational parameters (such as mass flow rate of working fluid, inlet turbine pressure, mass flow rate of air) and the plant performance (Wnet) decrease with the reduction of the thermal input of the binary plant. The plant operational parameters need to be adjusted over the whole plant life to maintain the performance due to the resource degradation. These main operational parameters are mass flow rate of working fluid and mass flow rate of air.

Implications:

The plant designers must evaluate the best design point by considering a thermal decrease of a geothermal resource over whole plant life. The initial thermodynamic properties of the geothermal resource cannot be used to design the binary plants as commonly implemented in the sector. The best design point needs to be analysed in detail and it depends on the level of a resource degradation over whole plant life.

The working fluid pumps need to be replaced after the half-life of the plant operation in order to maintain the plant performance. Installing a recuperator can improve the plant performance after the half-life of the operation with the technical constraints of the geothermal rejection temperature.

Because heat transfer areas of the preheater and vaporizer required by the binary plant system decrease over whole plant life, it is recommended to design the heat exchangers with the number of exchangers (shells) in the series. Therefore, the area of the heat exchangers can be reduced after the half-life of the operation without investing in new heat exchangers.

8.4. Future works

The research in this thesis provides the framework to design the ORC system based on a fixed set of operating conditions (heat resource and heat sink). The design process still neglects uncertainty and the results of the optimum design are very dependent on the assumptions about true values of the operating conditions. The future work will take into account the true stochastic nature of the geothermal resource. This approach allows designers to quantify the probability that the system will achieve the desired performance in the face of uncertainty.

Future design evaluation would concern a possibility to integrate other renewable heat resources such as biomass and solar thermal power to improve the thermodynamic performance of the plants. For example, developing the design guideline for a hybrid geothermal and solar-thermal plant. The hybrid plant is intended to have a better performance than a stand-alone plant.

Moreover, future work will consider the geothermal fluid characteristic in the implementation of the FSFFD approach. The silica factor is important for geothermal plant developments and operations especially if the fluid has a high concentration of silica.

REFERENCES

1. Bhattacharya, K.B.a.S., *Power Generation from Coal: Ongoing Developments and Outlook*. 2011.

2. Administration, U.S.E.I., *International energy outlook 2016.* Energy Information Administration (EIA), 2016.

3. Bertani, R., *Geothermal Power Generation in the World 2010-2014 Update Report.* 2015.

4. Watson, A., *Geothermal engineering: fundamentals and applications*. 2013, New York: Springer.

5. Barbier, E., *Geothermal energy technology and current status: an overview.* Renewable and Sustainable Energy Reviews, 2002. **6**(1): p. 3-65.

6. Franco, A. and M. Villani, *Optimal design of binary cycle power plants for water-dominated, medium-temperature geothermal fields.* Geothermics, 2009. **38**(4): p. 379-391.

7. Quoilin, S., et al., *Techno-economic survey of Organic Rankine Cycle (ORC) systems.* Renewable and Sustainable Energy Reviews, 2013. **22**: p. 168-186.

8. Bertani, R., *Geothermal power generation in the world 2005–2010 update report.* Geothermics, 2012. **41**: p. 1-29.

9. DiPippo, R., *Geothermal power plants: principles, applications, case studies and environmental impact*. 2008, Boston; Amsterdam; London: Butterworth-Heinemann.

10. Valdimarsson, P. *The Kalina power plant in Húsavik—why Kalina and what has been learned*. in *Electricity Generation from Enhanced Geothermal Systems Conference, Strasburg*. 2006.

11. Carey, B., et al. *2015 New Zealand Country Update*. in *Proceeding, World Geothermal Congress*. 2015.

12. Dym, C.L. and D.C. Brown, *Engineering design: representation and reasoning*. Vol. 2nd. 2012, New York: Cambridge University Press.

13. Dym, C.L., et al., *Engineering design: a project-based introduction*. Vol. 3rd. 2009, Hoboken, N.J: Wiley.

14. Sage, A.P. and J.E. Armstrong, *Introduction to systems engineering*. 2000, New York: Wiley.

15. Gazo, F., L. Lind, and G.N.S. Science, *Low enthalpy geothermal energy: technology review*. 2010, GNS Science: Taupo, N.Z.

16. Jaluria, Y., *Design and optimization of thermal systems*. Vol. 209.;209;. 2008, Boca Raton: CRC Press.

17. Calise, F., et al., *Thermoeconomic analysis and off-design performance of an organic Rankine cycle powered by medium-temperature heat sources.* Solar Energy, 2013.

18. Coskun, A., A. Bolatturk, and M. Kanoglu, *Thermodynamic and economic analysis and optimization of power cycles for a medium temperature geothermal resource.* Energy Conversion and Management, 2014. **78**: p. 39-49.

19. Quoilin, S., et al., *Thermo-economic optimization of waste heat recovery Organic Rankine Cycles.* Applied Thermal Engineering, 2011. **31**(14–15): p. 2885-2893.

20. Gabbrielli, R., *A novel design approach for small scale low enthalpy binary geothermal power plants.* Energy Conversion and Management, 2012. **64**: p. 263-272.

21. Bejan, A. and M.J. Moran, *Thermal design and optimization*. 1996: Wiley. com.

22. Cleveland, C.J., et al., *Energy and the US Economy: A Biophysical Perspective.* International Library of Critical Writings in Economics, 1997. **75**: p. 295-302.

23. Madhawa Hettiarachchi, H., et al., *Optimum design criteria for an organic Rankine cycle using low-temperature geothermal heat sources.* Energy, 2007. **32**(9): p. 1698-1706.

24. Klein, S.A., *Engineering Equation Solver, F-Chart Software.* Middleton, WI, 2008.

25. AspenTech, *Aspen plus. Aspen Technology, Inc., Wheeler Road, Burlington, Massachusetts, USA, http://support.aspentech.com/.* 2014.

26. Eastop, T. and A. McConkey, *Applied Thermodynamics for Engineering Technologists, 1993.* ELBS with Longman, Singapore.

27. Chen, H., D.Y. Goswami, and E.K. Stefanakos, *A review of thermodynamic cycles and working fluids for the conversion of low-grade heat.* Renewable and Sustainable Energy Reviews, 2010. **14**(9): p. 3059-3067.

28. Desai, N.B. and S. Bandyopadhyay, *Process integration of organic Rankine cycle.* Energy, 2009. **34**(10): p. 1674-1686.

29. Yamamoto, T., et al., *Design and testing of the Organic Rankine Cycle.* Energy, 2001. **26**(3): p. 239-251.

30. Bundela, P. and V. Chawla, *Sustainable development through waste heat recovery.* American Journal of Environmental Sciences, 2010. **6**(1): p. 83-89.

31. Bruno, J.C., et al., *Modelling and optimization of solar organic rankine cycle engines for reverse osmosis desalination.* Applied Thermal Engineering, 2008. **28**(17): p. 2212-2226.

32. DiPippo, R., *Second law assessment of binary plants generating power from low-temperature geothermal fluids.* Geothermics, 2004. **33**(5): p. 565-586.

33. Obernberger, I., P. Thonhofer, and E. Reisenhofer, *Description and evaluation of the new 1000 kWel Organic Rankine Cycle process integrated in the biomass CHP plant in Lienz, Austria.* Euroheat & Power, 2002. **10**: p. 1-17.

34. Peris, B., et al., *Experimental study of an ORC (organic Rankine cycle) for low grade waste heat recovery in a ceramic industry.* Energy, 2015. **85**: p. 534-542.

35. Chen, Q., J. Xu, and H. Chen, *A new design method for Organic Rankine Cycles with constraint of inlet and outlet heat carrier fluid temperatures coupling with the heat source.* Applied Energy, 2012. **98**: p. 562-573.

36. Dai, Y., J. Wang, and L. Gao, *Parametric optimization and comparative study of organic Rankine cycle (ORC) for low grade waste heat recovery.* Energy Conversion and Management, 2009. **50**(3): p. 576-582.

37. Preißinger, M., F. Heberle, and D. Brüggemann, *Advanced Organic Rankine Cycle for geothermal application.* International Journal of Low-Carbon Technologies, 2013: p. ctt021.

38. Peters, M.S., K.D. Timmerhaus, and R.E. West, *Plant design and economics for chemical engineers*. 2003, New York: McGraw-Hill.

39. Thuesen, G.J. and W.J. Fabrycky, *Engineering economy*. 2001, Upper Saddle River, N.J: Prentice Hall.

40. Guo, T., H. Wang, and S. Zhang, *Comparative analysis of natural and conventional working fluids for use in transcritical Rankine cycle using low-temperature geothermal source.* International Journal of Energy Research, 2011. **35**(6): p. 530-544.

41. Bao, J. and L. Zhao, *A review of working fluid and expander selections for organic Rankine cycle.* Renewable and Sustainable Energy Reviews, 2013. **24**: p. 325-342.

42. Rohsenow, W.M., J.P. Hartnett, and E.N. Ganic, *Handbook of heat transfer applications.* New York, McGraw-Hill Book Co., 1985, 973 p. No individual items are abstracted in this volume., 1985. **1**.

43. David Meyer, C.W., Frithjof Engel and Dr. Susan Krumdieck, , *Design and build of a 1 kilowatt organic rankine cycle power generator.* New Zealand Geothermal Workshop 2013 Proceedings, 2013(Rotorua New Zeland, 2013).

44. Peters, M.S. and K.D. Timmerhaus, *Plant design and economics for chemical engineers*. 1991, New York: McGraw-Hill.

45. Grassiani, M., *Siliceous scaling aspects of geothermal power generation using binary cycle heat recovery.* Transactions-Geothermal Resources Council, 2000: p. 475-478.

46. Kakac¸ S, L.H., *Heat Exchangers Selection, Rating and Thermal Design.* University of Miami., 1998.

47. Georges, E., et al., *Design of a small-scale organic rankine cycle engine used in a solar power plant.* International Journal of Low-Carbon Technologies, 2013. **8**(1): p. i34-i41.

48. Quoilin, S., V. Lemort, and J. Lebrun, *Experimental study and modeling of an Organic Rankine Cycle using scroll expander.* Applied Energy, 2010. **87**(4): p. 1260-1268.

49. Kakaç, S., A. Pramuanjaroenkij, and H. Liu, *Heat exchangers: selection, rating, and thermal design*. 2012: CRC press.

50. Hewitt, G.F., *Hemisphere handbook of heat exchanger design*. 1990: Hemisphere Publishing Corporation New York.

51. Qiu, G., H. Liu, and S. Riffat, *Expanders for micro-CHP systems with organic Rankine cycle.* Applied Thermal Engineering, 2011. **31**(16): p. 3301-3307.

52. Chys, M., et al., *Potential of zeotropic mixtures as working fluids in organic Rankine cycles.* Energy, 2012. **44**(1): p. 623-632.

53. Quoilin, S., *Sustainable Energy Conversion Through the Use of Organic Rankine Cycles for Waste Heat Recovery and Solar Applications*. 2011, University of Liège (Belgium.

54. Quoilin, S., S. Declaye, and V. Lemort. *Expansion machine and fluid selection for the Organic rankine cycle*. in *Proceedings of the 7th International Conference on Heat Transfer, Fluid Mechanics and Thermodynamics*. 2010.

55. Hicks, T.G. and T.W. Edwards, *Pump application engineering*. 1971, New York McGraw-Hill.

56. Dickenson, T.C., *Pumping manual*. 1995, Oxford: Elsevier Advanced Technology.

57. Drescher, U. and D. Brüggemann, *Fluid selection for the Organic Rankine Cycle (ORC) in biomass power and heat plants.* Applied Thermal Engineering, 2007. **27**(1): p. 223-228.

58. Wang, D., et al., *Efficiency and optimal performance evaluation of organic Rankine cycle for low grade waste heat power generation.* Energy, 2013. **50**(0): p. 343-352.

59. Hung, T.-C., *Waste heat recovery of organic Rankine cycle using dry fluids.* Energy Conversion and Management, 2001. **42**(5): p. 539-553.

60. Liu, B.-T., K.-H. Chien, and C.-C. Wang, *Effect of working fluids on organic Rankine cycle for waste heat recovery.* Energy, 2004. **29**(8): p. 1207-1217.

61. Hung, T.C., T.Y. Shai, and S.K. Wang, *A review of organic rankine cycles (ORCs) for the recovery of low-grade waste heat.* Energy, 1997. **22**(7): p. 661-667.

62. Hung, T.C., et al., *A study of organic working fluids on system efficiency of an ORC using low-grade energy sources.* Energy, 2010. **35**(3): p. 1403-1411.

63. Hong Gao, C.L., Chao He, Xiaoxiao Xu, Shuangying Wu and Yourong Li, *Performance Analysis and Working Fluid Selection of a supercritical Organic Rankine Cycle for Low grade Wste Heat Recovery.* energies, 2012: p. www.mdpi.com/journal/energies.

64. Kuo, C.-R., et al., *Analysis of a 50 kW organic Rankine cycle system.* Energy, 2011. **36**(10): p. 5877-5885.

65. Mago, P.J., et al., *An examination of regenerative organic Rankine cycles using dry fluids.* Applied Thermal Engineering, 2008. **28**(8–9): p. 998-1007.

66. Masheiti, S., B. Agnew, and S. Walker, *An Evaluation of R 134 a and R 245 fa as the Working Fluid in an Organic Rankine Cycle Energized from a Low Temperature Geothermal Energy Source.* Journal of Energy and Power Engineering, 2011. **5**(5): p. 392-402.

67. Rayegan, R. and Y. Tao, *A procedure to select working fluids for Solar Organic Rankine Cycles (ORCs).* Renewable Energy, 2011. **36**(2): p. 659-670.

68. Rayegan, R. and Y.X. Tao, *A procedure to select working fluids for Solar Organic Rankine Cycles (ORCs).* Renewable Energy, 2011. **36**(2): p. 659-670.

69. Roy, J.P., M.K. Mishra, and A. Misra, *Parametric optimization and performance analysis of a waste heat recovery system using Organic Rankine Cycle.* Energy, 2010. **35**(12): p. 5049-5062.

70. Saleh, B., et al., *Working fluids for low-temperature organic Rankine cycles.* Energy, 2007. **32**(7): p. 1210-1221.

71. Quoilin, S. and V. Lemort, *Technological and economical survey of organic Rankine cycle systems.* 2009.

72. Kuppan, T., *Heat exchanger design handbook*. Vol. Secondition. 2013, Boca Raton: CRC Press.

73. Dixon, S.L. and C. Hall, *Fluid mechanics and thermodynamics of turbomachinery*. 2013: Butterworth-Heinemann.

74. Branchini, L., A. De Pascale, and A. Peretto, *Systematic comparison of ORC configurations by means of comprehensive performance indexes.* Applied Thermal Engineering, 2013. **61**(2): p. 129-140.

75. Yari, M., *Exergetic analysis of various types of geothermal power plants.* Renewable Energy, 2010. **35**(1): p. 112-121.

76. Meinel, D., C. Wieland, and H. Spliethoff, *Economic comparison of ORC (Organic Rankine cycle) processes at different scales.* Energy, 2014. **74**: p. 694.

77. Shengjun, Z., W. Huaixin, and G. Tao, *Performance comparison and parametric optimization of subcritical Organic Rankine Cycle (ORC) and transcritical power cycle system for low-temperature geothermal power generation.* Applied Energy, 2011. **88**(8): p. 2740-2754.

78. Karellas, S., A. Schuster, and A.-D. Leontaritis, *Influence of supercritical ORC parameters on plate heat exchanger design.* Applied Thermal Engineering, 2012. **33-34**(1): p. 70-76.

79. Braimakis, K., et al., *Low grade waste heat recovery with subcritical and supercritical Organic Rankine Cycle based on natural refrigerants and their binary mixtures.* Energy, 2015. **88**: p. 80-92.

80. Zhu, Y.D., et al. *An integrated comparison for working fluids selection in both subcritical and supercritical ORC*. 2014.

81. Mikielewicz, D. and J. Mikielewicz, *A thermodynamic criterion for selection of working fluid for subcritical and supercritical domestic micro CHP.* Applied Thermal Engineering, 2010. **30**(16): p. 2357-2362.

82. Schuster, A., S. Karellas, and R. Aumann, *Efficiency optimization potential in supercritical Organic Rankine Cycles.* Energy, 2010. **35**(2): p. 1033-1039.

83. Kosmadakis, G., D. Manolakos, and G. Papadakis, *Experimental investigation of a lowerature organic Rankine cycle (ORC) engine under variable heat input operating at both subcritical and supercritical conditions.* Applied Thermal Engineering, 2016. **92**: p. 1-7.

84. Astolfi, M., et al., *Technical and economical analysis of a solar–geothermal hybrid plant based on an Organic Rankine Cycle.* Geothermics, 2011. **40**(1): p. 58-68.

85. Augustine, C., et al., *Modeling and analysis of sub-and supercritical binary Rankine cycles for low-to mid-temperature geothermal resources.* GRC Transactions, 2009. **33**: p. 689-693.

86. Greenhut, A.D., et al. *Solar–geothermal hybrid cycle analysis for low enthalpy solar and geothermal resources*. in *Proceedings world geothermal congress*. 2010.

87. Toffolo, A., et al., *A multi-criteria approach for the optimal selection of working fluid and design parameters in Organic Rankine Cycle systems.* Applied Energy, 2014. **121**: p. 219-232.

88. Turton, R., et al., *Analysis, synthesis and design of chemical processes*. 2008: Pearson Education.

89. Calise, F., C. Capuozzo, and L. Vanoli, *Design and Parameter Optimization of an Organic Rankine Cycle Powered by Solar Energy.* American Journal of Engineering and Applied Sciences, 2013. **6**(2): p. 178.

90. Clotworthy, A. *Response of Wairakei geothermal reservoir to 40 years of production*. in *World Geothermal Congress*. 2000.

91. Larsen, U., et al., *Design and optimization of organic Rankine cycles for waste heat recovery in marine applications using the principles of natural selection.* Energy, 2013. **55**: p. 803-812.

92. Maraver, D., et al., *Systematic optimization of subcritical and transcritical organic Rankine cycles (ORCs) constrained by technical parameters in multiple applications.* Applied Energy, 2014. **117**: p. 11-29.

93. Safarian, S. and F. Aramoun, *Energy and exergy assessments of modified Organic Rankine Cycles (ORCs).* Energy Reports, 2015. **1**: p. 1-7.

94. Quoilin, S., et al., *Performance and design optimization of a low-cost solar organic Rankine cycle for remote power generation.* Solar Energy, 2011. **85**(5): p. 955-966.

95. Amicabile, S., J.-I. Lee, and D. Kum, *A comprehensive design methodology of organic Rankine cycles for the waste heat recovery of automotive heavy-duty diesel engines.* Applied Thermal Engineering, 2015. **87**: p. 574-585.

96. Macián, V., et al., *Methodology to design a bottoming Rankine cycle, as a waste energy recovering system in vehicles. Study in a HDD engine.* Applied Energy, 2013. **104**(0): p. 758-771.

97. Jung, H.C., S. Krumdieck, and T. Vranjes, *Feasibility assessment of refinery waste heat to power conversion using an ORC.* Energy Conversion and Management, 2014. **77**: p. 396-407.

98. Uris, M., J.I. Linares, and E. Arenas, *Techno-economic feasibility assessment of a biomass cogeneration plant based on an Organic Rankine Cycle.* Renewable Energy, 2014. **66**: p. 707-713.

99. Khatita, M.A., et al., *Power generation using waste heat recovery by organic Rankine cycle in oil and gas sector in Egypt: A case study.* Energy, 2014. **64**: p. 462-472.

100. Clarke, J. and J.T. McLeskey, *Multi-objective particle swarm optimization of binary geothermal power plants.* Applied Energy, 2015. **138**: p. 302-314.

101. Wang, H., H. Wang, and Z. Ge. *Optimal design of organic rankine cycle driven by low-temperature waste heat*. in *World Automation Congress (WAC), 2012*. 2012. IEEE.

102. Song, J., C.-w. Gu, and X. Ren, *Parametric design and off-design analysis of organic Rankine cycle (ORC) system.* Energy Conversion and Management, 2016. **112**: p. 157-165.

103. Wang, J., et al., *Off-design performance analysis of a solar-powered organic Rankine cycle.* Energy Conversion and Management, 2014. **80**: p. 150-157.

104. Carcasci, C. and R. Ferraro. *Thermodynamic Optimization and Off-Design Performance Analysis of a Toluene Based Rankine Cycle for Waste Heat Recovery From Medium-Sized Gas Turbines*. in *ASME 2012 gas turbine India conference*. 2012. American Society of Mechanical Engineers.

105. Fu, B.-R., et al., *Performance of a 250 kW organic Rankine cycle system for off-design heat source conditions.* Energies, 2014. **7**(6): p. 3684-3694.

106. Savola, T. and I. Keppo, *Off-design simulation and mathematical modeling of small-scale CHP plants at part loads.* Applied thermal engineering, 2005. **25**(8): p. 1219-1232.

107. Wendt, D.S. and G.L. Mines, *Simulation of Air-Cooled Organic Rankine Cycle Geothermal Power Plant Performance.* 2013.

108. Manente, G., et al., *An Organic Rankine Cycle off-design model for the search of the optimal control strategy.* Energy, 2013. **58**: p. 97-106.

109. Walnum, H.T., et al., *Off-design operation of ORC and CO2 power production cycles for low temperature surplus heat recovery.* International Journal of Low-Carbon Technologies, 2011: p. ctr003.

110. Sohel, M.I., M. Sellier, and S. Krumdieck, *An adaptive design approach for geothermal plant with changing resource characteristics.* 2011.

111. Pambudi, N.A., et al., *Preliminary analysis of single flash combined with binary system using thermodynamic assessment: a case study of Dieng geothermal power plant.* International Journal of Sustainable Engineering, 2015. **8**(4): p. 258-267.

112. Pambudi, N.A., I. Ryuichi, and S. Jalilinasrabady. *Performance Evaluation of Double-flash Geothermal Power Plant at Dieng Using Second Law of Thermodynamics*. 2013. Stanford Geothermal Workshop.

113. Mines, G.L.e.a., *Evaluation of the impact of off-design operation on an air-cooled binary power plant.* Transactions - Geothermal Resources Council, 2002: p. 701-706.

114. M Kanoğlu, Y.C., *Improving the performance of an existing air-cooled binary geothermal power plants a case study.* Journal of Energy Resources Technology, 1999. **121**: p. 201.

115. Wendt, D.S. and G.L. Mines, *Interim Report: Air-Cooled Condensers for Next Generation Geothermal Power Plants Improved Binary Cycle Performance.* DOE Report, September, 2010.

116. Nellis, G. and S.A. Klein, *Heat transfer*. 2009, New York: Cambridge University Press.

117. Franco, A., *Power production from a moderate temperature geothermal resource with regenerative Organic Rankine Cycles.* Energy for Sustainable Development, 2011. **15**(4): p. 411-419.

118. Valdimarsson, P., *Geothermal power plant cycles and main components.* Short Course on Geothermal Drilling, Resource Development and Power Plants, 2011: p. 16-22.

119. Holdmann, G., *The Chena Hot Springs 400kW geothermal power plant: experience gained during the first year of operation.* Chena Geothermal Power Plant Report, Chena Power Plant, Alaska, 2007: p. 1-9.

120. Schefflan, R., *Teach yourself the basics of Aspen plus*. 2011, New York: Wiley.

121. Linstrom, P. and W. Mallard, *NIST Chemistry webbook; NIST standard reference database No. 69.* 2001.

122. Administration, E.I., *State Electricity Profiles 2007.* 2009.

123. Sanyal, S.K., *Cost of Geothermal Power and Factors that Affect It.* 2004.

124. Tester, J.W., et al., *The future of geothermal energy.* Impact of Enhanced Geothermal Systems (EGS) on the United States in the 21st Century, Massachusetts Institute of Technology, Cambridge, MA, 2006: p. 372.

125. Budisulistyo, D., R. Wijninckx, and S. Krumdieck, *Methodology of pre-feasibility study for a binary geothermal power plant utilizing low-moderate temperature heat sources.* Proceedings 37th New Zealand Geothermal Workshop, 2015.

126. Moustapha, H., *Axial and radial turbines*. 2003: Concepts NREC.

127. Mago, P.J., et al., *An examination of regenerative organic Rankine cycles using dry fluids.* Applied thermal engineering, 2008. **28**(8): p. 998-1007.

128. Turton, R., *Analysis, synthesis, and design of chemical processes*. 1998, Upper Saddle River, N.J: Prentice Hall PTR.

129. StatisticsNewZealand, *Economic Indicators - Capital goods price index.* 2014: p. http://www.stats.govt.nz/infoshare/default.aspx?AspxAutoDetectCookieSupport=1.

130. Gawlik, K. and C. Kutscher, *Investigation of the opportunity for small-scale geothermal power plants in the Western United States.* Transactions-Geothermal Resources Council, 2000: p. 109-112.

131. Roos, C.J., C. Northwest, and A. Center, *An overview of industrial waste heat recovery technologies for moderate temperatures less than 1000 F*. 2009: Northwest CHP Application Center.

132. Stefansson, V., *Investment cost for geothermal power plants.* Geothermics, 2002. **31**(2): p. 263-272.

133. Kranz, S., *Market survey Germany, GFZ Potsdam.* 2007: p. http://www.lowbin.eu/public/GFZ-LowBin_marketsituation.pdf,.

134. Kutscher, C.F. *The status and future of geothermal electric power*. in *Proceedings of the solar conference*. 2000. American Solar Energy Society; American Institute of Architects.

135. Zealand, R.B.o.N., *Reverse Bank of New Zealand Te Putea Matua.* 2014: p. http://www.rbnz.govt.nz/statistics/key_graphs/inflation/.

136. David, G., F. Michel, and L. Sanchez. *Waste heat recovery projects using Organic Rankine Cycle technology–Examples of biogas engines and steel mills applications*. in *World Engineers' Convention, Geneva*. 2011.

137. Power, A.E.A.C., *400 kW geothermal power plant at Chena hot springs, Alaska.* Final Report, 2007.

138. Hunt, T., *A Practical Guide to Exploiting Low Temperature Geothermal Resources.* 2006.

139. Entingh, D. and L. McLarty, *Renewable energy technology characterizations*. 1997, TR-109496 Topical Report, Prepared by Office of Utility Technologies, Energy Efficiency and Renewable Energy, US Department of Energy (USDOE) and EPRI.

140. CE Holt Company, P., California 91101, *Next Generation of Geothermal Power Plants.* Electric Power Research Institute (EPRI), 1996.

141. Hance, C.N., *Factors affecting costs of geothermal power development.* Geothermal Energy Association for the US Department of Energy, 2005.

142. Peng, D.-Y. and D.B. Robinson, *A new two-constant equation of state.* Industrial & Engineering Chemistry Fundamentals, 1976. **15**(1): p. 59-64.

143. Sullivan, J., et al., *Life-cycle analysis results of geothermal systems in comparison to other power systems*. 2010, Argonne National Laboratory (ANL).

144. King, C.W. and C.A. Hall, *Relating financial and energy return on investment.* Sustainability, 2011. **3**(10): p. 1810-1832.

145. Murphy, D.J., et al., *Order from chaos: A preliminary protocol for determining the EROI of fuels.* Sustainability, 2011. **3**(10): p. 1888-1907.

146. Frick, S., M. Kaltschmitt, and G. Schröder, *Life cycle assessment of geothermal binary power plants using enhanced low-temperature reservoirs.* Energy, 2010. **35**(5): p. 2281-2294.

147. Southon, M. and S. Krumdieck, *Energy Return on Investment (EROI) for Distributed Power Generation from Low-Temperature Heat Sources Using the Organic Rankine Cycle*. 2013, Resource.

148. Icerman, L., *Net energy analyses for liquid-dominated and vapor-dominated hydrothermal energy-resource developments.* Energy, 1976. **1**(4): p. 347-365.

149. Yu, G., et al., *Simulation and thermodynamic analysis of a bottoming Organic Rankine Cycle (ORC) of diesel engine (DE).* Energy, 2013. **51**: p. 281-290.

150. Quoilin, S., et al. *Working fluid selection and operating maps for Organic Rankine Cycle expansion machines*. in *21st International Compressor Conference at Purdue*. 2012.

151. Johnson, I., et al., *Waste heat recovery: technology and opportunities in US industry.* US Department of Energy, Office of Energy Efficiency and Renewable Energy, Industrial Technologies Program, 2008.

152. Jung, H.-C., L. Taylor, and S. Krumdieck, *An experimental and modelling study of a 1 kW organic Rankine cycle unit with mixture working fluid.* Energy, 2015. **81**: p. 601-614.

153. Lemmon EW, H.M., McLinden MO., *Reference fluid thermodynamic and transport properties-REFPROP.* Standard Reference Database 23, Version 8.0, National Insitute of Standard and Technology, 2007.

154. Lemort, V., et al., *Testing and modeling a scroll expander integrated into an Organic Rankine Cycle.* Applied Thermal Engineering, 2009. **29**(14): p. 3094-3102.

155. Winandy, E., C. Saavedra, and J. Lebrun, *Experimental analysis and simplified modelling of a hermetic scroll refrigeration compressor.* Applied thermal engineering, 2002. **22**(2): p. 107-120.

156. Rathore, M.M. and R.R. Kapuno, *Engineering heat transfer*. Vol. 2nd. 2011, Sudbury, Mass: Jones & Bartlett Learning.

157. Hsieh, Y.Y. and T.F. Lin, *Saturated flow boiling heat transfer and pressure drop of refrigerant R-410A in a vertical plate heat exchanger.* International Journal of Heat and Mass Transfer, 2002. **45**(5): p. 1033-1044.

158. Kuo, W., et al., *Condensation heat transfer and pressure drop of refrigerant R-410A flow in a vertical plate heat exchanger.* International Journal of Heat and Mass Transfer, 2005. **48**(25): p. 5205-5220.

159. Gnielinski, V., *G1 Heat Transfer in Pipe Flow*, in *VDI Heat Atlas*. 2010, Springer. p. 691-700.

160. Zukauskas, A., *Convective heat transfer in cross flow*. Vol. 6. 1987: Wiley, New York.

161. Woodland, B.J., et al., *Experimental testing of an organic Rankine cycle with Scroll-type expander.* 2012.

162. Purcell, J.E., *A comparison of positive displacement and centrifugal pump applications.* Proceedings of the 14th International Pump users Symposium.

163. Christopher Mills, M.B., Muhamad Ghazali, Nathan Marks, *Gast Turbine bottoming cycle.* ENME 408 Final Year Project, 2013.

164. Baik, Y.-J., et al., *Power enhancement potential of a mixture transcritical cycle for a low-temperature geothermal power generation.* Energy, 2012. **47**(1): p. 70-76.

165. Sanyal, S.K. and S.L. Enedy. *Fifty years of power generation at the Geysers geothermal field, California–the lessons learned*. in *36th workshop on geothermal reservoir engineering, Stanford, California*. 2011.

166. Cappetti, G., et al. *Fifteen years of reinjection in the Larderello-Valle Secolo area: analysis of the production data*. in *Proceedings*. 1995.

167. Lovekin, J., *Sustainable Power and the Life Cycle of a Geothermal Field.* Geothermal Resources Council Bulletin, 1999. **28, No. 3,**: p. 515-519.

168. NIWA, *The National Climate Database.* National Institute of Water and Atmospheric Research, 2015.

169. Cooke, D., *On prediction of off-design multistage turbine pressures by Stodola's ellipse.* Journal of engineering for gas turbines and power, 1985. **107**(3): p. 596-606.

170. Keeley, K., *A theoretical investigation of the part-load characteristics of LP steam turbine stages.* CEGB memorandum RD/L/ES0817/M88, 1988.

171. Hadi Ghasemi, M.P., Alessio Tizzanini, Alexander Mitsos, *Modelling and optimization of a binary geothermal power plant.* Energy, 2013. **50**.

172. Kanoglu, M., I. Dincer, and M.A. Rosen, *Understanding energy and exergy efficiencies for improved energy management in power plants.* Energy Policy, 2007. **35**(7): p. 3967-3978.

173. StatisticsNewZealand, *Economic Indicators - Capital goods price index.* http://www.stats.govt.nz/infoshare/default.aspx?AspxAutoDetectCookieSupport=1, 2015.

174. Walnum, H.T., et al., *Off-design operation of ORC and CO2 power production cycles for low temperature surplus heat recovery.* International Journal of Low-Carbon Technologies, 2011. **6**(2): p. 134-140.